

Energy Advances

Accepted Manuscript

This article can be cited before page numbers have been issued, to do this please use: N. A. Adzahar, A. G. Alsultan, H. V. Lee and Y. Taufiq-Yap, *Energy Adv.*, 2025, DOI: 10.1039/D5YA00078E.



This is an Accepted Manuscript, which has been through the Royal Society of Chemistry peer review process and has been accepted for publication.

Accepted Manuscripts are published online shortly after acceptance, before technical editing, formatting and proof reading. Using this free service, authors can make their results available to the community, in citable form, before we publish the edited article. We will replace this Accepted Manuscript with the edited and formatted Advance Article as soon as it is available.

You can find more information about Accepted Manuscripts in the [Information for Authors](#).

Please note that technical editing may introduce minor changes to the text and/or graphics, which may alter content. The journal's standard [Terms & Conditions](#) and the [Ethical guidelines](#) still apply. In no event shall the Royal Society of Chemistry be held responsible for any errors or omissions in this Accepted Manuscript or any consequences arising from the use of any information it contains.

Advances of supported-monometallic and bimetallic catalysts towards green aviation fuels: Review

View Article Online
DOI: 10.1039/D5YA00078E

Nur Athirah Adzahar^{1,2}, G. AbdulKareem-Alsultan^{1,2*}, Hwei Voon Lee³, Y.H. Taufiq-Yap^{1,2*}

¹*Catalysis Science and Technology Research Centre, Faculty of Science, Universiti Putra Malaysia, 43400 UPM Serdang, Selangor, Malaysia*

²*Department of Chemistry, Faculty of Science, Universiti Putra Malaysia, 43400 UPM Serdang, Selangor, Malaysia*

³*Nanotechnology and Catalysis Research Centre (NANOCAT), Universiti Malaya, 50603 Kuala Lumpur, Malaysia*

*Corresponding authors

*Professor Datuk ChM. Ts. Dr. Taufiq Yap Yun Hin

Catalysis Science and Technology Research Centre, Faculty of Science, Universiti Putra Malaysia, 43400 UPM Serdang, Selangor, Malaysia

Email address: taufiq@upm.edu.my (Y.H. Taufiq Yap)

*Dr. Abdulkareem Ghassan Abdulkreem Alsultan

Catalysis Science and Technology Research Centre, Faculty of Science, Universiti Putra Malaysia, 43400 UPM Serdang, Selangor, Malaysia

Tel: +60182534058,

Email: kreem.alsultan@yahoo.com

Abstract

The worldwide energy crisis is triggered by the increasing exhaustion of fossil fuel supplies along with a population increase in developing nations. In addition, fossil fuels are not environmentally benign due to their association with issues such as climate change, high toxic content, and non-biodegradability. Consequently, they are regarded as an unsustainable source of energy. Undoubtedly, green aviation fuel, also referred to as bio-jet fuel, is potential and sustainable long-term energy source that can help decrease our reliance on fossil fuels, owing to the availability and renewability of its feedstocks. In contrast to biodiesel, which is produced through the process of transesterification, green aviation fuel is produced using deoxygenation to eliminates oxygen and other impurities, resulting in a fuel that is chemically mimic to petroleum diesel. Thus, conventional homogeneous and heterogeneous catalytic systems for producing biodiesel from vegetable oil are no longer justifiable for the sustainable aviation fuel (SAF) industry in the foreseeable future. This is primarily due to the oxygen-containing



compounds in biodiesel (~10–12%), which increases its susceptibility to oxidation and degradation over time, and resulted to the formation of gum, clogging of filters, and decreased fuel storage stability, all of which are crucial concerns for aviation. Furthermore, jet engines are engineered to operate on drop-in fuels that closely resemble hydrocarbon-based jet fuel without requiring modifications. This review provides a detailed and systematic procedure for converting non-edible oils, such as palm kernel oil (PKO) into SAF utilizing bimetallic nickel cobalt onto magnetite support catalysts. The enhanced catalytic system can effectively convert palm kernel oil with a high yield and selectivity towards kerosene for aviation sectors via deoxygenation reactions. Using palm kernel oil as a raw material for SAF production will help address the problem of food security that arises from using food-grade oil for SAF production, while decreasing the overall manufacturing expenses for green fuel production. This article aims to highlight the use of heterogeneous bimetallic acid/base catalysts for the production of SAF from environmentally friendly and non-edible palm kernel oil. Future research should focus on optimizing bimetallic catalysts to improve the efficiency of sustainable aviation fuel (SAF) production from non-edible oils, with the aim of reducing energy consumption and minimizing environmental impact. Additionally, it is crucial to investigate alternative sustainable feedstocks and assess their scalability to ensure widespread adoption of green fuels in the aviation sector, addressing both food security and long-term energy needs. In conclusion, this study provides insights and potential advancements for the future.

Keywords : Green fuel; nickel-cobalt; palm kernel oil; aviation; iron catalysts

Table of Contents

Title	Pages
Introduction	3
1.1 Development of green fuel	6
Sustainable Aviation Fuel (SAF)/ Bio-jet fuel (BJF)	9





A. Fischer-Tropsch hydroprocessed Synthetic paraffinic kerosene (FT-SPK)	16
B. Synthesis-paraffin kerosene from hydroprocessed esters and fatty acids (HEFA)	19
C. Alcohol to jet synthetic paraffinic kerosene (ATJ-SPK)	21
D. Synthesized iso-paraffins from hydroprocessed fermented sugars (SIP)	22
E. Catalytic Hydrothermolysis Jet (CHJ-SPK)	23
1.2 Generations of Feedstocks for Green Fuel Production: From First to Advanced Biofuels	24
1.2.1 First generation feedstocks	25
1.2.2 Second generation feedstocks	27
1.3 Types of reaction and processes	31
1.3.1 Hydrodeoxygenation/ Hydrocracking (HDO)	31
1.3.2 Deoxygenation (DO)	33
1.4 Catalysts development for deoxygenation reaction	35
1.4.1 Catalysts overview	35
1.4.2 Homogenous vs Heterogenous catalysts	36
1.4.3 Noble metal catalysts	40
1.4.4 Non noble metal catalysts	43
(A) Metal carbides (CS), phosphides (P), nitrides (N), sulfided (S)-based catalysts	43
(B) Transition metal oxides (TMO) based catalysts	48
(I) Ni-based catalysts	48
(II) Co-based catalysts	50
1.4.5 Catalyst support	52
(I) Properties of iron element as catalyst support	54
1.4.6 Deoxygenation of bimetallic Ni-Co supported on Fe-based catalyst	57
1.5 Deactivation of catalyst	59
1.5.1 Sintering	60
1.5.2 Coking	62
1.5.3 Poisoning	64
1.5.4 Leaching	66
1.5.5 Catalysts' stability	67
1.6 Factors affecting reaction conditions	69
1.6.1 Reaction Temperature	69
1.6.2 Residence Time	71
1.6.3 Catalyst type and amount used	74
1.6.4 Types of feedstocks	76
1.6.5 Reaction Environment	78
1.7 Recent developments and future outlook in deoxygenation reaction on production of renewable biofuels	82

Introduction

The predominant fuel type for both commercial and military aircraft is jet fuel, which is mostly produced through petroleum refining. The excessive mobility of air passengers has led the global aviation sector to consume jet fuel at an unsustainable rate, resulting in a

significant increase in greenhouse gas (GHG) emissions. The New York Times reported in September 2021 that the earth is currently hotter than it has been for at least 1,000 years because CO₂-GHG gas concentrations have risen to nearly 900 million metric tons globally¹⁻³. NASA claimed that in October 2021, CO₂ levels had already surpassed the mid-1700s (280 ppm) and were 416 parts per million (ppm)^{4,5}. As a result, an increase in CO₂ levels frequently causes extreme weather, the effects of which may result in global financial crises and loss of life. Consequently, an increasing number of climate-conscious experts have sparked the creation of a new generation of jet fuel made from renewable biomass. A sustainable and clean-burning alternative to commercial jet fuel, biodiesel is a liquid fuel made of mono-alkyl esters of fatty acids. Unfortunately, the higher oxygen content in biodiesel appears to cause thermal instability, low volatility, poor combustion quality, and a heightened sooting propensity to limit its direct use in engines⁶⁻⁹. Therefore, a different procedure that produces less-oxygenated molecules with mimicked hydrocarbon structure within the jet range fuel (C₁₀-C₁₆) is necessary¹⁰.

Deoxygenation or hydrodeoxygenation reactions can be used to accomplish this. In contrast to deoxygenation, which involves the removal of oxygenated compounds in the form of CO₂/CO through direct C-O bond cleavage under H₂-free conditions, hydrodeoxygenation involves the addition of H₂ and removal of O₂ in the form of hydrocarbons and H₂O as a by-product¹¹⁻¹³. In contrast to deoxygenation, which results in a fuel fraction with one fewer carbon atoms than its fatty acids, hydrodeoxygenation yields a fuel fraction with a carbon length similar to that of its fatty acid^{6,11,14}. Deoxygenation has received increasing attention due to H₂-free reaction method that can provide fuel fractions while hydrodeoxygenation is not economically viable¹⁵⁻¹⁷. Fatty acids appear to be a potential feedstock for producing bio-jet fuel via a deoxygenation reaction. Apart from fatty acids, triglycerides (TGs) are another major component of both plant and animal fats and oils. When triglycerides are hydrolysed, fatty



acids are produced¹⁸. TGs and fatty acids can also be used as chemical intermediates to create alcohols, aldehydes, and alkenes, and using them as feedstocks for deoxygenation is advantageous^{19,20}. The qualities of the fuel, such as viscosity, flash point, and cetane number were improved by the presence of these intermediates. In addition to TGs and fatty acids, the deoxygenation procedure also demonstrated notable ability to remove the oxygen from lignin species from lignocellulosic biomass and enhanced aromatic hydrocarbons^{21,22}. The deoxygenation process was shown to be a very effective method for all feedstocks with majority of the deoxygenated TGs or fatty acid products have a bright yellow colour.

The catalytic deoxygenation process has been studied extensively in the past by employing sulfided metals, such as ReNiMo, NiMo, CoMo, and NiW, as well as noble metals, such as Pt and Pd^{23–28}. Although noble catalysts were found to be superior at deoxygenating feeds, they were unappealing owing to their high price and limited availability^{13,29–31}. On the other hand, sulfided catalysts are an issue because they might cause sulfur to seep out and contaminate the final product^{32,33}. Consequently, it is essential to develop catalysts that are both affordable and devoid of sulfur. It is interesting to note that because transition metal oxides like Ni, Co, Mn, Zn, and Ce may achieve results that are equivalent to those of noble metal-promoted catalysts, they are regarded as suitable catalyst promoters. It has been discovered that Ni has greater deoxygenation performance and endurance than noble metal catalysts with greater C–C or C–O bond cleavage activity^{34–36}. This is corroborated by a previous study in which a Ni-promoted catalyst produced a diesel selectivity of 80% at 390°C in inert environments^{37,38}. However, Ni-based catalysts favor excessive cracking, leading to poor coking activity, which can limit their stability and yield. Thus, previous studies have investigated the modification of Ni by adding Co metal, which demonstrated that deoxygenating palm fatty acid distillate over Co/AC catalyst produced 91% hydrocarbon fuel



^{39,40}. Notably, the Ni-Co catalyst has been shown to have a synergistic effect that can increase the DO activity even at low temperatures ^{41,42}.

It has also been shown that the catalyst support plays a significant role owing to its physicochemical properties and electronic interactions, which would affect the rate of the reaction and increase the yield of the desired deoxygenated product. γ -Al₂O₃, SiO₂, and TiO₂ are typically utilized as catalyst supports owing to their excellent oxygen storage capacity and intrinsic redox properties, which make them capable of facilitating the activation of oxygenated compounds ^{13,43,44}. However, catalyst supports with high acid strength such as zeolite (H-ZSM-5) and sulphated zirconia (SO₄²⁻/ZrO₂) were prone to promotes excessive cracking, as well as severe coke formation and deposition, which resulted rapid deactivation. To decompose the carboxylic group in vegetable-based oil, moderately acidic supports such as iron oxide support are needed. The use of iron oxide as a support can also minimize weight loss and make the catalyst easier to separate owing to its magnetic ability. Iron oxide has high oxyphilic effects, and redox reactions make it easier to break C-C and C-O bonds and boost the efficiency of the oxygen-removing agent ⁴⁵⁻⁴⁷. In addition, it also reduces polymerization and accentuates cracking and char generation. The presence of Lewis acid sites on iron oxide supports aids in reducing carboxylic acids to aldehydes, while Brønsted acid sites facilitate cracking and hydrogen transfer reactions ⁴⁸⁻⁵⁰. Therefore, the present work focuses heavily on the advancement of bimetallic nickel-cobalt supported catalysts on iron oxide for catalytic deoxygenation of second-generation crops in an absence of H₂ atmosphere.

1.1 Development of green fuel

Therefore, the creation of clean and renewable energy sources is gaining popularity. The United Nations adopted the "Transforming our World: the 2030 Agenda for Sustainable Development" on September 25, 2015, with the goal of promoting global sustainable



development and ensuring that "no one is left behind." For this initiative to be successful, it is crucial that the economic, social, and environmental aspects of sustainable development are interconnected^{51,52}. In addition to this initiative, the European Union has embraced the European Green Deal, which presents a growth strategy aimed at transforming the organization into a modern and competitive economy. The primary objectives are to maximize resource efficiency and, notably, to achieve net-zero greenhouse gas emissions by the year 2050^{28,51,53}. In order to limit global warming by 1.5°C over pre-industrial levels, the 2015 Paris Agreement calls for a reduction in greenhouse gas emissions, which is something that the Green Deal supports^{54–56}. From what has been discussed thus far, it is evident that the development of green fuels is a topic of great importance that also has favourable environmental effects.

Global energy consumption is at an all-time high due to changing lifestyles and a growing population. Currently, fossil fuels are the primary energy source. However, it was expected that fossil fuel resources would eventually run out because they are known to be non-renewable. According to a study published in the Statistical Review of World Energy, if global energy consumption continues to rise, the world's reserves of petrol and oil will run out in 41 and 63 years, respectively. Furthermore, the use of petroleum contributes significantly to the release of greenhouse gases (GHGs), which affect human health and the environment by causing sea-level rise, glacier retreat, and climate change^{57–60}. The global average temperature rises as a result of the climate system radiating more positively due to an increase in greenhouse gases. This is supported by statistics showing that atmospheric CO₂ levels have increased from 277 parts per million in 1750 to 417 parts per million in 2019, globally, leading to a 2°C increase in temperature over the pre-industrial revolution levels^{61–63}. Ice sheets and glaciers will also melt as global temperatures rise, endangering millions of people with diseases, such as malaria, starvation, flooding, and water shortages. Consequently, there has been a national



focus on developing renewable energy sources in an attempt to mitigate the negative impacts of the issues caused by the use of conventional fuels ^{64,65}.

Energy derived from naturally occurring processes that replenish itself is referred to as renewable energy ^{66,67}. Examples of such processes include solar, wind, biomass, geothermal and hydropower resources (tidal and wave) ^{66,68}. Renewable energy is superior to fossil fuels in many different ways, such as an endless supply, lowering the risk of atmospheric pollution by minimizing the emission of sulfur, carbide, and dust, and reducing the consumption of natural fossil fuels ^{69,70}. Moreover, renewable energy is clean, green, and low in carbon, along with a reduction in solid waste release and the protection of water resources. Recently, renewable energy has been widely used to generate electricity and energy of approximately 24.5% and 19.3%, respectively, and has been used in the industrial and domestic sectors ^{71–73}. Renewable energy can also be used to develop value-added products such as cosmetics and perfumes from fatty acids of fermenting sugars, food additives, and nutritional supplements from algae, plastics, lubricants, surfactants (oleo-furan), fertilizers, biogas, and renewable natural gas ^{74–76}. Furthermore, the development of green fuels in the transportation industry has significantly increased the use of renewable energy sources such as biomass (**Figure 1**).









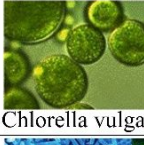



Categories	Biomass Sources	Production Process	Biofuel	Common Catalyst Type
First Generation	   Sunflower Wheat Corn	Biochemical (fermentation, transesterification, esterification)	Bioethanol	Enzyme catalyst, microorganisms (yeast)
			Biodiesel	Homogenous (NaOH, KOH, HCl, H ₂ SO ₄) and heterogenous catalyst (CaO, dolomite, AlCl ₃ , WO/ZrO ₂)
Second Generation	   Jatropha Ceiba PFAD	Biochemical Thermochemical	Bioethanol Biodiesel Bio-jet fuel/ Sustainable Aviation Fuel (SAF)	Bioethanol and biodiesel commonly used catalyst similar to first generation
Third Generation	   Chlorella vulgaris Microalgae Macroalgae			Bio-jet fuel/sustainable aviation fuel (SAF) used heterogenous catalyst such as Pd/C, zeolites, transition metal oxides
Fourth Generation	 Genetically engineered feedstocks with genomically synthesized microorganisms			

Figure 1: An overview of each type of green fuel generation ^{77–79}.

Sustainable aviation fuel (SAF)/ Bio-jet fuel

Air transportation plays a crucial role in the daily lives of developing countries. Civil aviation is a rapidly expanding mode of transportation and one of the fastest-growing areas in the industry ^{80,81}. In 2019, the International Air Transport Association (IATA) reported that air travel by people in emerging nations is expected to increase by up to 10% annually, resulting in a significant growth of 44% over the following 20 years ^{80,82}. The exponential expansion of air transport has resulted in a corresponding increase in environmental impacts, particularly the depletion of fossil fuels as its principal energy source. However, these challenges require special attention and consideration. The U.S. Department of Energy (DoE) forecasted that the commercial jet fuel market will expand to more than 230 billion gallons by 2050, which the current existing petroleum could not withstand; thus, another alternative approach to replace this petroleum fuel has been widely studied. This rise not only causes fossil fuels to diminish over time but also leads to an increase in CO₂ emissions ⁸³. Statistics studies from EIA show that global aviation emissions represent 2% of global GHG emissions, which rose in 2022 to



reach nearly 80% in 2019 (**Figure 2**), which is around \square 1000 MMT of CO₂, and forecasted by the International Civil Aviation Organization (ICAO), the value would triple by 2050^{84–86}. To overcome this issue, researchers worldwide have extensively studied and explored alternative approaches to replace fossil fuels in various sectors, including aviation^{52,87}.

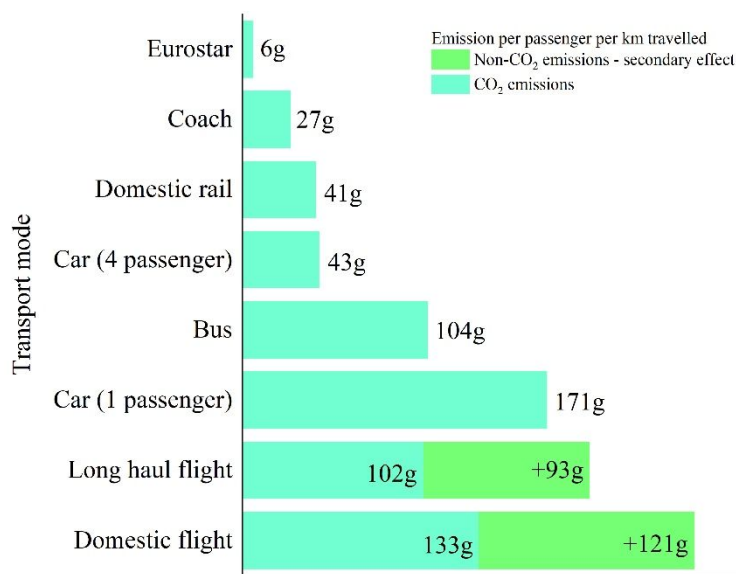
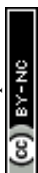


Figure 2: Emissions from different transportation mode per passenger per km travelled.

An effective approach is to advance and implement sustainable aviation fuel (SAF). SAF, commonly referred to as bio-jet fuel or biokerosene, is a liquid hydrocarbon alternative to hydrocarbons in the C₈-C₁₆ boiling point range. It shares similar properties with traditional fuels and is formulated for current aircraft usage^{88–90}. SAF is distinguished by its markedly reduced carbon impact compared with that of traditional jet fuel. SAF typically achieves a significant decrease in carbon dioxide emissions, typically falling within the range of 50–80% as opposed to conventional jet fuel sourced from fossil fuels. The extent of this decrease depends on the specific feedstock and production method used^{91,92}. The primary objective of the Carbon Offsetting and Reduction Scheme for International Aviation (CORSIA) is to offset any excess emissions over the established limitations by 2020 through the purchase of carbon credits from various businesses^{70,93,94}. In addition, it specifies the sustainability criteria for the



raw materials used. To be certified as sustainable, a fuel must adhere to the sustainability guidelines established by the CORSIA. These requirements include reduction of carbon emissions, enhancement of water quality, consideration of soil and air quality, and adherence to land and human rights. The proposal functions as an interim measure until the aviation sector can devise and use more environmentally sustainable technologies to mitigate carbon emissions. SAFs must comply with specific fuel property standards to ensure efficient absorption. These properties include energy content to improve aircraft performance, density to optimize fuel load and payload capacity, viscosity to ensure smooth engine operation, flash point for safe handling, freezing point for cold climate operations, low sulfur content to reduce emissions, and specific distillation characteristics for compatibility with aircraft engines^{95–97}. Achieving an appropriate balance between these characteristics is crucial for the advancement of SAFs that not only comply with precautions and operational demands but also have a positive environmental impact and assist in the future of greater sustainability for the aviation sector.

Jet A-1 is the conventional jet fuel that serves as a reference point for SAF in terms of its molecular makeup and overall fuel characteristics^{98–100}. Jet A-1 is typically composed of C₈–C₁₆ hydrocarbons. It is abundantly composed of paraffinic chains such as iso-, cyclo-, and n-paraffins, followed by aromatics^{83,98}. Given their low freezing points, superior thermal conductivities, and particular powers, iso-alkanes are the preferred alternatives. Cycloalkanes, however, satisfy certain requirements owing to their density and ability to swell. Both iso-alkanes and cycloalkanes offer the advantages of providing specific energy density, assuring thermodynamic durability; lowering specific emissions; boosting cargo capability; and prolonging endurance^{83,101}. Although aromatics are less packed with energy than the alkane group elements of jet fuel, these components are nevertheless required to keep the nitrile rubber sealant on airplanes from expanding excessively to minimize fuel leakage^{102,103}. The key



factors determining the fuel qualities of the standard are its H/C ratio of 2, lower heating value (LHV) of 43.2 MJ/kg, and complete absence of oxygen^{83,98,102,104}. The chemical properties of aviation fuels, such as Jet A essential relevance as they directly influence an immediate impact on the fuels' effectiveness, security, and impact on the environment. The compatibility of fuel molecules with engines for aircraft and equipment is crucial for effective discharge of energy, efficient ignition, and safe flight operations. Furthermore, strict compliance with aviation fuel specifications based on molecular functions is crucial for meeting rigorous industry regulations and guaranteeing consistency and dependability throughout the aviation industry. The chemical composition of aircraft fuels is intricately linked to their energy content, ignition characteristics, fluctuation, ignition point, thawing point, and pollutant features^{98,102,105}. Hence, a crucial area of research involves developing and refining the molecular composition of SAF to closely resemble those of traditional fuels. This enables improved fuel efficiency, reduced emissions, and a smaller carbon footprint than conventional fossil-based aviation fuels. Hence, it is imperative to thoroughly understand and assess the molecular functions of synthetic candidates for SAF to authorize their use in aircraft. This will help promote sustainable aviation practices, improve aircraft performance, and reduce environmental impact^{83,106}. The ASTM D7566, which includes the rigorous criteria necessary for SAF, received its initial route approval in 2009. The processes authorized according to ASTM D7566 are listed in **Table 1**. The aviation sector is responsible for approximately 3% of global GHG emissions, and has long been recognized as one of the major contributors of the transportation sector to global warming^{107–109}. With almost 37% of the world's jet fuel consumption going to the US, this country is the largest user^{110,111}. China is projected to overtake the United States as the largest worldwide market for jet fuel and air passengers by 2029^{112,113}.

View Article Online
DOI: 10.10039/D5TA00078E



Table 1: ASTM standard on production group of sustainable aviation fuel (SAF). View Article Online
DOI: 10.1039/D5YA00078E

ASTM D7566	Conversion Process	Possible Feedstocks	Blend limit (%)	Year
A1	Fischer-Tropsch synthetic paraffin kerosene (FT-SPK)	Coal, natural gas, biomass	50	2009
A2	Hydroprocessed ester and fatty acid (HEFA-SPK)	Vegetable oil, animal fat, waste oil	50	2011
A3	Synthesized iso- paraffinic (SIP)	Starch, carbohydrate, cellulose	10	2014
A4	Fischer-Tropsch synthetized paraffin kerosene with aromatics (FT- SPK/A)	Coal, natural gas, biomass	50	2015
A5	Alcohol to jet synthesized paraffin kerosene (ATJ-SPK)	Biomass from ethanol or isobutanol production	30 50	2016 2018
A6	Catalytic hydrothermolysis jet fuel (CHJ)	Fatty acids, fatty acid esters, vegetable oil	50	2020
A7	Hydroprocessed hydrocarbons, esters and fatty acids (HC-HEFA- SPK)	Algae	10	2020

An illustration of the chemical equation used to describe the catalytic deoxygenation of WCO is shown in **Figure 3**. The fatty acid composition profile of WCO revealed that the vast majority of its constituents were derivatives of the C₁₈ and C₁₆ fatty acids. This was the case for most of the constituents. In principle, the deCO_x procedure can eliminate the carboxyl and carbonyl groups present in C₁₈ and C₁₆ fatty acid derivatives. This results in the production of hydrocarbon fractions that are mostly composed of n-heptadecenes (n-C₁₇) and n-pentadecenes (n-C₁₅), in addition to the production of byproducts (CO₂, CO, and H₂O) (reactions A and D). During the course of the present study, a significant proportion of the n-C₁₅ fraction was recovered as opposed to mixtures of n-C₁₅ and n-C₁₇. This discovery provides evidence in favor of the idea that a mild cracking pathway is likely to occur. This route finally led to C-C cleavage of the n-C₁₇ fraction into the n-C₁₅ fraction (by the elimination of ethane) (Reaction B). It has been hypothesized that bimetallic CaO-La₂O₃ phases are responsible for the enhancement of certain deCO_x-mild cracking pathways. The cracking activities of the CaO/AC and La₂O₃/AC catalysts, which resulted in the synthesis of the n-C₁₁ fraction, demonstrated that CaO and



La₂O₃ were responsible for the cracking ability of CaO-La₂O₃/AC. This was confirmed by the cracking activity of these catalysts. Another option is the C-C cleavage that occurs on fatty acid derivatives, which leads to the production of C₁₆ fatty acids (reaction C). Subsequently, the fatty acid derivatives were subjected to a selective deCO_x reaction, which ultimately led to the production of n-C₁₅ hydrocarbon products (reaction D). Because it is impossible to avoid the cracking reaction, the hydrocarbons commonly go through the process of C-C cleavage, which leads to the creation of the short chain hydrocarbon n-(C₈-C₁₄) (Reaction E). This is because the cracking reaction cannot be avoided ¹¹⁴.

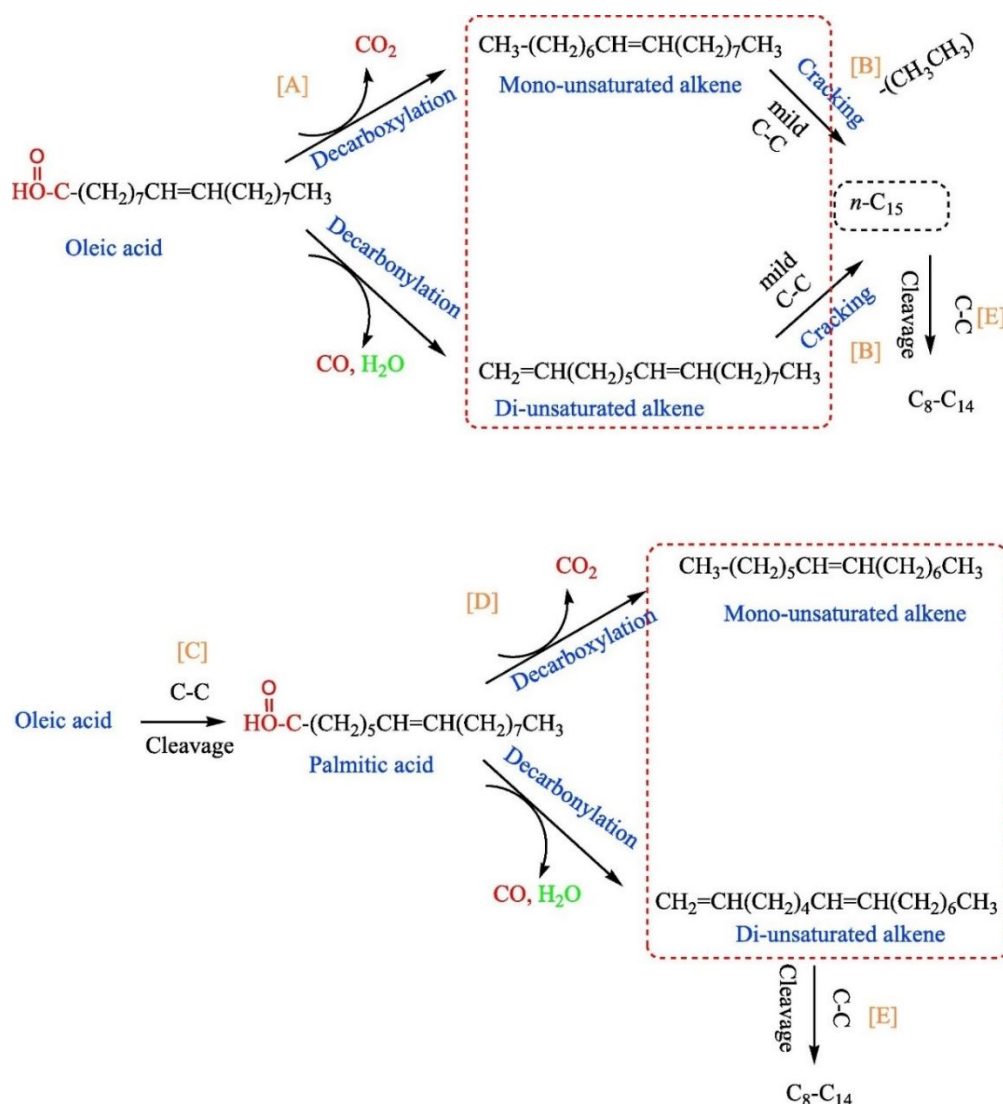


Figure 3: Proposed deoxygenation reaction pathway for the deoxygenation of WCO to hydrocarbon over CaO-La₂O₃/AC catalysts.



The suggested process for the catalytic deCOx of synthetic organic compounds is shown in **Figure 4**. This method makes use of a NiO-CD catalyst ¹¹⁵. The proposed chemical pathway was constructed using the hydrocarbon composition of the SO-based green fuel produced from the deCOx reaction and the fatty acid content of the indicated reactant, as determined by GC–MS analytical data. Both of these factors were considered when designing the route. The fatty acids in SO were responsible for most of the fatty acids in the feedstock. SO contained the following fatty acids: 40.1% oleic acid, 29.4% palmitic acid, and 14.1% stearic acid. The composition of this feedstock led to the production of green fuel, which contained a sizable quantity of hydrocarbons with designations C₁₅ and C₁₇. This particular type of diesel was produced. Given this result, it can be concluded that the production of hydrocarbon derivatives in C₁₅ and C₁₇ is facilitated by the deCOx of sulfur dioxide in the presence of a NiO-CD catalyst. In the first procedure, oleic acid was hydrogenated, leading to the synthesis of steric acid as an intermediate product (**Figure 3**). During the process, water gas shift (WGS) is the important pathway that creates significant amounts of in situ hydrogen throughout the reaction, which oleic acid's double bonds are saturated completely as a result of WGS pathway. Moreover, the NiO-CD catalyst accelerated the hydrogenation process by making it easier to break the carbon-oxygen bonds. As a result, oxygen atoms will be removed from the molecules of synthetic organic compounds (SO). In the next step, active sites composed of NiO and CaO on the dolomite catalyst support will cause this steric acid to undergo a deCOx reaction. In accordance with procedures 2 and 3, the decarboxylation and decarbonylation (deCOx) process removes carbon dioxide, carbon monoxide, and water from the stearic acid carbon chain. This may lead to the synthesis of heptadecane (C₁₇) and n-heptadecene (n-C₁₇). The carbon chain was eliminated as a result of this reaction. Based on the information shown in pathways 4, 5, and 6, more C-single bond cleavage would produce pentadecane, n-pentadecene, and lighter hydrocarbons with C₈-single bond C₁₄. To achieve this, heptadecane and n-heptadecene were



employed as solvents. This was supported by the findings of research conducted by prior studies on the removal of carbon dioxide from fatty acids using a NiO catalyst^{116,117}. Route 7 releases hydrogen peroxide and carbon monoxide, which allow palmitic acid to undergo a decarbonylation process that ultimately leads to the synthesis of pentadecane. The mechanism that leads to the production of n-pentadecene is the decarbonylation of palmitic acid, which is controlled by pathway 8. A second C-C cracking reaction of these C₁₅ hydrocarbons would result in a lighter hydrocarbon with a carbon range of C₈ single bond C₁₄, as demonstrated in routes 9 and 10. This occurs in a moderate environment. Decarboxylation and decarbonylation processes are preferred by the 1–10 approaches that have been suggested for the catalytic deCOx of SO, according to the produced NiO-CD catalyst.

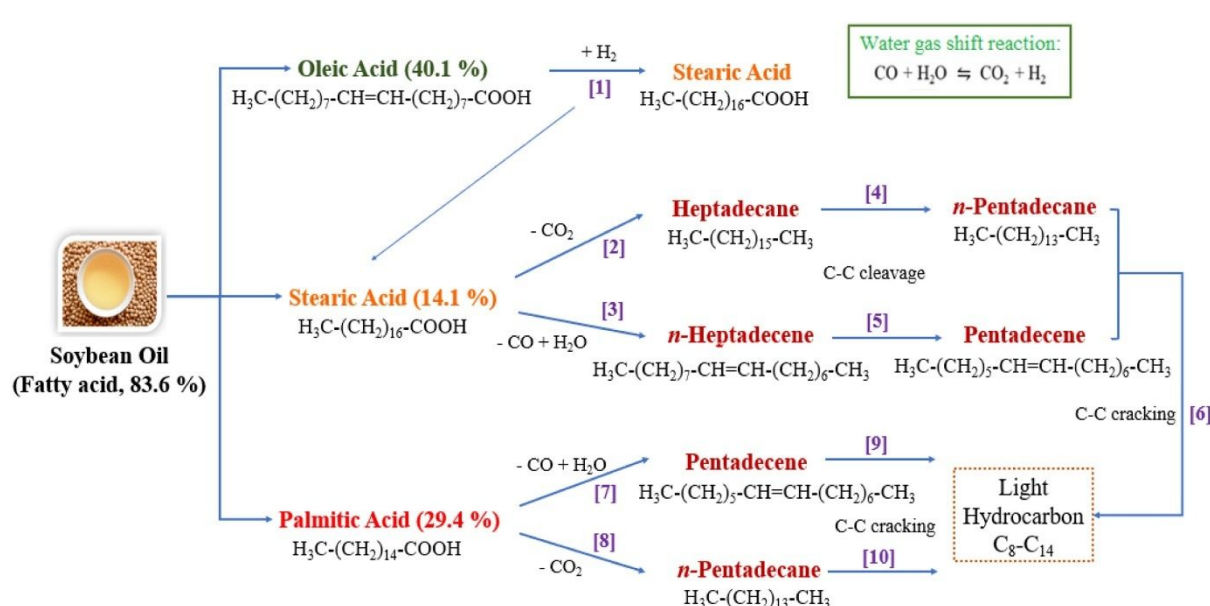


Figure 4: The proposed catalytic deoxygenation reaction mechanism of soybean oil using a synthesized NiO-CD catalyst¹¹⁸.

A. Fischer-Tropsch hydroprocessed Synthetic paraffinic kerosene (FT-SPK)

Syngas is transformed into liquid hydrocarbon fuels using the Fischer-Tropsch (FT) approach. The standard FT technique consists of six steps: feedstock pretreatments, waste gasification, vapour conditioning, gaseous acid elimination, FT synthesis, and syncrude



purification. The raw material was initially dried and treated to reduce humidity and particle size before it was gasified. Gasification followed the prior treatment of the biomass. Temperature, type of biomass used, gasifying agent used, particle size, heating velocity, working strain, equivalency proportion, enzyme addition, and reactor design are some of the variables that affect the quantity and characteristics of syngas produced ¹¹⁹. Gasification of FT always occurs at a high temperature (approximately 1300 °C) with high-purity oxygen and steam. For gasification, the common gasifier reactors are the fluid bed, moving or fixed bed, and entrained flow systems.

Additional research has analyzed different types of gasifier reactors in detail, and it has been suggested that ash and tar can be removed using a syngas cooling system next to the gasifier, which uses direct quench technology ¹²⁰. The syngas is injected into an acid gas removal system after the gasification process to eliminate the sulfur, CO₂, and H₂S present in the gaseous form of acid. Eliminating CO₂ may improve the economy and efficiency of the downstream synthesis process, whereas eliminating H₂S will keep the catalyst clean. The gas is then sent to a gas conditioning unit via a water-gas shift (WGS) reaction, where the correct ratio of CO and H₂ is adjusted. The H₂:CO ratio plays a significant role in the FT process, where it enters the reactor and produces the major product. Carboxylic acids, ketones, ethers, alkenes, and alkanes are the products of two main reactions that occur during FT: CO and H₂. Recycled FT gas and unconverted syngas may be returned to the FT reactor following reformation, where refining the liquid products is necessary to create several types of fuel and surplus gas can be utilized for electricity generation. The degree of selectivity of the catalysts is crucial for the target hydrocarbons.

There is another way to divide FT synthesis into low- and high-temperature ¹²¹. Fuel, solvent oil, and olefins are the principal byproducts of high-temperature FT, and lubricating base oil, naphtha fractions, diesel oil, and kerosene are the principal byproducts of low-



temperature FT. When the FT temperature is too low, large volumes of methane are produced as a by-product. The typical pressure range for the Fischer-Tropsch (FT) method is between one and several tens of atmospheres, where elevated pressures can lead to the formation of longer hydrocarbon chains ¹²².

Fe, Co, Ni, and Ru are frequently used as catalysts in FT process ^{123,124}. Ru has good selectivity and catalytic activity, but its high cost prevents frequent utilization ¹²⁵. The most popular catalysts for industrial production are Fe-based catalysts that have a long lifetime but a high space-time yield, and Co-based catalysts that are effective at allowing carbon chains to form, their byproducts contain fewer oxygen-containing molecules, and carbon deposition is difficult ¹²². Alkali metals, alkaline earth metals, copper, and other transition metals are common promoters that can be employed to modify the catalytic activity and efficiency ^{126–128}.

The primary challenges associated to the The main difficulties related to the FT-SPK pathway are the adoption of less complicated gasification methods, which often results to a decrease in the quality of the syngas. However, using plasma gasification for the manufacture of high-quality syngas requires a significant upfront investment for economic viability. Currently, commercially accessible biomass-derived gasified aircraft fuels are scarce in significant amount ¹²⁹. Another significant cost factor is the essential "cleanup" of raw syngas before Fischer-Tropsch synthesis ¹³⁰. This cleanup process involves multiple steps to eliminate various contaminants, and the complexity and cost increase owing to feedstock variability and varying levels of contaminants. In addition, adverse economics and unresolved syngas clean-up difficulties prevent commercial plants from manufacturing FT fuels via the BTL method ¹³¹. Additional costs and uncertainties to the process also come from the collection facilities from various places, the relatively inadequate heat amount, and the inconsistent amount and quality of the fuel ¹³². Considering the drop-in efficiency, the absence of volatile substances in



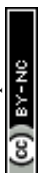
FT products may cause issues with fuel seepage because elastomer seals may not expand sufficiently¹³³.

The FT-SPK/A technology, which enhances the aromatic content of the FT fuel produced, was approved according to ASTM D7566 Annex 4. It is crucial to consider that fuels with high H/C ratios and low O/C ratios can be utilized to calculate the energy source content¹³⁴. Fuels with larger aromatic compositions have higher specific energies. FT fuels do not release aerosol emissions of sulfur dioxide (SO₂) or sulfuric acid (H₂SO₄) because of the thorough cleanup of intermediate syngas. This makes it possible to extend the life of hot path components (such as turbines and combustors) as the rate at which impurity deposits are decreased.

B. Synthesis-paraffin kerosene from hydroprocessed esters and fatty acids (HEFA)

The HEFA process is implemented for manufacturing bio-jet fuels by subjecting triglycerides (TGs), both saturated fatty acid (SFA) and unsaturated fatty acids (UFA), plant-based oils, residue from cooking oils, and animal-derived fats to hydrotreatment. Typically, this procedure consists of two steps. UFA are initially converted into SFA by catalytic hydrogenation, during which the TGs undergo a H₂ elimination reaction and produce a fatty acid¹³⁵. By hydrodeoxygenating and decarboxylating the SFA, C₁₅-C₁₈ paraffinic chains are produced¹³⁶. Propane, H₂O, CO, and CO₂ are the co-products. Noble metals onto zeolites or oxides support were the initially implemented as catalysts for this phase; however, as catalyst deactivation by poisoning, the production of cracking species, and process costs increased, the focus shifted to other transition metals, such as Ni, Fe, Cu, Mo, Co, and Fe, or composite bimetallic catalysts^{137–140}.

In the subsequent stage, the paraffinic hydrocarbons are subjected to a process called targeted hydrocracking and deep isomerization, resulting in the production of fuels that contain



highly branched alkanes. Activated carbon, Al_2O_3 , and zeolite molecular sieves are frequently used as catalysts in this step, together with Pt, Pd, or other expensive metals ^{141–144}. A moderately acidic zeolite catalyst that supports Ni exhibits good activity. However, a highly acidic catalyst causes over-cracking and lowers the yield of isomers. Fractionation was used to separate the combined liquid fuels into naphtha, light gases, paraffinic kerosene (jet fuel), and paraffinic diesel. Triglycerides were hydrocracked in a single step by Azkaar et al. using Ru-modified faujasite zeolite catalysts ¹⁴⁵. When hexadecane was utilized as the feedstock, they were able to obtain a high yield of jet-fuel range hydrocarbons (71%) with a reasonably high selectivity by using 2.5 wt.% Ru deposited on a hierarchical micro-mesoporous USY zeolite to complete deoxygenation and cracking in a reactor ¹⁴⁵. To convert used cooking oil into jet green fuel, Li et al. suggested using a nickel-based mesoporous zeolite Y catalyst ¹⁴⁶. High jet-range alkane yields of 40.5% and low jet-range aromatic hydrocarbon yields of 11.3% were achieved at an optimal temperature of 400 °C. Using a three stage catalytic method, Wu et al. created jet fuel from vegetable oils based on triglycerides that contained aromatic components ¹⁴⁷. The first step involves catalytically cracking vegetable oils over a zeolite catalyst into light aromatics. Second, by alkylating light aromatics with the help of an ionic liquid, $\text{C}_8\text{--C}_{15}$ aromatics are created. Third, by hydrogenating aromatics for 6 h at 200 °C and 5 MPa over a Pd/AC catalyst, the aromatics were transformed into saturated cycloparaffins. As they are high-energy green fuels, bio-jet fuels made by HEFA can be used in aircraft engines without blending. The fuel has a high cetane number, strong cold flow characteristics, high thermal stability, and less tailpipe smog; however, it has a low aromatic concentration, which makes it less lubricating and more prone to fuel leaks ¹⁴⁸.

View Article Online
DOI: 10.1039/D5TA00078E



C. Alcohol to jet synthetic paraffinic kerosene (ATJ-SPK)

View Article Online
DOI: 10.1039/D5YA00078E

A range of events, including dehydration, oligomerization, hydroprocessing, and distillation, can be employed to create green fuels from alcohols such as methanol, ethanol, or higher alcohols^{149,150}. Ethanol, butanol, and isobutanol are commonly used in commercial manufacturing as intermediaries to convert biomass to jet fuel. It usually involves a four-step upgrading procedure to produce hydrocarbons from alcohols in the aviation fuel range. A middle distillate is created by oligomerizing olefins in the presence of catalysts after the alcohol is first dehydrated to form olefins. The jet-fuel ranged hydrocarbons are created by hydrogenating middle distillates, followed by distillation^{151,152}.

Al_2O_3 , transition metal oxides, zeolites, and heteropolyacid catalysts are frequently used as ethanol dehydration catalysts^{153–155}. Phung et al. conducted a comparison between alumina and silica alumina in the context of commercial zeolite catalysts used for ethanol dehydration¹⁵⁶. H-zeolites are undoubtedly more active on a catalyst weight basis when compared to silica alumina and alumina. The ethylene output from H-FER and faujasite was maximum (99.9%) at 573 K¹⁵⁶. Ethylene was then subjected to a catalytic oligomerization procedure in which either homogeneous or heterogeneous catalysts were used. When the reaction conditions were optimized, the selectivity for linear -olefins was 96%. For ethylene oligomerization, Shimura et al. created a heterogeneous catalyst composed of $\text{NiO}/\text{SiO}_2\text{-Al}_2\text{O}_3$, which is extremely active, selective, and stable¹⁵⁷. After hydrotreatment and isomerization, these oligomers can transform into branched alkanes, from which distillation can yield jet fuel. One or more olefins, such as 1-butene, cis-2-butene, trans-2-butene, and isobutene, can be produced when isobutanol is dehydrated^{158–160}. The common catalyst for dehydrating isobutanol involves the use of $\gamma\text{-Al}_2\text{O}_3$ with its moderate acidity. However, catalysts such as inorganic acids, metal oxides, zeolites, and acidic resins have also been identified. Kim and colleagues investigated the dehydration of 1-octanol using the Al_2O_3 catalyst¹⁶¹. It was

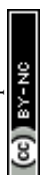


discovered that crystal phase changes also affected the strong Lewis acid sites and catalytic activity of Al_2O_3 thus increasing the conversion 1-octanol and octene yield ¹⁶¹. Dehydration is followed by the oligomerization of isobutene to produce jet-range alkenes. Phosphoric acid impregnated on solid supports was a pioneering industrial catalyst for the oligomerization of light olefins, and more catalysts have been studied in recent years, including sulfonic acid resins, acid solids like sulfated zirconia and sulfated titania, nickel-doped zeolites and nickel supported on sulfated zirconia ^{157,162–164}. Since they have both Lewis and Brønsted acid sites, zeolites are among the most appealing stable acid catalysts; however, they are easily deactivated during oligomerization. The catalysts for isobutene oligomerization were mesostructured aluminosilicates, according to Fang et al. ¹⁶⁵. The catalyst was durable and possessed strong acidic sites with high strength. The data show that Ni ions and acidity dominate the product distribution at 523 and 723 K, respectively, where micropore acidity benefits reactions at 723 K, whereas mesopores have an advantage at 523 K ¹⁶⁵.

Butanol can also be converted into jet fuel by using the same process as isobutanol and a similar catalyst. Zeolite, zirconium, solid acid catalysts, HPW ($\text{H}_3\text{PW}_{12}\text{O}_{40}$), and mesoporous silica groups are commonly used catalysts for the dehydration of butanol. To synthesize butenes via butanol dehydration, Buniazet et al. used a mesoporous material made from ferrierite as the catalyst ¹⁶⁶. The catalyst was discovered to have excellent catalytic activity, selectivity, and stability, with selectivity for linear butenes higher than 80% ¹⁶⁶. Next, hydrogenation and distillation are used to transform the by-products into jet fuel.

D. Synthesized iso-paraffins from hydroprocessed fermented sugars (SIP)

The SIP method utilizes fermentation to transform carbohydrates into fuels resembling alkanes. This approach differs from the alcohol to jet process, which requires an alcohol intermediate. It is based on the advancement of genetic engineering and screening techniques,



which allow for the modification of the way bacteria metabolize sugar ¹⁶⁷. Fermentation products vary widely, but they are largely influenced by the type of substrate used, the fermentation method applied, and the microorganisms involved ^{168–170}. Through sugar fermentation, the mevalonate pathway in yeast cells can be used by Amyris' biochemical technology to produce farnesene. Farnesene is a hydrocarbon molecule that can take the role of petrochemicals in a range of products, including diesel and jet fuel ¹⁷¹. SIP conversion has been described in detail by Davis et al., who studied that SIP included six main steps: pretreatment and conditioning, enzymatic hydrolysis, hydrolysate clarity, biological conversion, product purification, and hydroprocessing ¹⁷². The commercialization of the biological conversion of sugar to aviation fuel is being carried out by LS9 company ¹⁷³. LS9 has focused on creating a method to directly produce alkanes through a single-step fermentation process, except for the fatty acids that are generated aerobically via the fatty acid biosynthesis pathway. This method produces diesel without the need for hydrogen, hazardous inorganic catalysts, high pressures, higher temperatures, or complicated unit operations ^{174,175}. Further research is needed on the other intermediates produced during sugar fermentation. Owing to the low temperature of fermentation and the SIP's limited (10%) fuel blend, both these factors result in a low energy input. It is also noted as being more appropriate for manufacturing valuable compounds.

E. Catalytic Hydrothermolysis Jet (CHJ-SPK)

The Catalytic Hydrothermolysis Jet (CHJ-SPK) pathway received ASTM certification in 2020 for blending limits up to 50% ¹²⁹. It is based on hydrothermal liquefaction (HTL) technology for the conversion of lipid feedstocks such as fatty acid esters and free fatty acids. However, the processing steps for HTL and bio-crude upgrading are still in the pilot stage of development.



1.2 Generations of Feedstocks for Green Fuel Production: From First to Advanced Biofuels

[View Article Online](#)

DOI: 10.1039/D5YA00078E

More than 350 oil-bearing crops are found worldwide and have the potential to be used as sources for biodiesel production. This is considered to be one of the most important variables in the manufacture of green fuels. The choice of feedstock is a critical factor that significantly impacts the overall complexity of the production process, the severity of the operating conditions, and the overall profitability of renewable fuel production. Phan & Phan emphasized the importance of selecting bio-energy feedstock with precision, as the cost of these raw materials can represent up to 75% of the total expenses associated with bio-fuel production¹⁷⁶. The feedstock should ideally meet two primary criteria: cost-effectiveness in terms of production and scalability in terms of production volume. The accessibility of raw materials for the production of biofuels is contingent upon the climatic conditions, geographical positioning, local soil quality, and agricultural methods employed in a given country. Numerous fuel crops and land biomass have been researched and considered as potential sources of feedstock for the development of sustainable fuels. Three generations of feedstocks act as sources for achieving sustainable green fuel development and decreasing the oil dependency of the transport industry. They are known as first-, second-, and third-generation feedstocks.

The composition of vegetable oil is a crucial criterion for determining its appropriateness as a feedstock. The oil composition determines the quality of the resulting green fuel. Diverse varieties of consumable vegetable oils, along with inedible oils containing distinct fatty acid contents, are employed in the manufacturing of green fuels. The primary fatty acids found in both edible and inedible oils are oleic, linoleic, stearic, and palmitic acids. The oils contain fatty acids that can be classified into two categories: saturated and unsaturated fatty acids. The first group consisted of stearic, palmitic, and dihydroxystearic acids, whereas the



second group consisted of oleic, linoleic, ricinoleic, palmitoleic, linolenic, and eicosenoic acids. The government stopped producing first-generation biodiesel in 2007 in response to a debate over its possible negative social effects, including food safety and environmental contamination¹⁷⁷. Recent years have seen significant potential for the sustainable development and emission reduction of third-generation biodiesel, which is mostly sourced from microalgae. Nevertheless, increasing the output of third-generation biodiesel to satisfy the urgent energy requirements of nations such as China remains a challenge^{178,179}.

1.2.1 First generation feedstocks

First-generation feedstocks that consist of edible oil crops, such as rapeseed, soybean, sunflower, palm, and coconut oil, can potentially be converted into green fuel via thermochemical processes. **Table 2** shows the fatty acid composition of the edible oil feedstock containing high unsaturated fatty acids, which is expected to generate long carbon chain mainly C₈-C₂₀ fractions via selective deoxygenation reaction, as one carbon will be removed from the parent fatty acid chain of the feedstock. For instance, rapeseed oil and sunflower oil have been widely used as the main sources of green fuel production in Europe. This can be confirmed by Rogelio et al., who produced renewable diesel-based hydrocarbons on three bifunctional catalysts (Pt/H-Y, Pt/H-ZSM-5, and sulfided NiMo/ γ -Al₂O₃) using rapeseed oil at certain parameters. The results revealed that NiMo/ γ -Al₂O₃ gave the highest yield of green fuel, successfully converting rapeseed into green fuel¹⁸⁰. Yuitsu et al., successfully produced green fuel under conditions of 300 °C/1 MPa (H₂ pressure) with Pd/C for 120 min in a yield of 92 mol% on rapeseed oil¹⁸¹. Soybean oil has also been a major source of green fuel using different catalysts, such as Pt/SAPO-11 and NbO₄P^{182,183}. Coconut oil is commonly used in Asian countries, particularly the Philippines, whereas palm oil is predominantly used in Malaysia and Indonesia¹⁸⁴. Malaysia is ranked as the second-largest exporter of palm oil, following



Indonesia. Malaysia generated approximately 17.7 million tonnes of palm oil across 4.5 million hectares of land^{185–187}. Edible oils play a dual role, acting as essential raw materials for motor fuels while also supplying crucial nutrients that should not be disregarded. As an illustration, soybeans have a high protein content (35–40%) that contains all the necessary amino acids needed for the development and growth of individuals, supporting excellent health at every stage¹⁸⁸. Furthermore, soybean oil contains a significant amount of linoleic acid, which is a type of omega-6 fatty acid required for the diet of all mammals. This fatty acid is present in soybean oil at a concentration of 51%, as well as in rapeseed oil at a concentration of 22.3%, and plays a crucial role in reducing the risk of cardiovascular illness¹⁸⁹. However, palm oil's substantial quantity of saturated nutrients can function as antioxidants, which aid in lowering the likelihood of specific tumor forms. Although it has been demonstrated that different types of edible oils can be used as raw materials for green fuel production, there is ongoing controversy surrounding the use of food resources for automotive fuels. This practice has the potential to disrupt the global food supply and demand market, jeopardize food security, and contribute to rising prices of staple foods in impoverished and developing nations. Likewise, it gives rise to significant environmental concerns, such as the pollution of soil and water, the obliteration of ecosystems, the dissemination of agricultural illnesses and pests, and long-term sustainability challenges related to low energy and cultivation yields for crops such as corn, sugarcane, and soybeans^{190–194}. Thus, the ability of fuel crops to replace fossil fuels and achieve sustainable production is being questioned. Thus, scientists have begun to focus on relatively non-food-based feedstocks that are inexpensive and economically viable. One potential approach to decrease the use of vegetable oils for diesel generation is to utilize non-edible oils.

View Article Online
DOI: 10.1039/D5TA00078E



Table 2: Types and fatty acid composition of potential edible oil feedstock.

View Article Online
DOI: 10.1039/D5YA00078E

Feedstock	Palm	Soybean	Sunflower	Corn	Coconut
Primary sources	Malaysia & Indonesia	U.S.A	Europe	U.S.A	Philippine
Availability (mill metric tonnes)	65.5	53.7	16.6	60	61.4
Price (USD)* (Nov 2017) (per metric ton)	688	772	1,000	300	1523
Oil in seed or kernel (%)	30-60	15-20	25-37	48	65-72
Saturated fatty acid	48	14	11	16	90
Unsaturated fatty acid	50	81	89	84	9
Acid value (mgKOHg ₋₁)	0.5	0.6	<1.1	0.223	<3

1.2.2 Second generation feedstocks

The global interest in non-edible oil resources is driven by their abundance, especially in barren areas that are not suited for growing food crops ^{195,196}. They provide numerous benefits, such as the eradication of food competition, a decrease in deforestation rates, improved efficiency, enhanced environmental sustainability, the generation of profitable secondary products, and substantial cost-effectiveness compared to edible oils. Considerable consideration has been given to the long-term effects of global food or fuel issues on the use of edible oil as a green fuel source ¹⁹⁷. Due to their high oil content, availability, and capacity to survive in deserted territories and harsh climates, non-edible plant oils have drawn considerable attention as a new generation feedstock. Additionally, geographical weather has a significant impact on growth ¹⁹⁸. Therefore, they may be cultivated with less extensive care, thus lowering the cost of production. A number of non-edible plant species, including trees, also have extended life spans, some of which can reach 100 years, which is encouraging for the sustainability of the food supply. Examples of well-known non-edible crops, such as palm kernel oil, *Jatropha curcas* oil (JCO), ceiba oil, and *sterculia* oil, have been widely used in the manufacturing of liquid green fuels, particularly in the production of biodiesel. It was discovered that non-edible plant seed or kernel raw materials have a higher oil content than raw materials from food plant sources. **Table 3** shows the free fatty acid values of non-edible



oils, in which ceiba oil had the highest oil content (25-28%), followed by tung oil and cotton seed oil (16-20%). The majority of the oils were classified as non-edible because they contained significant quantities of free fatty acids (FFAs), which include a higher proportion of unsaturated fatty acids compared to saturated carbon, as indicated by the breakdown of fatty acids in inedible oil. This suggests that deoxygenating such feedstocks could produce a product primarily composed of unsaturated hydrocarbon fractions.

Table 3: Types of inedible oils along with free fatty acid (FFA) contents.

Oil properties	Sterculia	Palm kernel oil	Ceiba
Acid value (mg KOH/g)	11.9	3.4	11.9
FFA value (%)	5.9	1.7	5.9
Fatty acid composition of oil (%)			
Caprylic acid (C8:0)	-	6.5	-
Decanoic acid (C10:0)	-	10.9	-
Lauric (C12:0)	0.1	7.5	0.1
Myristic (C14:0)	0.1	32.6	0.1
Palmitic (C16:0)	19.2	19.8	19.2
Palmitoleic (C16:1)	0.3	-	0.3
Stearic (C18:0)	2.6	7.9	2.6
Oleic (C18:1)	17.4	10.2	17.4
Linoleic (C18:2)	39.6	-	39.6
Linolenic (C18:3)	1.5	7.9	1.5
Arachinic (C20:0)	0.56	0.3	0.56
Malvaloyl (C18:CE)	18.5	-	18.5
Others	0.34	-	0.34

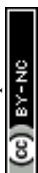
Jatropha curcas L. is a non-edible crop belonging to the Euphorbiaceae family, with a small tree or large shrub up to 5-7m tall. *Jatropha curcas* is indigenous to tropical America, but it is currently widely distributed in numerous tropical and subtropical areas across Africa and Asia¹⁹⁹. This crop exhibits resilience in challenging climates and soil conditions, such as non-arable and desert soils with little requirement for energy and water resources; it is easily established and demonstrates rapid growth and longevity, producing seeds for a span of 50 years. This *jatropha* plant also contains various parts with medicinal value and is often used for erosion control²⁰⁰. *Jatropha* the wonder plant produces seeds with an oil content of 20-60%



while 40-60% in kernels, reported to be 1590 kg/ha. *Jatropha* oil is rich in fatty acids and comprises chains ranging from C₁₆ to C₁₈. These carbon chains have a structure similar to that of diesel fuel, making them a highly promising potential source of oil. Additionally, *Jatropha* plants have additional benefits such as their ability to sustain extreme weather, substantial fat content, affordable price of kernels, quick span of development, and swift development.

The perennial herb *Sterculia foetida* L. is a member of the Sterculiaceae family and is referred to as a waterproof oil. This plant is indigenous and is highly suited to tropical and subtropical regions. The typical lifespan of this plant exceeds 100 years. This plant is a tall, upright deciduous tree that can reach a height of 40 m and girth of 3 m. Its branches are organized in whorls and spread horizontally. This oil seed has numerous applications, serving not only as a culinary ingredient, but also as an illuminant in the pharmaceutical, soap-making, and surface-coating industries. The desiccated seeds contained 51.8% fat, 12.1% carbohydrate, 21.6% protein, 5% sugar, 5.5% cellulose, and 3.9% ash. The husks provide an oil with a light-yellow fatty content that is light yellow that constitutes 50-60% of their composition. The identified fatty acids are oleic acid (20.5%), linoleic acid (12.9%), palmitic acid (11.9%), sterculic acid (6.8%), and margaric acid (2.3%).

Ceiba pentandra L., commonly referred to as kekabu or kapok, is a member of the Malvaceae family. It originated in Southeast Asia and grew in Southeast Asia, India, Sri Lanka, and tropical America. The tree was cultivated in a naturally occurring humid and sub-humid tropical environment, and it is typically resistant to drought. The trees bear leathery, ellipsoid, and hanging capsules, which contain seeds with an oil content of 25-28% (w/w) of each fruit, while the trees yielded 1280 kg/ha of oil. This plant has a low nutritional value because it contains a large amount of fiber. Tye's study revealed that its fibre comprises 34-64% cellulose and has significant promise for the production of cellulosic ethanol ²⁰¹. These fibers are commonly utilized as filling materials, such as beds and pillows ²⁰². This plant contains a



distinctive pair of cyclopropane fatty acids (malvalic acid) that exhibit higher reactivity than the polyunsaturated carbon bond when exposed to ambient oxygen. Therefore, this hydrocarbon chain decreased the ability of *C. pentandra* oil to resist oxidation. According to Bindhu et al., cyclopropane fatty acids (specifically malvalic acids) result in higher viscosity and faster oxidation than palmitic acid ²⁰³.

Malaysia is a major global supplier of palm oil, accounting for 28% of global production and 33% of global exports ²⁰⁴. Although palm oil has long been used to produce biodiesel, Malaysia has begun to focus on developing jet fuel based on palm oil due to the current crisis and increasing demand ²⁰⁵. However, the growth of palm oil has resulted in additional environmental problems. The renewable feedstock used to make jet fuel should not have a large carbon chain impact due to indirect land-use change (ILUC) ⁹³. However, oil palm has a significant advantage over other feedstocks because it is more economically viable to produce and yield a higher amount of oil than other feedstocks ^{206,207}. In addition, it can provide a more stable source of income and has an economic life of over 20 years ²⁰⁸. As the palm oil sector develops, it will contribute to reducing poverty and promoting economic progress in emerging nations ²⁰⁹. Because palm oil is widely available in Malaysia, its use as a renewable resource to produce bio-jet fuel is both possible and highly profitable.

For cooking purposes, palm oil is obtained from the fleshy portion of the fruit through a straightforward streaming and pressing process, whereas palm kernel oil (PKO) is obtained from the fruit kernel. Palm oil is a tropical perennial plant that grows in low-lying and humid areas such as Malaysia, Indonesia, and Thailand. The palm oil has been reported to reach a maximum height of 20-30 meters and the tree has a single stem and is unbranched ²¹⁰. Moreover, the fruit can be obtained from the farmed oil palm for 40–50 years starting in the fourth year of growth producing up to 2000 fruitlets with the juicy orange-reddish-colored fruits ²¹⁰. In addition, palm oil is a high oil yield crop that produces approximately 10 times



more oil than soybeans, with an average annual production of 4-5 tonnes of oil/ha/year ²¹¹. At room temperature, crude palm oil present in a semi-solid state and is composed of lauric acid (48%) and myristic acid (6%), which have good oxidative stability and acute melting points and are abundant in palm kernel oil ²¹². Palm oil, with its economical price and maximum output per acre among all vegetable oil feedstocks, is a sustainable resource that holds promise for green fuel production ^{213,214}. Typically, two types of natural oils are derived from fruit: palm oil and palm kernel oil. These oils have distinct chemical and physical properties. Furthermore, crude palm kernel oil (CPKO), which is obtained through extraction, can be further refined into refined palm kernel oil (PKO) via mechanical pressing or the use of solvents such as hexanes. Refined palm kernel oil is commonly utilized in non-edible products such as cosmetics, personal care items, and soaps due to its chemical composition, physical properties, and similarities to coconut oil ²¹⁵. PKO exhibits a significant proportion of lauric acid (C12:0) at approximately 50%, which distinguishes it from palm oil, which is generally composed of palmitic acid (C16:0) and oleic acid (C18:1) at approximately 40% each. Despite the greater cost of CPKO compared to palm oil, this disparity has been diminishing owing to the implementation of policies that promote the expansion of farmed areas for palm in green fuel programs. Consequently, a sustainable supply of CPKO is readily generated ^{216,217}. Hence, these data are intriguing and compelling for investigating PKO as a sustainable raw material for BHK production in comparison to palm oil because its fatty acid chain has a carbon atom count within the range often found in kerosene.

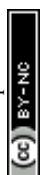
1.3 Types of reaction and processes

1.3.1 Hydrodeoxygenation/ Hydrocracking (HDO)

As stated earlier, it is not recommended to directly use renewable sources for fuel, owing to engine compatibility issues with renewable green fuel. As a result, various



enhancement techniques, including hydrodeoxygenation, have been devised to generate green energy compatible with modern infrastructures. Hydrodeoxygenation involves the conversion of unsaturated fats in vegetable-based oils to saturated fats. The process involves the removal of oxygenated molecules from triglycerides using heterogeneous catalysts at a precise temperature and high pressure while using H₂ gas to cleave the C-O bonds ^{147,218}. Generally, the reaction begins with the conversion of the carboxyl group into a carbonyl functional group. The reduction process involves the hydrogenolysis of the carbonyl bond, resulting in the formation of an aldehyde molecule. This process occurs through the adherence of oxygen molecules to the active sites, which is followed by the dissociation of hydrogen from these sites. The oxygen atom is then eliminated from the active site in the form of water, while the aldehyde undergoes reduction to form a primary alcohol and reacts with hydrogen to yield an alkane and water ²¹⁹. The main approach for achieving ultimate elimination involves dehydration, which results in the formation of alkenes. Conversely, alkanes are generated through hydrogenation. The rate-limiting process involves the transformation of the carboxyl group into a carbonyl group. The reaction progresses via the following sequence: first, reduction to an aldehyde, then reduction to an alkane, and finally reduction to an alcohol. The two stages of HDO are in opposition, and when the catalyst comes into contact with highly adsorbed acids, it can hinder the adsorption of alcohols and result in a shift in the selectivity towards deoxygenation ²²⁰. The technique relies heavily on H₂, and hence requires a continuous flow of H₂ to achieve the desired result. The primary objectives of HDO are to reduce the O/C ratio and concurrently increase the H/C ratio ²²¹. The catalytic support also plays a pivotal role in determining catalyst selectivity. Supports exhibiting greater acidity demonstrated improved effectiveness in the dehydration of alcohol functional groups.



The outcome was that the n-alkane generated the same number of carbon atoms as the starting fatty acids in triglycerides, making n-alkane green fuels more desirable as sustainable fuels with superior qualities than traditional diesel-based fuels (such as a high cetane number)^{26,222,223}. In addition, two potential side reactions may occur during the HDO process: the water gas shift reaction and methanation reaction. These processes result in an increase in hydrogen intake²²⁴. The primary volatile by-products resulting from the HDO of TG-based oils are CO₂, CO, H₂, and C₃H₈^{225,226}. Unfortunately, the disadvantage of the hydrodeoxygenation process is its high cost, which is mostly caused by the significant amount of hydrogen utilized in the process²²⁷. Consequently, extensive studies have been conducted to develop a new cracking method for the generation of certain diesel fractions in an atmosphere with free hydrogen, known as deoxygenation.

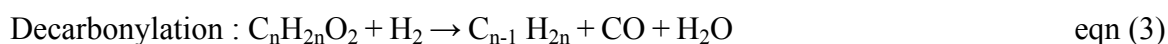
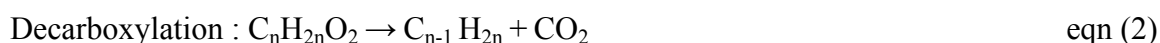
1.3.2 Deoxygenation process (DO)

Deoxygenation consists of two processes occurring simultaneously (decarboxylation and decarbonylation), in which oxygenated molecules are removed from triglycerides to produce by-products (CO, CO₂, and H₂O), which can then be used to create hydrocarbons resembling fuel in the absence of H₂ gas. Decarboxylation is the process of removing a carboxyl group, where oxygen (O₂) is expelled as carbon dioxide (CO₂) from the carbon chain of TGs²²⁸. Meanwhile, the decarbonylation reaction has two primary reaction pathways: β -elimination and γ -hydrogen transfer²²⁸. β -Elimination is a chemical process that results in the production of carboxylic acids and unsaturated glycol difatty esters (UGDE) from triglycerides (TGs). Subsequently, the hydrogenation of UGDE results in the release of fatty acids and the formation of a lesser quantity of straight paraffin chains²²⁹. However, the γ -hydrogen transfer process initiates the unravelling of the C-C bond within the acyl group, leading to the emergence of a terminal olefin that is less than two carbons than the fatty acids. This process predominantly



yields alkanes as the main product and releases CO₂ as a by-product²²⁸. The primary outcome of the decarboxylation reaction is alkanes, with carbon dioxide being produced as a secondary by-product.

Conversely, decarbonylation reaction involves the elimination of a carbonyl group to generate a paraffin molecule that has a single less carbon than the TGs and generates carbon monoxide as a by-product²²⁹. During decarbonylation, fatty acid intermediary states release formic acid as the primary output instead of CO₂²²⁹. Subsequently, the process of formic acid decomposition might occur through two concurrent pathways: dehydration and hydrogenation. Carbon monoxide (CO) and water (H₂O) were released during dehydration. In contrast, dehydrogenation produces carbon dioxide (CO₂) and hydrogen gas (H₂), which are utilized to generate alkenes or olefins¹⁸. The equations are depicted as below:



Remarkably, this reaction has several advantages over hydrodeoxygenation, despite the fact that both processes successfully produce green fuel and jet fuel. First, deoxygenation uses inexpensive catalysts and requires little to no H₂, making it more economically desirable. In contrast, hydrodeoxygenation employs H₂ gas to saturate unsaturated hydrocarbons and removes O₂ as H₂O to generate renewable fuel^{230,231}. For this reason, hydrodeoxygenation uses H₂ more than deoxygenation; thus, production costs and operating expenses for hydrodeoxygenation are higher than those for deoxygenation. Moreover, the use of H₂ in the reaction also leads to environmental issues, making HDO environmentally unfriendly. Finally, the decarboxylation pathway improves the catalytic stability, as no water is produced during the reaction. Acid-heterogeneous catalysts are essential for the production of green fuels. For



oxygen removal from fatty acids by C-O cleavage via a deoxygenation process, highly acidic catalysts are employed to dramatically boost the product yield and selectivity.

1.4 Catalysts development for deoxygenation reaction

1.4.1 Catalysts overview

Catalysts are crucial for expediting certain chemical processes, hence enhancing performance and maximizing output standards and productivity²³². A catalyst is a material that accelerates the progress of a chemical reaction toward equilibrium without significantly consuming itself. However, the equilibrium of the process is unaffected by the catalyst. In 1835, Berzelius first used the term "catalyst" to describe a concept that might explain a variety of occurrences that appeared to be unrelated to one another²³³. For instance, it has been demonstrated that the production of alcohol from plant materials is achievable when ferments are added in small quantities. When one or more reactants and catalysts form a chemical bond, new routes for the conversion of these reactants into products are created, allowing the catalyst to be renewed. Additionally, only chemical reactions that are thermodynamically viable can benefit from catalytic activity. A catalyst performs its function in both forward and reverse reactions when the reaction is reversible²³⁴. The catalyst should be able to continuously cycle between the reactant and reactant catalyst without depletion. Various alkali-, acid-, and enzyme-based catalysts have been used to produce green fuel^{235–239}.

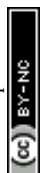
In reality, the catalysts must be regenerated and changed. Manufacturing catalysts is a significant industry; billions of dollars' worth of catalysts are sold each year globally. The catalysts can be solids, liquids, or gases. Most modern catalysts consist of fluid or solid surfaces. Homogeneous catalysis refers to catalytic reactions that occur in a single gas or liquid phase, characterized by the homogeneity of the phase in which they occur. Heterogeneous catalysis refers to the process of catalysis occurring in mixtures consisting of several phases,



such as a gas-solid mixture. The catalytic activity of a catalyst is a measure of the speed at which the catalytic process occurs. It can be expressed as the rate of the catalytic reaction, a rate constant, or as the conversion or temperature necessary for a certain reaction under predetermined conditions. The ability of the catalyst to focus a reaction on specific products was measured by selectivity. Selectivity cannot be defined by a single definition, but is sometimes referred to as the ratio of activities. It is the ratio of the rate of the desired reaction to the total rate of all reactions that use the reactants. The distribution of products is another way to describe selectivity. In addition to being assessed for activity and selectivity, the stability of the catalysts was also assessed. The rate at which the activity or selectivity is lost in a catalyst is gauged by its stability. Essentially, stability can be measured by the rate at which deactivation occurs, such as the pace at which the desired catalytic reaction changes or the rate at which the temperature of the catalyst must be adjusted to compensate for the loss of activity. Catalysts that have become inactive are often subjected to treatment to revive or restart their functionality. The regenerability of a catalyst refers to the extent to which it can be successfully restored; however, its definition is ambiguous.

1.4.2 Homogeneous vs Heterogeneous catalysts

Industrial catalysts frequently exhibit intricate compositions and structures. The catalyst is composed of catalytically active phases, supports, binders, and promoters. The most frequently used metals, metal oxides, and metal sulphides are catalytically active substances in solid or liquid form. On rare occasions, they are employed in purest forms. There are some crucial aspects that need to be considered when choosing suitable catalysts for deoxygenation, such as acidity, basicity, surface area, pore size, pore volume, and crystallite size. Traditionally, homogeneous acid or alkali catalysts have been employed to create green fuels, especially in biodiesel production. Homogeneous catalysts are catalysts that are in the same phase as

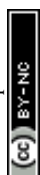


reactants, principally by a soluble catalyst in solution (liquid-liquid form), where either acid or alkaline depends on the properties of the substances used, such as HCl, H₂SO₄, NaOH, KOH, etc. These types of catalyst are more favored due to affordable and yielding more product even in short time reaction ^{240,241}. This was confirmed by the study of Abhishek using H₂SO₄ as a catalyst for the conversion of *S. obliquus* lipids to FAME, which yielded 96.68% under low temperature ²⁴². This was also aligned with the investigation of Ogunkunle using KOH to transesterified milk bush seed oil, which showed nearly complete methanolysis with a FAME value of 94.33% under optimal conditions ²⁴³. However, some problems occur when utilizing homogenous catalysts, including difficult separation, instrument corrosion, requirement for extensive cleaning, contamination, and expensive materials ^{244,245}. As a result, research is primarily focused on finding suitable catalysts that are easy to separate, have high conversion efficiency, and cause less corrosion to the reaction vessel in addition to the fact that chemical reactions can take place on the surface of these catalysts such as heterogeneous catalysts. Heterogeneous catalysts are catalysts that are in distinct phases from reactants, such as solid-liquid form or solid-gas forms. Heterogeneous catalysts have also been divided into basic and acidic types, yet this hetero-catalyst is in solid or powder form that can be repeatedly recycled and easy to discretize. Therefore, it might serve as a catalyst for promoting eco-friendliness by minimizing hazards, reducing catalyst usage, preventing losses, and enhancing the efficiency and sustainability of the catalysts ²⁴⁶. This could be verified by comparison with Abhishek, which showed no cycle of reusability for H₂SO₄, while three reusability cycles were performed for the tungsten zirconia catalyst and achieved a FAME conversion of 94.58% ²⁴². This was also corroborated by another study by Nurul Saadiah, which revealed that the reaction over the CaO/SiO₂ catalyst reached 87.5% at 2 h along with the seventh reuse cycle, with a slightly remarkable reduction in yield ²⁴⁷.



Heterogeneous catalysts encompass both monometallic and bimetallic systems, which are typically dispersed on various supports to enhance their activity and stability. These catalysts can be broadly classified based on their active components into noble metals, nitrides, sulfides, phosphides, carbides, and non-noble metal catalysts. Monometallic catalysts, defined by the presence of a single active metal or metal promoter supported on a support, are widely recognized for their straightforward synthesis, facile characterization, and cost-effectiveness. These catalysts offer well-defined active sites and have demonstrated considerable efficacy across a range of catalytic processes, including hydrogenation and methanation, particularly when employing transition metals such as Ni, Pd, or Pt. For example, Huang et al. reported the selective deoxygenation of lauric acid over a Pt/TiO₂ monometallic catalyst at 30 °C under 1 bar H₂ with LED irradiation (365 nm, 18 W), achieving an impressive 93% selectivity toward n-C₁₁ hydrocarbons, underscoring the catalyst's efficiency under mild reaction conditions²⁴⁸. Despite these promising outcomes, monometallic catalysts frequently encounter intrinsic limitations, including restricted catalytic activity, selectivity, and stability when exposed to harsh operational environments. For instance, Ni-based monometallic catalysts are prone to sintering and carbon deposition during deoxygenation, leading to catalyst deactivation, secondary reaction and diminished performance²⁴⁹. Moreover, although precious metal catalysts such as Pt exhibit high intrinsic activity, their high cost and scarcity pose significant barriers to large-scale industrial deployment. These challenges underscore the imperative for continued research aimed at enhancing the durability, efficiency, and economic viability of monometallic catalysts, particularly for applications demanding robust and sustainable catalytic systems. **Table 4** highlights the prior studies on homogeneous and heterogeneous catalysts.

In contrast, bimetallic catalysts leverage the synergistic interactions between two different metals, which can significantly enhance catalytic performance by improving activity,



selectivity, and resistance to deactivation. The addition of a secondary metal can modify the electronic and geometric properties of the primary metal, stabilize active sites, and promote better dispersion, leading to superior catalytic behaviour. For instance, Tan et al. studied on the catalytic deoxygenation of stearic acid into biofuels using FeNi/AC catalyst. The results demonstrated the best catalytic performance with stearic acid conversion of 99% and linear C₁₇ selectivity of 94%²⁵⁰. This shows that bimetallic catalysts have been shown to have high conversion along with increase the efficiency performance of catalysts owing to the synergistic interaction between the two active metals and the existence of equal base-acid properties in the catalysts. Despite these advantages, bimetallic catalysts present challenges related to their synthesis and structural control, such as preventing phase segregation, dealloying, and ensuring uniform metal distribution. Moreover, the complexity of these systems complicates mechanistic understanding and scale-up for industrial use. However, these obstacles are gradually being overcome by new developments in synthesis techniques, such as controlled co-impregnation, atomic layer deposition, and additive manufacturing, as well as computational modelling methodologies, such as density functional theory (DFT) and machine learning. These developments make it possible to rationally build bimetallic catalysts with precisely regulated composition and structure, offering specialized activity, selectivity, and durability for a range of uses in chemical synthesis, energy, and environmental remediation. Although monometallic catalysts are still useful in applications where simplicity and economy are important considerations, bimetallic systems are becoming more and more popular in catalysis because of their better tunability and capacity to overcome the inherent drawbacks of single-metal catalysts.



Table 4: Literature studies on homogenous and heterogeneous catalysts.View Article Online
DOI: 10.1039/D5YA00078E

Catalyst	Feedstock	Conditions	Product distribution (%)	Ref.
H ₂ SO ₄	S. obliquus	60°C, 4h, 30:1, 10wt.%	96.68	242
KOH	Milk bush seed oil	65°C, 2h, 9:1, 3wt.%	94.33	243
CaO/SiO ₂	Palm oil	60 °C, 2h, 3 wt.%, 15:1	87.5	247
Ni/AC	WCO	N ₂ - 60ml/min, 500 °C, 15 mins	24–85	249
FeNi/AC-500	Stearic acid	N ₂ - 360 °C, 1 h	Conversion - 88 C ₁₇ - 97 %	249
Ni-Fe/ZSM-5/SAPO-11	Palm oil and triolein	H ₂ -60 bar, 300 °C, 2h	Palm oil-62 Triolein- 64	142

1.4.3 Noble metal catalysts

Noble metal catalysts such as Pd, Pt, Rh, and Ru have been widely employed in the DO reaction. The data indicate that these noble metal catalysts are promising with high catalytic activity and selectivity during the DO reaction, as they contain unfilled d-electron orbitals, making it easy to adsorb reaction species at lower temperatures. Among these metals, Pd with high dispersion properties had been recognized as this catalyst selectively produce more products towards paraffins chains formation due to its high dispersion properties. **Table 5** presents an overview of recent research focused on the deoxygenation of natural oils and analogous model compounds into diesel-range hydrocarbons, highlighting the predominant role of noble metal catalysts in advancing this field over recent years. This was studied by Why et al. to investigate effect of Pd metal on three different support which is carbon, vanadium oxide and zeolite support on generation of bio-jet fuel from WCO. The results exhibited Pd/C has highest yield □99% with 73% of jet fuel selectivity ²⁵¹. The fuel properties were also studied, indicating that the produced liquid product achieved the ASTM standard by having better low-temperature fluidity at 15 °C and combustion effect, which is due to the high paraffinic hydrocarbon selectivity with low aromatic content. Further examination of the variation ratio of blended Jet A-1 has also been investigated ²⁵². Notably, the bio-jet fuel



catalyzed by the Pd/C catalyst with P20%J80% showed the best ratio. This was because of the chemical composition, which contained □73% bio-jet fuel (~73%), □ 24% iso-paraffins, and a small molecular weight of non-paraffinic compounds compared to other ratios, making the properties similar to those of the existing jet fuel. Srihanun et al. also corroborated that monometallic Pd on an alumina support can also produce a high green fuel yield of 86%, but the addition of Fe to the catalyst increases the performance of the catalyst yielding a 96% of green fuel yield with high selectivity towards green fuel ¹⁸⁶. Apart from Pd, Pt has also been widely used as a catalyst for the production of green fuels. Zheng showed that bimetallic Pt-Ni has higher stability and activity owing to the synergistic effect of Pt-Ni along with the promotion of C=O hydrogenation and improved Ni dispersion. The results discovered that bimetallic catalyst producing 52.67% and 40.25% for hydrocarbon and aromatic respectively while lowering the coke deposition to 7.26% ²⁵³. This is also supported by Janampelli et al., who revealed the conversion of the 4Pt-8MoOx/ZrO₂ catalyst to green fuel at a lower temperature of 200 °C, making it a favorable DO catalyst ²⁵⁴. Other metals, such as Re, Ru, and Rh, have also been employed as catalysts with superior catalytic performance, making them desirable as catalysts for green fuel production ^{255–258}. However, the high cost of noble metals has prevented their widespread use in industrial applications. Moreover, earlier research has shown that adsorbed chemical intermediates, such as carbon monoxide, heavy organic compounds, and carbonaceous deposits, can poison the active metal site of palladium, making it more prone to deactivation. Thus, an another alternative way to substitute into more effective compounds has been researched.

Research on the utilization of Ru in the hydrodeoxygenation process of microalgae oil was carried out by Ali et al. ²⁵⁹. At a low reaction temperature of 140 °C, a high heptadecane yield of 93% was achieved over a mesoporous carbon-supported Ru (Ru/C) catalyst derived from starch. Furthermore, it would be desirable to design catalysts that are impervious to



contaminants to convert WCO. Xu and colleagues successfully synthesized an exceptionally active Ru-HAP catalyst by using an ion-exchange method. With this catalyst, it was possible to hydrogenate renewable oils into long-chain alkanes at relatively low temperatures (the conversion was completed at 200 °C). At least five recycling cycles demonstrated the high stability of the Ru/HAP catalyst, as well as its high tolerance to a variety of pollutants, such as salts, sugars, and amino acids. Both these attributes have been proven. Apart from its application in the hydrogenation of many oil sources, such as WCO, palm oil, and jatropha oil, this catalyst has also shown a high degree of tolerance. Metastable calcium carboxyl phosphate was produced as a result of the widely distributed Ru nanoparticles anchored on the HAP substrate and absorbed fatty acids. The significant role of this component was directly responsible for the high activity and stability of the Ru/HAP compound. A number of authors have also noted that substituting another metal or metal for Ru in catalysts may alter product selectivity. For example, Zhou et al. investigated the effect of Re incorporation into Ru/TiO₂ catalysts in the context of the selective deoxygenation of ethyl stearate and found that it produced a promotion effect. Their results showed that the addition of Re had a promoting effect. The catalyst, which consisted of 1wt.% Ru/TiO₂ in the absence of Re, produced a substrate conversion of 98%. Additionally, a strong selectivity toward n-C₁₇H₃₆ (n-C₁₈/n-C₁₇ = 0.5) was demonstrated by the catalyst. The catalyst was also able to achieve this conversion. The ratio of n-C₁₈ to n-C₁₇ may rise significantly if the amount of Re in the mixture is increased from 0.5 - 10wt.%. This suggests that there is room for the ratio to increase further. Over the course of their investigation, they learned that the addition of Re increases the number of weak acid sites and promotes Ru growth. They arrived at this conclusion during the course of their investigations.

View Article Online
DOI:10.1039/D5TA00078E



Table 5: Research on the deoxygenation of natural oils and other analogous model molecules to diesel-ranged hydrocarbons over noble metals has been the main focus of recent years.

Catalyst	Feedstock	Conditions	Product distribution (%)	Ref.
Pt/ZIF-67/ zeolite 5A bead	Palmitic acid	300 °C, 20 bar CO ₂ , 2 h, batch reactor	n-C ₁₅ = 92	260
Pt/NMC	Lauric acid	300 °C, without H ₂ , 3 h, mini-batch reactor	n-C ₁₁ = 99	261
Pt/HAP-AE	Stearic acid	260 °C, 10 bar N ₂ , 4 h, batch reactor	n-C ₁₇ = 91	262
PtSn/SnO _x	Stearic acid	320 °C, 10 bar N ₂ , 4 h, batch reactor	n-C ₁₁ = □ 94 n-C ₁₅ = □ 92	260
Pd/C	Stearic acid	260 °C, 28 bar H ₂ , 6 h, batch reactor	n-C ₁₇ = 92 n-C ₁₈ = <1.0	263
Pd/HPA-SiO ₂	Soybean oil	200 °C, 10 bar H ₂ , 24 h, batch reactor	n-C ₁₅ -C ₁₈ = □ 90	264
Pd@PPN	Stearic acid	150 °C, 20 bar H ₂ , 14 h, batch reactor	n-C ₁₇ = 84 n-C ₁₈ = 6	265
Al-modified Pd@SiO ₂	Methyl palmitate	260 °C, 30 bar, 5 h, batch reactor	n-C ₁₅ = 28 n-C ₁₆ = 71	266
Ru/C (ZnCl ₂ starch)	Microalgae oil	140 °C, 50 bar H ₂ , 6 h, batch reactor	n-C ₁₇ = 93	259
Ru-Re ₁₀ /TiO ₂	Ethyl stearate	220 °C, 30 bar H ₂ , 2 h, batch reactor	n-C ₁₇ = 22% n-C ₁₈ = 70%	267
Ru/La(OH) ₃	Jatropha oil	240 °C, 40 bar H ₂ , 8 h, batch reactor	n-C ₁₇ = 65 % n-C ₁₅ = 12 %	268
SiNA-Rh	Stearic acid	200 °C, 10 bar H ₂ , 24 h, microwave reactor	n-C ₁₇ = 94%, n-C ₁₈ = □ 1	257

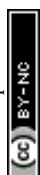
1.4.4 Non noble metal catalysts

(A) Metal carbides (CS), phosphides (P), nitrides (N), sulfided (S)- based catalysts

This has progressively deviated the research effort toward the development of cheaper and more efficient catalysts with high catalytic activity, such as non noble metals which been tabulates in **Table 6**. This involves the development of non-noble metal-based catalysts, such as carbides, sulfides, nitrides, and phosphides, on catalyst supports for the conversion of TGs and model compounds into hydrocarbons. Thikhamporn et al. reported on Ni–Mo sulphide catalysts producing highest yield of C₁₄–C₁₈ yield of 75.3 wt.% with recyclability up to 4 cycles. This might also be due to the high acidity, which leads to high activity ²⁶⁹. Moreover,



sulfured catalysts such as NiMo-PS/MgO-Al₂O₃ and NiMo-CS/AC catalyst been observed and the results showed octadecane and heptadecane as main products, in which NiMo-PS/MgO-Al₂O₃ more favoured that might related to the metal oxyphilic capacity ²⁷⁰. Furthermore, inclusion of P and CS could promotes the catalysts' structure and allowing a sulphide to prevails on the surface of both catalysts thus presenting high catalytic activity with different active sites ²⁷¹. However, some issues emerged while carried out HDO using sulfided-based catalysts such as an impairment catalytic activity in the earlier reaction time of corresponding catalyst and the necessity for more prominent process conditions such as pressure and temperature thus making it unfavorable to be used in this reaction. Carbides are non-noble-metal-supported catalysts that can be used to produce hydrocarbons. Tran et al. demonstrated the effect of bimetallic carbides on the production of diesel-range hydrocarbons using canola oil, and the results showed that Mo-W carbides/C catalysts converted more than 95% with a cracking ratio of < 3% at a low temperature of 250 °C ²⁶⁵. Another study by Fei et al. examined the efficacy of molybdenum carbide nanoparticles on a carbon nitride support (MoC/CN) catalyst. The results showed impressive performance, with a conversion rate of 94.3% and selectivity rate of 90.3% at 310 °C. This success can be attributed to the presence of more active sites, enhanced dispersion of active sites by the abundance of pyridinic and pyrrolic N onto molybdenum, and incorporation of Mo metal ²⁷². Nevertheless, the carbide catalyst surface's degradation and accumulation of carbon could result in the reduction of active sites, which could reduce the catalyst's performance. Therefore, the production of green fuels has enabled the use of nitride-based catalysts. Nitride and carbide catalysts possess numerous similar structural characteristics; however, nitride catalysts tend to be more oxidation-resistant. Wang examined the conversion of methyl palmitate (MPA) to green fuel using a Co₃Mo₃N catalyst, and the data obtained showed the highest yield (99.5%) with selectivity to hexadecane of up to 95% under mild conditions ²⁷³. This might be due to the interaction of Co-Mo nitrides with the



unique dual-site fining of the electronic and structural configuration of the $\text{Co}_3\text{Mo}_3\text{N}$ catalyst, thus leading to the desired hydrodeoxygenation route with high stability up to 72h. Another study also confirmed that nitridation of the catalyst plays a pivotal role in its properties, thus increasing the activity of the catalyst. This might be due to the excellent dispersion of active metals and promoters on the support and the formation of $\gamma\text{-Mo}_2\text{N}$ species, thus successfully hydroprocessing rapeseed oil with high efficiency ²⁷⁴. Phosphide-based catalysts have been extensively studied for the production of green fuels. Kaewtrakulchai investigated the effect of transition metal phosphide-supported porous biochar on the hydrocracking of bio-jet fuel ²⁷⁵. The results showed that Fe-P produced a high percentage of paraffin while lowering the aromatic content from 21% to 14% owing to its high acidity, surface area, and catalyst dispersion ²⁷⁵. However, increasing the number of active sites can promote the isomerization of short chains, leading to the formation of branched paraffins (iso-paraffins). In addition, the high acidity of the Fe-P catalyst leads to excessive fractions that result in a high proportion of undesirable products, such as C_4 and C_5 gaseous hydrocarbons ²⁷⁵. Ruangudomsakul also examined the hydrogenation on mixed-phase nickel phosphides catalyst. Remarkably, the Ni_xP_y catalyst produced more green fuel than commercial Ni_2P owing to the presence of mixed Ni_2P and Ni_{12}P_5 in Ni_xP_y ¹⁸⁷. It was noticed that more favored decarboxylation and decarbonylation processes produced C_{15} and C_{17} alkanes as the major products, in which the presence of dominant phase Ni_2P might have an impact. Thus, catalysts constructed from transition metal oxides (TMOs), such as Ni, Cu, and Mo, have been progressively explored for the oxygen deprivation of fatty acids to straight hydrocarbons of gasoline- and kerosene-range hydrocarbons, as well as for the green fuel-like approach.



Table 6: Literature studies on metal carbides (CS), phosphides (P), nitrides (N), sulfided (S)-based catalysts on production of green fuel.

Catalyst code	Feedstock	Conditions	Solvent	Product selectivity	Reference
NiMoS ₂	Palm oil	T:300°C, t:2 h, P:30 bar H ₂ , batch reactor	n-Decane	n-C ₁₅ = 22 n-C ₁₆ = 20 n-C ₁₇ = 30 n-C ₁₈ = 28	269
Ni ₃ S ₂	Palmitic acid	T:300 °C, P:50 bar H ₂ , batch reactor	Dodecane	n-C ₁₅ = 94 n-C ₁₆ = 6	276
Ni-MoS ₂	Palmitic acid	T:300 °C, P:50 bar H ₂ , batch reactor	Solvent-free	n-C ₁₅ = 45 n-C ₁₆ = 55	276
Sulfided ReNiMo/y-Al ₂ O ₃	Oleic acid	T:350 °C, t:1 h, P:40 bar H ₂ , batch reactor		n-C ₈ -C ₁₂ = 4 n-C ₁₃ -C ₁₈ = 77	277
Ni ₂ P/Al ₂ O ₃	Palmitic acid	T:300 °C, P:40 bar H ₂ , t:1 h, flow reactor		n-C ₁₅ = 76 n-C ₁₆ = 23	278
MoP/Al ₂ O ₃	Palmitic acid	T:300 °C, P:40 bar H ₂ , t:1 h, flow reactor		n-C ₁₅ = 3 n-C ₁₆ = 22	278
Ni ₂ P/AC	Palm oil	T:350 °C, 40 bar H ₂ , t:6 h, flow reactor	Solvent-free n-Hexane	n-(C ₁₃ -C ₂₀) = 98	279
NiC	Coffee oil	T:400 °C, P:40 bar H ₂ , t:5 h, batch reactor		n-(C ₈ -C ₁₆) = 42 n-(C ₁₃ -C ₂₀) = 23	280
MoWC/C	Canola oil	T:250 °C, P:450 psi H ₂ , t:2 h, batch reactor		n-C ₁₈ : 50 n-C ₁₇ : 34	265
Mo _{2.56} CN _{0.50}	Palmitic acid	T:300 °C, P:40 bar H ₂ , t:1.2 min, fix-bed reactor	n-Decane	n-C ₁₆ = 86	281

Ketene intermediate (3) was produced as a consequence of the activation of the fatty acid molecule on the sulfur vacancy site of Ni-MoS₂ (1 → 2). This process is illustrated in **Figure 5**. A Mo cation and a nearby basic sulfur atom, which were engaged in the C-O cleavage and α -proton abstraction processes, respectively, were utilized to produce this intermediate. The goal of the interaction between the carbonyl carbon and Mo cation was to improve the



synthesis of C_{15} hydrocarbons. This interaction resulted in the weakening of the C-C bond and an increase in the proportion of ketene species with DCO (3). Because the sulfur anions on MoS_2 are less basic and have fewer electrons than those on $Ni-MoS_2/Ni_3S_2$, there may be a change in product selectivity on MoS_2 , which could explain why ketene species production was restricted (3). This may be related to the fact that MoS_2 exhibits distinct product selectivity. However, although these compounds can be used to achieve high selectivity for desired products, the use of metal sulfides presents a number of environmental challenges. Consider sulfur as an example. Under hydrothermal conditions, sulfur can leak into the reaction fluid. The sulfur may be absorbed into the liquid fuel product or precursor as a result of this leaching. This might cause the catalyst to become inactive, which would shorten its lifespan and add to the environmental contamination.

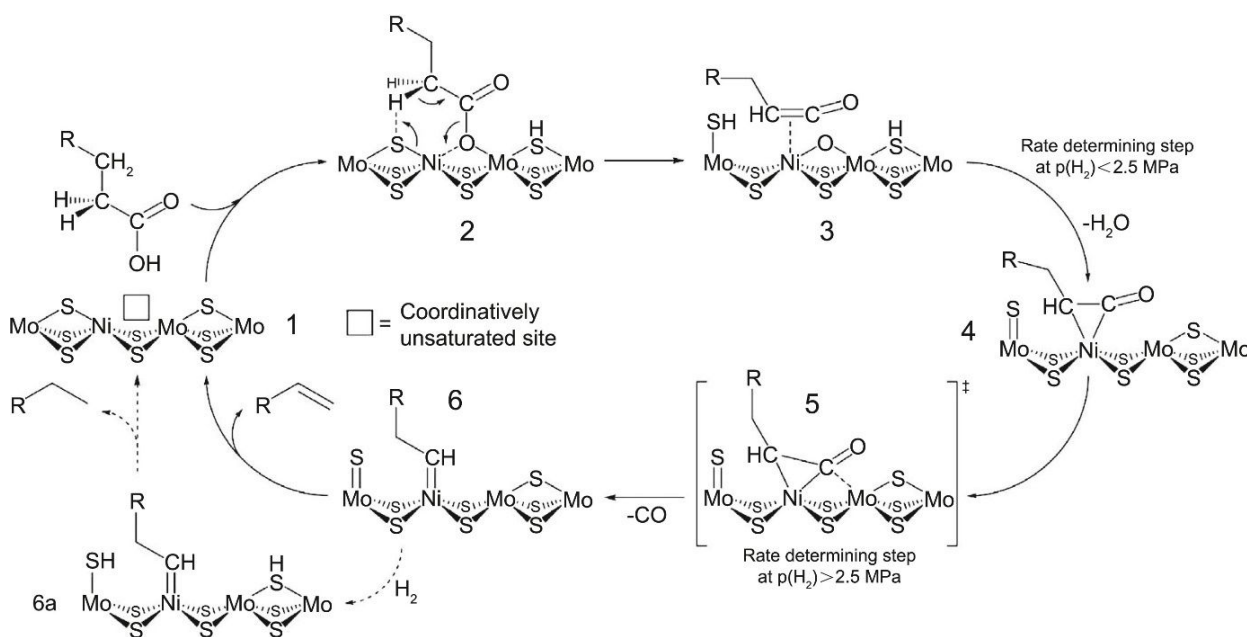


Figure 5: A hypothesized mechanism for the decarbonylation of fatty acids on $Ni-MoS_2$. Reprinted with permission from ref ²⁷⁶.



1.4.4.2 Transition metal oxides (TMO) based catalysts

View Article Online
DOI: 10.1039/D5YA00078E

(I) Ni-based catalysts

Among TMO, Ni has sparked interest due to comparable performance and endurance comparable to noble metal catalysts in the conversion of triglycerides and fatty acids to hydrocarbons molecules. Furthermore, this Ni species is easily synthesized, resulting in cost-effective production, exceptional hydrogen activation capabilities, and favorable electrical properties that can induce chemical reactions reminiscent of precious metals (e.g., Pd and Pt), including the unravelling of C–C or C–H bonds in hydrocarbon processes³⁴. This supports the findings of Zhang by using phosphotungstic acid loaded on a Ni/MCM-41 (HPW-Ni/MCM-41) catalyst, and it was shown that Ni metal catalyzed methyl palmitate through hydrodeoxygenation and dehydrogenation of methyl palmitate to produce 1-pentadecene and then produced jet fuel range hydrocarbons with an increment yield of 86% with selectivity to n-alkanes and iso-alkanes of 47% and 8%, respectively. Moreover, Lee investigated a Ni/Al-SBA-15 catalyst under N₂ atmosphere at 20 bar and 280 °C for 2 h, and the data revealed that 83% conversion to jet fuel hydrocarbon from methyl palmitate showed that Ni metal alone could successfully produce high conversion due to acidic sites due to Ni. In contrast, Tan examined under H₂ conditions for 4h at 330 °C, and the results revealed that the exposed Ni₂P/Zr-SBA-15 catalyst produced hydrocarbon yield of approximately 61-74%. Another separate study using non-edible oil, karanja oil been investigated by Ramesh et al. under H₂ atmosphere showing more than 90% jet fuel was produced using NiMoS/Ti-K catalyst for 6h reaction time. Ni-MOF catalysts have also been employed to produce jet-fuel hydrocarbons using different linkers, as illustrated by Zhu et al. using a 1,3,5-benzenetricarboxylate denoting catalyst as Ni-BTC/MCM-41, which was observed to produce only 53% jet fuel selectivity. In addition, Cheng et al. produced a Ni-DOBDC catalyst using 2,5-dihydroxy terephthalic acid as linkers, and 82% of the jet fuel-like products were produced. However, many previous studies



Open Access Article. Published on 25 June 2015. Downloaded on 7/17/2025 11:25:37 AM.
This article is licensed under a Creative Commons Attribution-NonCommercial 3.0 Unported Licence.



have shown that monometal Ni-based catalysts producing low gasoline or kerosene-range hydrocarbons as the formation of coking poses a serious barrier to the stability of Ni-based catalysts; as a result, catalysts may be inactive and lower the yield. This could be seen in the investigation of Hunsiri, which produced □71% yield using the Ni/Beta catalyst under a H₂ atmosphere. Apart from that, Kuttiyathil using Ni/Zeo catalyst showing the production of jet fuel 40-70% and Li producing 24–85 wt.% yield on Ni/AC catalyst, in which both condition under N₂ conditions. Although both studies were performed at 500 °C, the yield was not too high, which might be due to the sintering of the Ni species at high reaction temperatures. Hence, adding a second metal such as La, Ce, or Co strongly stabilized the active Ni sites and increased the Ni dispersion, thus improving the selectivity to the desired hydrocarbons^{282,283}. A thorough summary of earlier research on Ni-based catalysts for the generation of sustainable aviation fuel (SAF) is provided in **Table 7**.

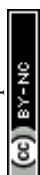
Table 7: Previous literature on Ni-based catalysts on SAF production.

Catalyst	Feedstock	Reaction condition	Yield (%)	Reusability cycles	Ref.
Phosphotungstic acid HPW-Ni/MCM-41	Methyl palmitate	H ₂ -2MPa, 390 °C, 6h	86	NA	284
Ni/Al-SBA-15	Methyl palmitate	N ₂ - 20 bar, 280 °C, 2 h.	83	NA	285
Ni ₂ P/Zr-SBA-15	Jatropha oil	H ₂ - 45 bar, 330 °C, 4 h	61-74	NA	286
Ni-BTC/MCM-41(1,3,5-benzenetricarboxylate)	Methyl palmitate	H ₂ -2MPa, 390 °C, 6h	53	NA	287
Ni/NH ₄ -Beta	Palm olein	H ₂ - 30-40 bar, 300-360 °C, 4-8h	>62	NA	288
Ni/SiO ₂ -ZrO ₂	Biobased difurfurilydene acetone	H ₂ - 2MPa, 280 °C, 24h	65	NA	289
Ni-Fe/ZSM-5/SAPO-11	Palm oil and triolein	H ₂ -60 bar, 300 °C, 2h	Palm oil-62 Triolein-64	NA	142
Ni-DOBDC (2,5-dihydroxy terephthalic acid)	Methyl palmitate	CO ₂ - 2MPa, mass ratio of 1:40, 430 °C, 8h	82	NA	290

NiMoS/Ti-K	Karanja oil	H ₂ - 30 bar, 350 °C, 6h	>90	NA	291
Ni/Beta	Palm olein	H ₂ - 40 bar, 320– 360°C, 5 h	71–74	NA	292
Ni/Zeo	Salicornia bigelovii seeds	N ₂ - 80 ml/min, 300-500°C, 10 mins	40-70	NA	293
Ni/AC	WCO	N ₂ - 60ml/min, 500 °C, 15 mins	24–85	NA	249

(II) Co-based catalysts

It is interesting to note that despite Co's lower acidity than Ni, Co-based catalysts behave differently from Ni-based catalysts. Further research on the effects of Co revealed a stronger selectivity for the decarboxylation pathway. **Table 8** provides a thorough summary of previous study findings on Co-based catalysts for the generation of green fuel. According to a recent report on the deoxygenation of PFAD over acid-base catalysts, the results revealed that Co/AC catalyst demonstrated the best level of deoxygenation efficiency and excellent selectivity towards synthesis of the liquid product (n-C₁₅+n-C₁₇)³⁹. Further study by de Barros et al. revealed that the Co/EAC catalyst presented almost 98.4% conversion of jet-fuel hydrocarbon from macauba pulp oil. Gamal examined PFAD using Co₁₀Mo₁₀/AC under N₂ flow, with a yield of 92%²⁹⁴. Asikin et al. also confirmed by a study on Co₅W₁₀/Silica Alumina using tung oil, giving out the jet fuel range to 84% with the 4th times reusability with a slight reduction in yield and n-C₈-C₁₆ selectivity. Study by Athirah and team also presenting 83.4% of yield was produced during deoxygenation under N₂ from coconut using acid-base catalyst, CoO-NiO/Kaolin. Nonetheless, monometal Co-based catalysts show low catalytic activity as Co species favor the decarboxylation pathway. This supports the results of Choo et al. (2020) on the effects of several TMO catalysts supported on zeolite Y. The Co-Y catalyst exhibited the lowest transformation (58%) for the deoxygenation of triolein to green fuel in an H₂-free





environment. This was also aligned with the investigation by Muangsuwan et al. on CoMo/Al₂O₃, with the lowest yield □ of 20%. Furthermore, Baharudin reported that Co/SBA-15 yielded only 16%. However, bimetallic Ni-Co/SBA-15 showed the highest hydrocarbon content (88.1%), with a high selectivity to jet fuel. This might be caused by a synergistic interaction between the high hydrogenolysis capacity of Ni and the reduced Brønsted/Lewis acid, which encouraged decarboxylation and prevented the cracking and polymerization of heavy hydrocarbons. This was confirmed by Safa et al. using a Co(10wt.%)–Ag(10wt.%) /AC revealing 92% hydrocarbon yield with 8 consecutive run, as silver metal favouring the decarbonylation along with decarboxylation by Co producing high performance on catalytic activity thus producing high yield with high selectivity. Thus, it is advised to use bimetallic materials such as Ni-Co catalysts that producing synergistic effect on acid-basic sites both metal species, boosting boost catalyst’s stability with high deoxygenation activity and simultaneously inhibiting coke formation. Furthermore, a catalytic support is crucial for augmenting the effectiveness of metal promoters in catalysts by strengthening catalyst reliability, facilitating metal dispersion, and reducing deactivation.

Table 8: Literature review on Co-based catalysts for green fuel production.

Catalyst	Feedstock	Reaction condition	Yield (%)	Reusability cycles	Ref.
Co/AC	Palm fatty acid distillate	350°C, 1h, 3wt. %	~72%	NA	39
Co/SBA-15	Palm fatty acid distillate	350°C, 3h, 10wt. %	~50	NA	294
Co/SBA-15	PFAD	N ₂ - 10 wt. %, 350 °C, 2h	Co/SBA-15 (16) Ni–Co/SBA-15 (88)	5	35
Co/EAC	Macauba pulp oil	H ₂ - 30 bar, 350 °C, 4 h	98	NA	295
Co ₁₀ Mo ₁₀ /AC	PFAD	N ₂ - 3wt. %, 350 °C, 1h, 50ml/min	92	6	294

Co ₃ O ₄ /Si ₂ O ₃ Al ₂ O ₃	Jatropha and palm oil	H ₂ - 2/30bar, 250/300°C, 6-8h	67-74	NA	296
Co-Y	Triolein	Partial vacuum-100mbar, 380 °C, 2h	58	NA	297
BOMoCo	Waste cottonseed oil	N ₂ - 500°C, 2 mL min ⁻¹	□ 60	NA	298
Co(10wt.%)-Ag(10wt.%) /AC	Coconut shell waste	N ₂ - 1wt.%, 350°C, 2h	92	8	299
CoMo/Al ₂ O ₃	Palm empty fruit bunch (PEFB)	H ₂ - 2 MPa, 300-350 °C, 1h, 10wt.%	□ 20	NA	300
Co ₅ W ₁₀ /Silica Alumina	Tung oil	N ₂ - 350°C, 2h, 5 wt.%	84	4	301
Co-Mo/Al ₂ O ₃	Neem seed	N ₂ - 1atm, 350–550 °C, 30–240 min	47-53	NA	302
CoO-NiO/Kaolin	Coconut oil	N ₂ - 330°C, 2h, 5wt.%	83	NA	303

1.4.5 Catalyst support

The choice of a suitable catalyst support is essential in catalyst conception, as it can affect the specific reaction route selected, including the acid/base properties, interactions between the metal and support, and geometric configuration. This choice also affects the distribution of products and enhances the efficiency of the supported catalysts, ultimately leading to increased catalytic activity. Prior research has demonstrated that the physical characteristics of the catalyst support can alter the distribution of the active site throughout its surface and impact the interaction between the support and the active site. The support might exhibit chemical inertness or interact with the active component, which is the true catalyst. The reactions that occur between the active catalyst and support material affect the selectivity and activity of the catalyst. The support material indirectly assists in the catalytic reaction process by adsorbing the reactants near the embedded catalysts, even though it does not directly participate in the reaction. Additionally, the metal support plays a vital role in modifying the



chemical properties of the catalysts and adjusting the activity of the catalytic reaction, while also improving the dispersion of the active metal.

Additionally, common catalysts are mostly composed of porous supports³⁰⁴. Most supports are robust solids that can be manufactured with various surface areas and pore-size distributions. Catalyst supports require chemical robustness, substantial surface area, and the capability to efficiently disseminate metal or metal oxide particles on their surfaces, especially when noble metals are used as catalyst promoters. Supports provide the catalyst with its physical framework, appearance, mechanical robustness, and specific reactivity, particularly for bifunctional catalysts. The performance of supported metals is affected by the surface chemical composition, namely the functional classes, as well as the physical characteristics of the surfaces. Considering these requirements, a range of oxide- and carbon-based elements have been used as materials to support catalysts.

Among these materials, zeolite has been utilized as a catalyst support in the DO reaction because of its high acidity, strictly uniform pore diameter, and high surface area. However, the strong acidity that leads to the deposition of carbonaceous materials on the active sites makes it prone to catalyst deactivation. Thus, AC has gained researchers' interest in producing highly feasible catalyst supports for the DO reaction as a low-cost and highly porous material. Nonetheless, it is difficult to reactivate, and the appearance of inorganic impurities such as potassium, sulfur, and nitrogen, which require prior pre-treatment, make it undesirable for use as a catalyst support.

Thus, another catalyst material was chosen to act as a catalyst support in the DO reaction: an oxide support. This is because of its superior oxygen retention ability and inherent redox characteristics, which enable it to aid in the activation of oxygenated molecules. γ - Al_2O_3 , SiO_2 , and TiO_2 are typically utilized as oxide catalyst supports because they are common materials for hydroprocessing conventional fuels. Inevitably, the cracking process requires the



support of acidic catalysts, because they provide more sites for oxidized chemical consumption or H₂ breakdown. Moreover, acidity of the support can enhance C–O hydrogenolysis activity. However, it is not suggested to employ strong acid support catalysts, such γ -Al₂O₃, since this might lead to significant degradation of the catalyst by promoting the development of coke and an indiscriminate breaking reaction. Consequently, it was essential to employ a moderately acidic material, such as an iron-based catalyst, in order to solubilize the carboxylic group present in the vegetable-derived oil.

(I) Properties of iron element as catalyst support

Iron (Fe) is the fourth most abundant transition element in the Earth's crust, which is safe for the environment and an incredibly important metal to society³⁰⁵. Iron in its pure form exhibits malleability and ductility, with a melting point of 1538°C. It has a solid density of 7.87 g/cm³ and exhibits magnetic characteristics. Despite its apparent prevalence, pure iron metal is rarely used in our surroundings. Instead, a substantial quantity of iron collected from its ore is employed in the production of various alloys, such as steel, which incorporates carbon. The primary ores utilized for iron extraction include hematite, limonite, magnetite (a magnetic ore), and siderite. This shows that Fe element exist in varies oxidation states, including 0, +1, +2, and +3, which leads to different forms, including Fe, FeO, Fe²⁺, Fe³⁺, FeOOH, Fe₂O₃, and Fe₃O₄, due to electron transition that has different physical and chemical properties suitable for different types of reaction^{305–307}. These classes of materials are widely feasible, reliably manipulable, environmentally sustainable, and simply produced through the use of various techniques.

As it is commonly found in the Earth's crust, making it a low-cost production material, Fe-based catalysts have been widely applied in medical, biological, and chemical applications, such as magnetic resonance imaging (MRI) and manufacturing pigments. Furthermore, it also



been employed as heterogeneous catalyst in various advanced oxidation processes (AOPs) such as catalytic ozonation, Fenton oxidation, electrocatalysis, photocatalysis, Fischer-Tropsch process, gasification and sulphate radical-based AOPs as well as adsorption of some contaminants^{308–315}. These studies show that Fe-based catalysts exhibit high catalytic activity along with a strong affinity for oxygen, favoring redox reactions and making them desirable for producing green fuel. It also appears that Fe-based catalysts have better water-gas shift reactions with a lower H₂/CO ratio and strong oxophilic effects, making it easier to break C–O bonds by binding to oxygen from the C=O of oleic acid³¹⁶. The strong attraction between the oxygen-deprived spaces within the iron oxide species enables them to enhance the adhesion and activation of oxygenated compounds more effectively than Ni³¹⁷. This is supported by a prior study by Peng et al., who found that by adjusting the Ni/Fe ratio, bimetallic Ni-Fe catalysts allowed for high phenolic conversion and greatly improved selectivity to phenol or cyclohexane³¹⁸. According to another study by Deplazes et al., the selectivity for toluene increased while the selectivity for cyclic components on the deoxygenation of m-cresol decreased³¹⁹. In addition, Fe-based catalysts improve the surface area and dispersion of host metal elements, enhance the yield and selectivity of the product, and act as electronic/chemical promoters to alter metal catalysts. Widayat et al. showed that the biodiesel yield reached 86.78% using α -Fe₂O₃–Al₂O₃ as a catalyst³²⁰. Furthermore, Zhang et al. investigated the impact of a Fe₂O₃ catalyst on the ignition and pollution properties of a diesel engine. They observed noteworthy conversion rates of 72.3% for NO and 76.1% for NO_x in an engine powered by diesel fuel³²¹. Given its significance in promoting eco-friendly fuel substitutes, NO_x emissions are a crucial factor. The Euro VI standard has implemented harsh regulations, mandating a 95% decrease in NO_x emissions from heavy-duty diesel engines. This is due to the fact that 90% of NO_x emissions are known to come from the combustion of fossil fuels,

View Article Online
DOI: 10.1039/D5TA00078E



with diesel engines being responsible for 70% of these emissions. These regulations highlight the significant potential of Fe_2O_3 as a catalyst.^{322,323}

However, an ineffective separation method could result in catalyst loss and reduce the reusability cycle of the reaction, making the catalyst less favorable (**Figure 6**). Therefore, magnetic materials, including Fe_3O_4 , serve as viable substitutes for catalyst support components due to their cost-effectiveness, simplicity of synthesis and functionalization, minimal toxicity, and ability to be readily recovered using an external magnetic field^{324–326}. Additional beneficial characteristics of these magnetic iron oxide nanoparticles include an enhanced saturation field, substantial surface area, high number of functional groups, and remarkable thermodynamic and chemical durability^{327–330}. In addition, using a magnetite catalyst not only preserves the magnetic features, but also increases the recovery rate while maintaining its catalytic strength and reusability. Magnetic catalysts have been widely applied in various applications^{331–336}. Prior research has also demonstrated that magnetic catalysts have superior catalytic activity in the generation of biodiesel compared to homogeneous catalysts. This is attributed to the magnetic characteristics of the particles, which lead to improved efficiency and durability^{325,337}. In addition to its cost-effectiveness and high catalytic activity, this magnetite catalyst has a remarkable impact on carbon combustion. It rapidly forms highly reactive iron oxide condensation sites, which occur faster than carbon particles. Consequently, it reduces the activation energy for soot formation and alters the chemistry of fine particle emissions. This leads to an increase in alkane, organic carbon, and fragments components, particularly in the manufacturing process of renewables fuel such as SAF and green fuel^{338,339}. Nevertheless, magnetic elements tend to form larger clusters because of their electromagnetic dipole-dipole attractions, which inhibit the effective dispersion of the magnetic catalyst and thus affect its surface area^{340,341}. Thus, this magnetic catalyst requires the inclusion of a metal promoter to avoid agglomeration. The study focuses on synthesizing synergistic acid-base Ni-



Co loaded on the Fe_3O_4 surface to produce high hydrocarbon yield with selectivity towards diesel-range, gasoline-range, and kerosene-range hydrocarbons via deoxygenation reaction under N_2 conditions using non-edible oil.

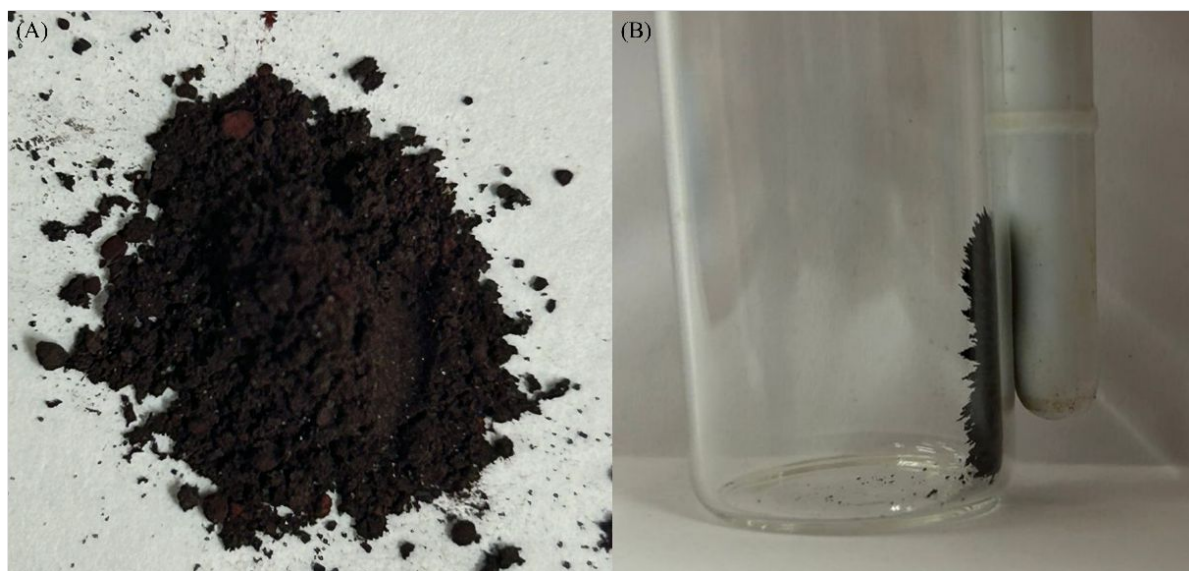


Figure 6: Images of (A) Prepared Fe_3O_4 catalyst and (B) Fe_3O_4 catalyst attracted to magnetic bar.

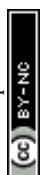
1.4.6 Deoxygenation of bimetallic Ni-Co supported on Fe-based catalyst

Figure 7 illustrates the mechanistic roles of nickel, cobalt, and iron in the deoxygenation reaction, highlighting how their synergistic interactions contribute to high yield and enhanced catalytic efficiency. Nickel (Ni) is the primary site of hydrogen dissociation in the deoxygenation of triglycerides and fatty acids. It efficiently cleaves molecular hydrogen (H_2) into atomic hydrogen, which is necessary for further hydrogenation processes (**Pathway I**). Ni also promotes the hydrodeoxygenation (HDO) and decarbonylation (deCOx) pathways by facilitating the breakage of C–O bonds within fatty acid chains (**Pathway II**)³⁴². These routes eliminate carbon monoxide (CO) and water (H_2O), respectively, as forms of oxygen. Significantly, Ni sites are essential for reducing the activation energy barriers related to these bond-breaking processes, which makes it possible for triglycerides to be efficiently converted



into hydrocarbons. On the other hand, by promoting the breakage of C–C bonds and the elimination of carbon dioxide (CO₂) as a by-product, cobalt (Co) primarily supports the decarboxylation route (**Pathway III**)³⁴³. Oxygenated intermediates are further stabilized by the catalyst's oxygen vacancy concentration and redox flexibility, preventing coking-induced catalyst deactivation. For example, earlier research has shown that Ni supported on SAPO-11 produces a greater percentage of C₈–C₁₈ alkanes (~26%) than Co/SAPO-11 catalysts (<20%), underscoring the different catalytic functions of these metals³⁴⁴. However, to attain the best activity and selectivity, monometallic systems' catalytic efficacy is sometimes insufficient on its own. This restriction emphasizes the need to create bimetallic catalysts, in which the electronic structure of the catalyst is substantially altered by the synergy between Ni and Co. By optimizing reactant and intermediate adsorption and lowering activation barriers for both C–C and C–O bond breakage, this change improves selectivity toward jet fuel-range hydrocarbons (C₈–C₁₆)¹⁰⁰.

Meanwhile, the iron oxide (Fe₃O₄) support contributes additional functionality by providing Lewis acid sites (Fe³⁺ centers) that polarize carbonyl groups in triglycerides¹⁰⁰. This polarization lowers the activation energy required for decarboxylation and decarbonylation reactions (**Pathway IV**). Moreover, the dynamic redox cycling between Fe²⁺ and Fe³⁺ promotes the formation of oxygen vacancies, which facilitates efficient oxygen removal and helps maintain catalyst stability and activity³⁴⁵. Mechanistically, hydrodeoxygenation (HDO) involves proton transfer at Co–Fe interfacial sites and hydrogen addition at Ni sites, leading to the formation of water and saturated hydrocarbons (**Pathway V**). Thus, by successfully balancing the deCO_x and HDO routes through complementing electrical and structural alterations, the Ni–Co/Fe₃O₄ catalyst system improves deoxygenation efficiency. Co encourages C–C cleavage and stabilizes oxygen intermediates, Ni activates hydrogen and cleaves C–O bonds, while the Fe₃O₄ support supplies necessary acid sites and oxygen



vacancies. These elements work in concert to enhance catalyst performance, stability, and selectivity, which makes this system extremely promising for the production of renewable fuel.

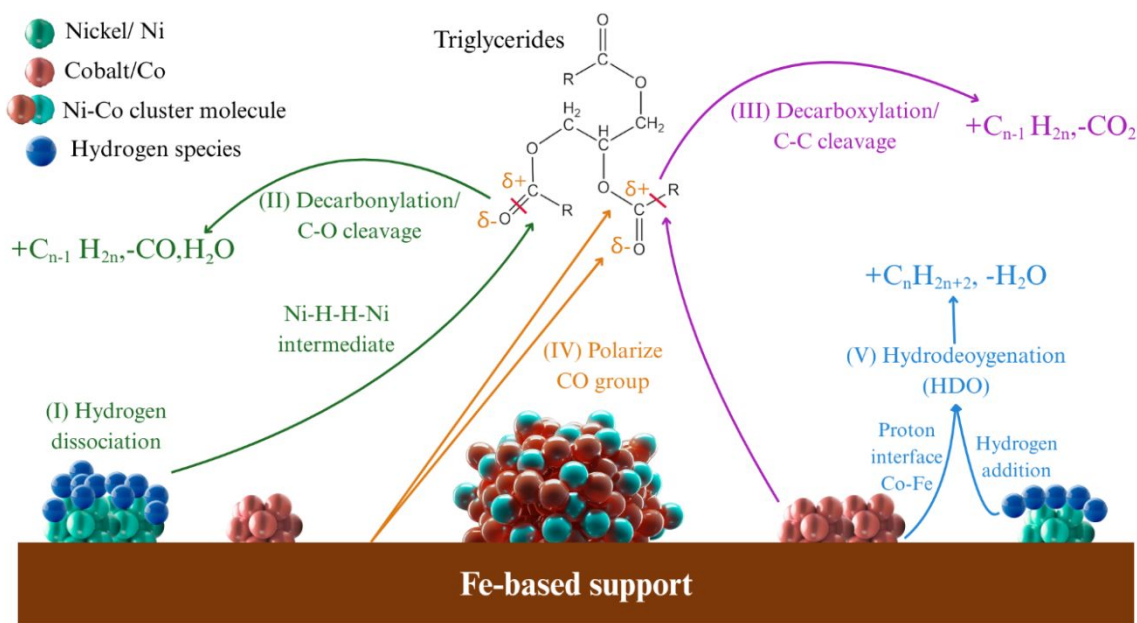


Figure 7: Diagrammatic representation of the mechanistic functions of iron, cobalt, and nickel in the deoxygenation process.

1.5 Deactivation of catalyst

The automobile and commercial catalytic industries face a persistent and significant concern regarding catalyst degradation and the progressive reduction in catalytic activity in which the replacement of catalysts can result in considerable capital expenditures. Deactivation has a substantial impact on the functioning, architecture, advancement, and investigation of commercial catalytic systems. Any process that is adequately regulated gradually encounters a decline in its activity. A wide range of physical and chemical elements may play an important role, and they can be divided into four broad categories: poisoning, metal leakage, sintering, and coking.

1.5.1 Sintering

View Article Online
DOI: 10.1039/D5YA00078E

Sintering, also known as thermal degradation, is a time-dependent thermal process that causes catalysts to undergo molecular and physical modifications. This incorporates alterations in the catalyst's surface area resulting from factors such as crystallite growth, support loss, or chemical transformation that occurs during active phase–support reactions. Sintering is commonly occurred at elevated reaction temperatures exceeding 500 °C with the assistance of moisture vapor. This sintering could be caused by metal or support sintering, where there are three main processes involved: high-temperature vapor transport, atomic migration, and crystallite migration. While vapour transportation took place during support sintering, both crystallite and atomic migration typically happened during metal sintering. The process of crystallite growth begins with the complete crystallite migrating over the support surface, followed by collision and amalgamation, the process by which elements combine to create a single mass. Meanwhile, metal atoms separate from crystallites and migrate across the support surfaces before being ensnared by larger crystallites. This process is known as atomic migration. The substance evaporated and condensed into water particles during vapor movement. Water vapor has a major impact on the porosity of the catalysts because the water particles obstruct the active sites, resulting in a surface area of the catalyst that is less active. As a result, less of the surface was exposed to the reactants, reducing the surface-to-volume ratio. Two illustrative scenarios of restricting steps in the sintering process are the disengagement of metal-containing compounds from metal crystallites and the entrapment of atomic metals on the support surface. However, these examples are excessively straightforward and have failed to consider the possibility that these mechanisms operate concurrently and collaborate via multifaceted physical and chemical processes.

The sintering process is influenced by several key elements, including temperature, environment, metal type and dispersion, types of promoters, as well as catalyst surface and



permeability. Sintering commonly occurs at numerous stages of a catalyst's life cycle, such as through the calcination process in synthesis and catalytic regeneration. As this sintering process is thermally induced, increasing the reaction temperature exponentially increases the sintering rate of the catalyst. Thus, using a stabilizer support or high thermal stability of the support will aid in minimizing the structural collapse or modification of the morphology of catalysts. This is because the sintering rates of the porous molecules are low as the crystallite diameter decreases, approaching the pore size. Dickinson and team studied on conversion of guaiacol from o-cresol via hydrodeoxygenation at 653°C and H₂ pressure of 305 bar using Ni/SiO₂-Al₂O₃ catalyst. The results showed that sintering occurred after a higher temperature was projected, increasing the particle size of Ni to be increased up to 36 nm from 3.8 nm after the reaction, resulting in a 20% decrease in guaiacol conversion within 400 min ³⁴⁶. Apart from that, Kim et al.. also reported the loss of active metal sites during HDO of Pt/Zr-P, in which the surface area deduced to 5m²/g after 114h of reaction time. This demonstrates that support materials with a substantial surface area undergo an alteration in phase, transitioning into a form with a smaller surface area owing to the loss of Pt metal during the reaction ³⁴⁷.

Indeed, under a H₂ atmosphere, the stability of noble metal crystallites often decreases as the metal melting temperature decreases. Rh > Pt > Ir > Ru is the order in which the metal stability decreased under O₂. The degree of unpredictability of the metal oxides is determined by their volatility and the durability of the metallic oxide-support association. In addition, by taking up defect sites or generating new phases, additives and impurities can affect the thermal characteristics of the support. For example, the sintering process can be accelerated by alkali metals such as barium, nickel, calcium, and lanthanum oxides, which produce spinel phases that are thermally resistant. Additionally, chlorine promotes sintering and particle formation in titanium and magnesium at elevated temperatures. This sintering processes induces the closure

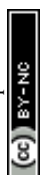


of pores, leading to the encapsulation of the active metals and a subsequent decrease in the efficacy of the catalyst.

1.5.2 Coking

In addition to sintering, coking is a deactivation mechanism that affects the catalytic activity of the catalysts. Coking is a process in which species within the fluid state are physically deposited onto the surface of catalysts, obstructing their pores or active sites and resulting in a decline in activity. Catalytic fouling transpires when solid deposits obstruct the adsorption of reactants by suffocating the pore spaces and active sites³⁴⁸. At a more advanced stage, catalyst particles have the potential to dissolve, leading to the possibility of reactor gaps becoming clogged. Carbonaceous material- and coke-forming processes include chemical absorption of different carbons or concentrated hydrocarbons, which can function as catalyst inhibitors. However, one of the most notable examples is the mechanical deposition of carbonaceous species, such as carbon and coke, in porous catalysts. While coke is created by the breakdown or precipitations carbon chains on catalyst surfaces, carbon is usually the result of CO disproportionation and is composed primarily of polymerised heavy hydrocarbons³⁴⁸. In these processes, many forms of carbon and coke are produced, each with its own unique shape and reactivity. When the temperature drops below 250°C, carbon dioxide will dissociate on metal surfaces to generate adsorbed atomic carbon. Raising the temperature causes more amorphous, reactive carbon to develop in the 250°C > T < 600°C range, and more refractory, less reactive graphitic carbon to form at T > 600°C³⁴⁹. These carbonaceous species structures formed in the catalytic processes depends on type of catalyst, reactant and reaction.

It has been suggested that increased catalyst acidity tends to encourage the development of cokes deposits³⁵⁰. Ausavasukhi also investigated the hydrodeoxygenation of m-cresol to form benzene, toluene, and xylene³⁵¹. A pool of condensate products was found on the surface



of the Ga/ZSM-5 catalyst, which resulted in coking during the reaction. This finding was also confirmed by Zanuttini et al. in which coke formation occurred during deoxygenation of m-cresol over Pt/ γ -Al₂O₃ ³⁵². It also been noticed that formation of phenolic species into graphitic coke as those species are very susceptible to oligomerization and polymerization ^{353,354}. Regarding hydrocarbon processes, coke deposits exhibit an olefinic pool rather than a phenolic pool. Adsorbed polyaromatics produced by olefin cyclization, alkylation, and oligomerization constitute the olefinic pool ³⁵⁵. It also found that formation of coke during the hydrogenolysis using Pt supported on Al₂O₃, CeO₂, La₂O₃ and ZnO due to acetol oligomerization ^{356,357}. Similarly, it has also been found that spent MoO₃ catalysts for the HDO process contain carbonaceous species including soft coke and oxycarbide carbon ^{358,359}.

For the coking analysis of spent catalysts, temperature controlled oxidation (TPO) and thermal gravimetric analysis (TGA) were frequently employed for evaluating the coke by the process of desorption amount, and composition. In order to remove coke, carbonaceous species must be burned or oxidized on a catalyst at a temperature that increases. The amount of coke included in the catalyst would be represented by the total weight loss in TG following the coke elimination. Similarly, the TPO peak resulting from the converting coke into CO₂ by oxidizing processes provides details about the quantity and temperature at which coke oxidizes. Various carbon species can be distinguished using this method based on their thermal reactivity in the presence of oxidation ^{360,361}. TPO is a promising technique since it can represent total coke morphologies and uses minimal powder-like coke samples.

Coking is caused by a varies factors such as acidity or basicity of the catalyst or the presence of molecules containing oxygen in the deoxygenated product ^{362–364}. Recent research has indicated that the presence of robust acidic regions on the catalyst enhances the formation of large polyaromatic molecules. These compounds serve as precursors for coke formation and are generated via the processes of aromatization, polymerization, and polycondensation. This



was noted in research by Choo et al. on the implementation of supported zeolite Y catalysts for the deoxygenation of triolein to green fuel ²⁹⁷. The results revealed that a large amount of Brønsted acidity in the zeolite Y catalyst produced higher concentrations of intermediates that tended to form coke, simultaneously lowering the catalytic activity of the zeolite Y catalyst ²⁹⁷. The coking performance was remarkable when a significant amount of unsaturated feed was used in the deoxygenation process. Unsaturated species may act as inhibitors by firmly adhering to the layer of catalyst and/or by engaging in the creation of coke thus concurrently lower the activity of reaction ^{135,365}. Other studies have shown that 17wt.% of coke was discovered on spent Ru/C using TGA analysis during HDO of guaiacol. The coking resulted from the deposition of polyaromatic hydrocarbons, which decreased the conversion within 5h reaction time ³⁶⁶. Notably, rich phenolic-oxygen-containing species during the reaction could lead to severe coking activity ³⁶⁷. Consequently, modified supports featuring a greater pore size or moderate acid strength can improve the C-O hydrogenolysis activity while simultaneously reducing coking. The latter strategy minimizes secondary reactions of deoxygenated products. Nevertheless, when the coking effect intensifies and the reaction proceeds, these catalysts remain susceptible to catalytic renewal.

1.5.3 Poisoning

The chemisorption of reactants, products, or contaminants on active sites deactivates the catalyst and renders inaccessible for the catalytic reaction to occur, which results in poisoning. This process, known as chemisorption, involves the bonding of undesirable compounds to the catalyst's active sites, which can change the surface's geometric structure, physically obstruct the active sites, change their chemical makeup (chemical reconstruction), and affect the electronic capacities of other species to dissociate and adsorb on the catalyst surface ³⁶⁷. Numerous prevalent carcinogens consist of inorganic anions that exhibit a high



inclination for adsorption onto the outside surfaces of metal catalysts, in conjunction with organic functional groups. This comprises organic molecules (nitrogen-containing compound, carbon monoxide, halides, cyanides, sulfides, and phosphates. Various factors can influence catalyst poisoning, including the production of volatile substances in the reaction (reactive byproducts, inhibitors, contaminants, corrosive substances, and moisture), the presence of a catalytic framework that promotes adsorption, and the occurrence of profound circumstances (high temperature and pressure) that can lead to structural changes and unwanted side reactions³⁶⁷.

In deoxygenation processes, certain chemical species may perform as toxins by deactivating the metal catalysts. As an illustration, the application of sulfide, phosphide, or chlorine-based starting materials may result in degradation of catalysts. This could be attributed to the strong binding of these substances on metals, which hinders or alters the subsequent adsorption of reactants. Mortensen et al. studied the effects of sulfur, chlorine, and potassium on nickel-based catalysts for hydrodeoxygenation²⁶⁸. It was revealed that without impurities, Ni/ZrO₂ could withstand over 100h operation however, employing Ni/ZrO₂ into sulfur compound resulting complete loss of activity and rapid deactivation of the catalysts. In addition, exposing the Ni/ZrO₂ catalyst to a chlorine compound causes the Ni particles to be sintered, thus deactivating the catalyst.

Apart from that, water which is one of the side-product in deoxygenation and hydrodeoxygenation processes, might interfere with the major reactions taking place on the active sites of catalysts by aggressively adhering to their surfaces. Evidently, literature study on phenol hydrodeoxygenation using Mo₂C/ZrO₂. The data displayed that the water oxidized the Mo₂C into MoO₃ which lowering the HDO activity which decrease the yield to 19% within 80h stream³⁶⁸. In addition, Li et al. also following the trend which the water oxidizing the phosphide into phosphate, lessen the activity while covering the active sites of phosphide³⁶⁹.



Furthermore, Li et al. also reduced the activity when covering the phosphide's active sites, continuing the trend where water oxidizes phosphide into phosphate²⁶⁸. Asikin et al. observed that while using an active Co-CaO clamshell catalyst to deoxygenate triolein under free-H₂ conditions, the reaction resulted in the conversion of the catalyst to an inactive CaCO₃ phase³⁷⁰. Similar results were noted for MgO catalysts, where MgO underwent a reaction and was transformed into an inactive carbonate phase (MgCO₃)³⁷¹. It has been observed that the ingestion of toxic gases will be prominent when the deoxygenation process is conducted completely within an enclosed reaction environment.

1.5.4 Leaching

Leaching, according to the IUPAC definition, involves the dissolution of active substances from an immobile phase, such as a catalyst, towards a partially soluble fluid³⁷². The progressive reduction in the number of active sites caused by this leaching ultimately leads to the elimination of catalytic activity, which occurs when the active phase components, especially metal fragments, are extracted from the catalyst. Both high-temperature chemical reactions and solubilization in liquid media can induce leaching. Catalyst leaching can be caused by the following: (i) solvents that are destructive or indistinguishable with the catalyst; (ii) stringent reaction conditions characterized by elevated temperature, high pH, extended duration, and rapid oxidation/reduction rates; and (iii) catalyst's structure, choice of catalyst support, and synthesis method. Degradation that occurs through leaching when aggregate or supported catalysts are employed can be elucidated through chemical transformations or direct dissolution in a solvent³⁷³. In catalysts with low solubility in water, metal oxides, hydroxides, and carbonates substances dissolve quickly in solutions due to their hydrophilic nature and this process known as solubilization which occurs as these chemicals are forced into the solutions³⁷³. Hydrotalcites, which are a type of layered double hydroxide with the chemical formula

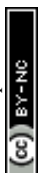


$\text{Mg}_6\text{Al}_2\text{CO}_3(\text{OH})_{16}\cdot 4\text{H}_2\text{O}$, can selectively remove Mg from solid base catalysts such as MgO when they are dissolved in water ³⁷⁴. Conversely, On the other hand, leaching via chemical alteration may arise when the elements of the catalyst combine with the substances involved in the process to produce a soluble or passive substance. This may be because metal oxide catalysts, which are more hydrophilic under hydrothermal conditions, generate hydroxides. Similarly, the release of active phases from the support can be attributed to the solvolysis of the metal-oxygen link ³⁷⁵.

The deoxygenation process may result in the leaching of active metal when exposed to acidic hydrothermal conditions, where H_2O is produced as a side-product and the feedstock contains a significant amount of acidic oxygenates, which include acetic acid and formic acid. After 300 h of reaction, approximately 10% of the Ru metal was eliminated from the RuSn/C catalyst during the conversion of levulinic acid to γ -valerolactone at 453 K and 35 bar ³⁷⁶. Zhao et al. demonstrated the existence of acidic conditions that exacerbate the leaching of Ni metal ³⁷⁷. As the leaching conditions were shifted to a 15wt.% acetic acid solution, the quantity of Ni leaked increased. Specifically, for the Ni/HZSM-5 catalyst, the concentration rose from 5ppm to 580ppm, while for the Ni/ Al_2O_3 -HZSM-5 catalyst, it increased from 1.5ppm to 690ppm after 90 hours ³⁷⁷. This demonstrates that leaching inevitably leads to consequences including the depletion of active sites. Nonetheless, the degradation of supported metal catalysts can potentially be mitigated through the use of metals and supports with more robust metal-support interactions ³⁷⁷.

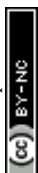
1.5.4 Catalysts' stability

Catalyst deactivation processes critically undermine catalyst stability, thereby limiting their industrial applicability. To address these challenges, various strategies have been developed to mitigate deactivation and enhance catalyst durability. One effective approach



involves incorporating stabilizing elements to form more robust phases, as irreversible phenomena such as metal leaching and sintering pose significant obstacles to catalyst longevity. For example, the incorporation of SiO₂ as a structural promoter in core-shell Pd@Al₃-mSiO₂ catalysts has been demonstrated to effectively protect the active metal from sintering and leaching, thereby preserving catalytic performance ²⁶⁶. Similarly, Liu et al. reported that introducing SiO₂ into Ni₂P-Pd/ α -Al₂O₃ catalysts enhanced stability by a factor of three, underscoring the critical role of support modification in catalyst robustness ³⁷⁸. Coking remains one of the most prevalent deactivation pathways during deoxygenation reactions. To counteract coke formation, rational catalyst design focusing on structural optimization, thermal regeneration, and strengthened metal-support interactions is essential. For instance, doping Ni catalysts with erbium (Er) has been shown to improve coke resistance during the hydrodeoxygenation of jatropha oil, attributed to reduced Ni particle sizes and the generation of surface oxygen vacancies that inhibit carbon deposition. In another study, the incorporation of lanthanum (La) into Ni/SiO₂ catalysts led to the formation of La₂O₃ and La₂O₂CO₃ phases, which effectively suppressed coke accumulation and significantly enhanced catalyst stability and reusability ³⁷⁹.

Regarding catalyst poisoning, strategies aim to minimize the adsorption strength of poisons or transform them into less harmful species. For example, Rabaev et al. demonstrated that adding the amine surfactant hexadecylamine during SAPO-11 crystallization inhibited hydrothermal desilication, markedly improving the hydrothermal stability of the catalyst ³⁸⁰. Despite these advances, deactivation remains a complex issue requiring further investigation, particularly through the development and optimization of regeneration protocols such as thermal, chemical, or reductive that can partially restore catalyst functionality. Nevertheless, repeated regeneration cycles often lead to gradual performance deterioration. Therefore, ongoing research prioritizes the development of catalysts with enhanced thermal stability, coke



resistance, and regeneration capability. Such advancements are pivotal for realizing sustainable and economically viable bio-jet fuel production technologies, ensuring catalysts maintain high performance over extended operational lifetimes.

1.6 Factors affecting reaction conditions

This section explores various factors affecting the DO process, including feedstocks, the reaction environment, reaction temperature, the amount of catalyst, and the use of solvents. The discussion focuses on how these parameters potentially impact the efficiency and selectivity of biomass deoxygenation, ultimately affecting the production of green fuels.

1.6.1 Reaction Temperature

One of the key variables that determines the products generated during the hydrotreating reactions is the reaction temperature. According to a study by Bezergianni et al., the yield of gasoline increased with reaction temperature, going from 0% at 330°C to 10.2% at 398°C, depending on yield conversion to the desired product along with selectivity, eradication of heteroatom components, and saturation point of the double bond ³⁸¹. Higher temperatures cause the oil to fracture, which converts the heavier diesel molecules into lighter gasoline molecules. In contrast, the amount of oxygen recovered was insignificant when the temperature was low, and it exhibited a substantial increase as the temperature increased, accompanied by the absence of heteroatoms such as nitrogen and sulfur in the resultant liquid product ³⁸¹. Another study by Anand and Sinha discovered that while hydrocracking triglycerides over a sulfided CoMo catalyst, the triglycerides initially transformed into oligomerized hydrocarbons at lower temperatures; however, as the temperature increased, C₁₅-C₁₈ hydrocarbons were produced ³⁸². In addition, while hydrotreating pomace oil, Pinto et al. examined the gas and liquid compositions ³⁸³. It was noted that an increase in the utilization of hydrogen at higher



temperatures over extended periods of time led to a 22% increase in the quantity of lighter gaseous hydrocarbon mixtures. This suggests that the increasing temperature promoted an extensive cracking reaction, thus producing a more gaseous product ³⁸³. Further evidence shows that decarboxylation and decarbonylation reactions may have been encouraged by the rise in temperature resulting from the 30% and 40% increases in CO and CO₂, respectively. At 300 °C, only 3% of the light fractions contained fatty acids, 96% of which were transformed into hydrocarbons. The hydrocarbon content increased to 99% as the temperature increased to 430 °C, and the fatty acids decreased. However, at 300 °C, the heavier fractions produced only 50% hydrocarbons and 47% fatty acids. Ninety% of the hydrocarbons were converted when the temperature reached 430 °C, but only 10% of the fatty acids were converted ³⁸³.

A study by Simacek et al. also showed that rapeseed oil was converted almost completely at 310 °C, whereas it was fully converted at 360 °C ³⁸⁴. In a different study, Kikhtyanin et al. discovered that, while utilizing Pd/SAPO-31 as a catalyst, the ideal temperature range for fully converting sunflower was 320–350 °C ³⁸⁵. Hancsok, on the other hand, was able to fully convert sunflower at 350 °C using Pt/HZSM-22/Al₂O₃ catalyst ³⁸⁶. Furthermore, a study was undertaken by Bezergianni et al. to investigate the influence of the reaction temperature on the hydrotreatment of compounds comprising heavy gas oil (HGO) and waste cooking oil (WCO), in which a NiMo catalyst was employed and other variables remained constant throughout the experiment ³⁸⁷. In their study, they used 70/30 HGO/WCO feedstock at 350 °C to achieve a maximum conversion of 48%. The researcher also discovered that the HGO concentration of a combination decreased with increasing conversion across the board ³⁸⁷. Lower temperatures were associated with decreased hydrogen consumption because only reactions related to saturation and heteroatom removal take place there, although cracking also occurs there. However, cracking reactions also occur at these lower temperatures. Srifa et al. conducted research on hydrotreated palm oil that was subjected to a temperature of



approximately 270°C. The outcome of this process is oil solidification at room temperature.

The solidified product is mainly composed of palmitic and stearic acids, supplemented by trace amounts of triglycerides³⁸⁸. Therefore, these results show that the product solidifies at ambient temperature during the hydrotreatment process at temperatures below 270 °C.

A substance produced by increasing the temperature further consists of molecules of hydrocarbons, lipids, or fatty acids that are freely present. The higher molecules break down into smaller molecules when the reaction temperature is high³⁸⁹. For the majority of the feedstock, it was found that rising reaction temperatures accelerated the rate of DO. Nevertheless, in the majority of circumstances, there is a significant decrease in the selectivity for DO at elevated temperatures, which is caused by an increased generation of aromatic products and a higher rate of heat degradation. This emphasizes the necessity of determining an optimal reaction temperature that balances the selectivity and rate of dissolved oxygen. In addition, the reaction temperature has minimal influence on the selectivity towards the desired DO pathways, such as deCO_x or HDO yet the specific catalyst chosen influences the direction of the DO pathway.

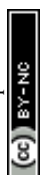
1.6.2 Reaction time

Residence time is defined as the ratio between the mass of the liquid input rate and the weight of the catalyst in the reaction mechanism^{389,390}. The reaction time metric is a fundamental aspect in the production of green fuel. Throughout each experiment, this characteristic is consistently researched, and the aggregate results show that conversion rates grow in direct correlation with the response times. The range of reaction times can be adjusted from 30 min to 48 h, and possibly longer. Significantly, the maximum reaction varied depending on the reaction components, including the feed, catalyst used, temperature, and pressure. An investigation conducted by Srifa et al.. examined the impact of residence period



on the production of hydrocarbon-diesel-fuel such as crude palm oil (CPO) using a 5% Pd/C catalyst ³⁹¹. By extending the reaction period from 0.25 to 5 h, they discovered that the optimal diesel output of 91% occurred around the 3-hour period ³⁹¹. Mohammed et al. also revealed that the Pd/AC catalyst produced the highest 93% conversion of diesel-like fuel from waste cooking oil over 2h reaction time ³⁹². Gamal et al. also investigated the effect of the residence time of the Co₁₀Mo₁₀/AC catalyst on the production of renewable diesel from palm fatty acid distillate (PFAD), which contains 55.69% palmitic acid (C₁₆) followed by 22.76% oleic acid (C₁₈) ²⁹⁴. The parameter was studied for 1h up to 4h and the results obtained showed that from 1-2h showing progressive increase in yield (75%–92%) and diesel selectivity ranging from 70 up to 89% was observed ²⁹⁴. Furthermore, Ding et al. examined the effectiveness of methyl laurate on a Co/ZSM-5 catalyst ³⁹³. The outcomes illustrate that the Co/ZSM-5 catalyst successfully converted methyl laurate into dodecane, with 68% selectivity for C₁₁ and 18% selectivity towards C₁₂ alkanes at 280°C with 4 hours reaction period ³⁹³. In addition, it was observed that prolonged reaction times enhanced the production of CO gas by favoring the decarbonylation route ³⁹⁴. Further cracking of the deoxygenated liquid product resulted in an increase in lighter fractions, which were almost similar to those of sustainable aviation fuels composed of C₈-C₁₆. Therefore, it is obvious that sufficient retention times are necessary to provide optimal interaction between both precursor and catalysts in order to produce the desired products including diesel-like fuel or kerosene-like fuel and gasoline-like fuel.

Unfortunately, it is not recommended to have a prolonged reaction time, considering the adverse effects on product selectivity. It has been reported that prolonging the reaction time causes the fatty acid to split into a lighter hydrocarbon fraction, decreasing the yield due to increased C-C cleavage, which aggravates the lighter hydrocarbons. This is because extended reaction times resulted in higher yields of undesirable side products such as ethane and methane, as long-chain hydrocarbons continued to break down into shorter hydrocarbons. et



al. reported that as the reaction period was extended, the products experienced side reactions, including cracking, isomerization, cyclization, and dimerization, resulting in a reduction in the amount of the desired hydrocarbons ³⁹⁵. This is also consistent with the findings of Sahar et al.. at 4h, the conversion of green fuel by the Pd/C catalyst dropped to 52% only ³⁹². This also can be seen from Azira's finding, where when the reaction duration of the NiCo/SBA-15 catalyst was increased to 3h, the selectivity towards bio-jet fuel started to decrease ³⁹⁶. This was probably due to the widespread cracking of fatty acids, resulting in the production of shorter hydrocarbon chains ³⁹⁶. Another study also showed that up to 4h of reaction time, the yield was reduced to \square 60% as a more undesirable side product such as gaseous or char was formed, resulting in the build-up of chemicals from undesirable side reactions (condensation, cyclization, and re-polymerization), obstructing the active centers of the reaction sites ²⁹⁴.

However, a shorter contact period resulted in insufficient time for the catalyst to initiate the deoxygenation reactions. Nevertheless, a contact period that was too brief resulted in an inadequate amount of time for the catalyst to initiate the DO process. Itthibenchapong et al. ³⁹⁴ reported that a shorter residence time in a solid-liquid reaction system implies an elevated liquid hourly space velocity (LHSV) across the reagent and catalyst. This can result in a decrease in HDO generation and an increase in deCOx output ³⁹⁴. This also coincides with Mezaal's finding on the conversion of palm oil into renewable fuel using a scale-derived hydroxyapatite (HAP) catalyst, in which the One-Variable-At-A-Time (OVAT) varied from 30 min to 240 mins during ³⁹⁷. The data showed that the HAP catalyst produced less than 30% of the hydrocarbon yield during the 30 min reaction period. In addition, another researcher carried out a study on the DO reaction by Ag₂O₃(10)-La₂O₃(20)/AC nanocatalyst on WCO, and the results indicated that less than 60% of hydrocarbons were produced in 30 min ³⁹⁸. Syazwani further stated that the initial biodiesel production was hindered by a poor yield due to insufficient mixing and dispersion of the feedstock and methanol within a short timeframe



³⁹⁹. The aforementioned studies suggest that achieving the optimal reaction time is crucial for enhancing deoxygenation activity through decarboxylation.

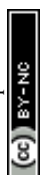
1.6.3 Catalyst type and amount used

Homogeneous and heterogeneous catalysts are the two main types of catalysts used in the manufacture of bio-jet fuels. However, heterogeneous catalysts, which do not require any additional mechanisms for removal from green fuel products, are the most widely employed catalysts. Two categories of catalysts are used in heterogeneous reactions: noble metal and transition metals catalysts. These catalysts are supported by SBA-15, zeolites, carbon, and alumina ³⁵. Compared to transition metals, noble metal catalysts are more expensive and have a shorter lifetime. Based on observations by Morgan and colleagues, who found that the 20Ni/C catalyst demonstrated better deoxygenation promotion by generating C₈-C₁₇ fractions (>80%) than noble-metal-promoted catalysts when deoxygenating various feedstocks (triolein tristearin, soybean oil) ⁴⁰⁰. This demonstrates that transition metals can also boost the production of green fuels. Basicity and acidity also play an important role in the production of green fuels. The high acidity of the catalyst improved the elimination of oxygen and the breaking of C-C bonds, leading to augmented generation of linear hydrocarbons. However, an excessive number of acidic sites can cause aggressive cleavage of C-C bonds, leading to the creation of undesirable side products such as CO, CO₂, CH₄, and CH₂. This reduces the selectivity for the desired product. Furthermore, excessive acidity might result in deactivation of the catalyst due to coking, which subsequently reduces the effectiveness of the catalyst ⁴⁰¹. On the other hand, basicity sites, known as the incorporation of a coke inhibitor species, are highly effective towards decarboxylation pathways and are highly resistant to CO adsorption, reducing coke formation, thus making it more sustainable ^{398,402}. However, the basic sites that appear to be inactive for decarbonylation pathways often make it unselective to produce



hydrocarbons, thereby reducing the yield. Therefore, it was proposed that the production of catalysts with a synergistic interaction between the acidic and basic sites could improve the catalyst stability and increase the deoxygenation activity.

Furthermore, the amount of catalyst employed in the DO reaction can significantly influence the rate of the reaction, quantity of the desired product produced, and selectivity of the products. A previous study discovered that the use of a Pd/C catalyst for eliminating oxygen from stearic acid had a substantial impact on the speed of the reaction and the selectivity of the intended products (n-heptadecane and heptadecene) ⁴⁰³. The impact of the catalyst dosage on the DO of stearic acid into dodecane was investigated under helium flow at a temperature of 300 °C and a pressure of 6 bar. The data showed that the conversion and reaction rates increased monotonically as the amount of catalyst was altered ⁴⁰⁴. Further experiments were conducted using varying quantities of the NiMo/Al₂O₃ catalyst ranging from 0 to 0.126 g. The results demonstrated that increasing the amount of catalyst led to an increase in the yield and selectivity towards straighter hydrocarbons, while reducing the formation of intermediate and undesired side products ⁴⁰⁵. This may be due to the higher number of available active sites on the catalyst surface when a higher amount was used. This was confirmed when Arvela and colleagues found that 4wt.% Pd/C catalysts yielded a higher yield and selectivity towards n-heptadecane during the deoxygenation of tall oil fatty acids ⁴⁰⁶. Conversely, when a small amount of catalyst is used in DO reactions, polymerization occurs, thereby enhancing the production of aromatics and other unwanted by-products. This can be seen in Chen's study, which showed that polymerization occurred when less silver nanoparticle catalyst was used for the production of CO₂ in exhaust gas ⁴⁰⁷. Hence, the precise quantities of the catalyst play a critical role in defining the highest possible amount and quality of the specified hydrocarbon output. In addition, the higher concentration of catalyst resulted in a reduced rate of catalyst



deactivation and an increased preference for n-alkanes. This demonstrates that the production and selection of an optimal catalyst are crucial for maximizing the output of the desired product.

1.6.4 Types of feedstocks

Usually, deoxygenation experiments are performed using various types of feedstock, such as triglyceride-based oil and algae biomass. Model compounds have also been selected as feedstock because of the similar molecular structures of vegetable oils^{408–410}. Some examples include various fatty acids such as behenic acid, palmitic acid, and stearic acid, as well as fatty acid esters such as stearic acid ethyl ester. The utilization of saturated fatty acids involves decarboxylation to generate linear hydrocarbons with enhanced selectivity, while unsaturated fatty acids undergo hydrogenation followed by decarboxylation to produce n-heptadecane, with stearic acid acting as the intermediary product²³¹. Furthermore, the composition of the chosen feedstocks is also a significant factor that dictates the composition and quality of the ultimate products generated throughout the process. These hypotheses could be validated by conducting studies involving multiple raw materials, such as stearic acid, soybean oil, and PFAD, with a Pd-based zeolite catalyst in an environment free of H₂, and the results demonstrated the highest bio-jet fuel yield⁴¹¹. Further investigation was conducted on the HDO of a model compound of palmitic and stearic acid by using Pd onto a mesoporous carbon catalyst with dodecane solvent at 300 °C, and the results demonstrated that the conversion rates of both feedstocks were identical⁴¹². This outcome is consistent with that which had been observed for the DO of heptadecanoic acid, stearic acid, nonadecanoic acid, arachidic acid, and behenic acid⁴¹³. The main liquid products of the catalytic deoxygenation of palmitic acid and stearic acid were n-pentadecane and n-heptadecane, respectively. These findings demonstrate that using saturated feedstock instead of unsaturated feedstock consistently provides benefits for DO experiments.



Similar experiments using commercial Pd/C catalysts have been conducted using saturated and unsaturated feedstocks with dodecane as the solvent at 300 °C for 360 min⁴⁰³. The initially observed reaction rates for stearic acid (0.63 mmol/min-g_{cat}) and stearic acid ethyl ester (0.70 mmol/min-g_{cat}) were both slightly higher than those for behenic acid (0.36 mmol/min-g_{cat}). The degradation of stearic acid ethyl ester by the Pd/C catalyst was more pronounced in comparison to that of stearic acid. This may be interpreted as stearic acid ethyl ester with a conversion of only 38%, whereas stearic acid reached 60%, which may be attributed to the increased production of unsaturated products that diminish the selectivity for n-alkanes. The existence of additional unsaturated molecules in the substrate or output may result in their adsorption onto the surface of the catalyst because of the C=C scission of the alkyl chain, which promptly renders the catalyst inactive. An additional investigation was conducted on bimetallic layered double hydroxides (LDH) and Ni/Al₂O₃ catalysts under N₂ conditions⁴¹⁴. The results indicated that soybean oil exhibited the greatest propensity for coking and cracking reactions, confirming that a greater concentration of unsaturated chemicals in the reactant increases the probability of undesirable coking and cracking⁴¹⁴. In addition, the presence of unsaturated compounds serves as a bridge for cyclization and dehydrogenation events that produce undesirable aromatic products²³¹. Previous research suggests that the deoxygenation of stearic acid ethyl ester (SAEE) leads to the formation of carbon monoxide (CO) as the primary gaseous constituent because of the stability of the ethoxy group in SAEE¹⁸. The coexistence of these effects in the DO process, caused by the presence of unsaturated molecules in the feedstock, can result in noticeable catalyst deactivation, reduced DO activity, and a large decline in hydrocarbon selectivity. Therefore, it can be deduced that utilizing saturated feedstock in DO processes can improve DO activity and the selectivity of the products.



1.6.5 Reaction environment

View Article Online
DOI: 10.1039/D5YA00078E

It is commonly acknowledged that the reaction atmosphere has a major impact on the reaction route in deoxygenation research. Deoxygenation and product selectivity improved noticeably in the presence of H₂. Heriyanto reported a green fuel yield of approximately 78 % using NiMo/ γ -Al₂O₃ at 400°C for 4 h under a 60 bar H₂ environment ⁴¹⁵. Another study by Frida et al. al. also reported that NiO/NbOPO₄ yielded 86% conversion of renewable diesel from palm oil, with a C₁₅ selectivity of 58% ⁴¹⁶. Further study by Tang and colleagues also revealed high jet fuel components, comprising 55% of C₈-C₁₆ using a magnetic Ni-Fe/SAPO-11 catalyst on rapeseed oil ⁴¹⁷. In addition, the Ru/HAP+ HZSM-5 catalyst produced □92% hydrocarbon yield in an H₂ environment ⁴¹⁸. While the utilization of H₂ can enhance the conversion and hydrocarbon output, it also results in an escalation in operational expenses. Due to the elevated H₂ pressure, the utilization of costly specialised equipment becomes necessary, and it is also linked to potentially significant safety concerns with hydrogen recycling in the enlarged facility. Consequently, deoxygenation in an inert environment, such as nitrogen (N₂), becomes a more attractive option.

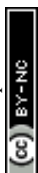
This can be seen in Elaine's report on the deoxygenation of palm kernel oil (PKO) using a Pd/C catalyst. Pd/C produced a significant quantity of liquid product (□99%) with a favorable level of selectivity for jet paraffins (□73%) that had attributes similar to Jet A1 ²⁵¹. An additional investigation conducted by Azira Razak focused on producing jet fuel from WCO at 350°C for a duration of two hours, while maintaining a 5% catalyst loading. According to the findings, the 5Ni5Co/SBA-15 and 5Ni5Co/SBA-15-SH catalysts shown outstanding activity by producing around 78-80% hydrocarbon with selectivities ranging from 78-92% ³⁹⁶. In a previous study, Xing evaluated the impact of the reaction conditions on the deoxygenation of oleic acid using a Ni/HZSM-5 catalyst at 360°C ⁴¹⁹. The findings demonstrated that, whereas the synthesis of C₈-C₁₅ alkanes was boosted in N₂ atmosphere, yielding approximately 65.05



mol% in H₂ atmosphere, the yields were reduced due to the catalytic cracking effect, yielding 49.67 mol%. Additionally, when H₂ was increased from 2 MPa to 4 MPa in the H₂ environment, more aromatic hydrocarbons were formed, the molar proportion of straight chains decreased, and the N₂ pressure ranging from 1-4 to MPa remained unchanged⁴¹⁹. This implies that lowering N₂ did not significantly alter the product and that no olefins were found in N₂, but more aromatic compounds were found when H₂ was present. Based on these results, it is possible to produce green fuel without relying on an external source of H₂.

There is a significant relationship between the atmospheric conditions and the performance of the process as well as the solvent-free deoxygenation pathway path. There are situations in which the hydrogen concentration can potentially play a significant role in determining the predominant reaction route. Decarboxylation, decarbonylation, and hydrodeoxygenation are processes that significantly increase the amount of hydrogen required. It was because of this that the current situation came about. With an increase in the initial hydrogen pressure, both the hydrodeoxygenation activity and the product yields improved considerably. During the hydrodeoxygenation process of the model chemical, insufficient stoichiometric hydrogen is present to complete the conversion into the hydrocarbons that are required. This is a concern, because hydrocarbons are expected to be produced. The concentration of linearly saturated C₁₅–C₁₈ hydrocarbons was found to be 48.6% in an autoclave batch reactor that included 40 bar of pure hydrogen, according to Malins et al.⁴²⁰. During this time, hydrogen was free of impurities. However, when the pressure was increased to 60 and 100 bar, the concentration of hydrogen increased to 91.7% and 93.3%, respectively⁴²¹. This occurred because of the increasing hydrogen content.

It is possible that the composition of the product changes as a consequence of a different primary reaction pathway. According to the information provided in²⁹⁶, shorter hydrocarbons are formed when an inadequate supply of hydrogen in the state makes the cracking process



easier to carry out. For the purpose of conducting an experiment to explore the effects of air conditions on the deoxygenation of oleic acid, an autoclave batch reactor became the instrument of choice and **Figure 8** illustrates the results of the study ⁴¹⁹. The effects of air quality were investigated during the course of the study. In addition to preventing the cracking reaction, hydrogen sulfide (H₂S) improves the production of the required hydrocarbons. Using a semi-batch quartz reactor with a capacity of 50 mL and partial vacuum of one bar, oleic acid was decarboxylated to produce unsaturated 8-heptadecene. The production of shorter olefins was accomplished using a straightforward procedure that involved a cracking event. It has been demonstrated that a C–C bond is more thermodynamically stable than a C=C bond ⁴²², which explains why a situation like this does exist. The deoxygenation of oleic acid results in the production of gaseous carbon monoxide, carbon dioxide, and water as byproducts. A number of additional processes, including water-gas shift (WGS), Fischer-Tropsch synthesis, and methanation, were incorporated into the system after it was previously extended. It is possible that this results in an increase in the hydrogenation of olefins, which in turn may lead to the generation of more hydrogen. The formation of linear hydrocarbons is possible through hydrogenolysis, a process that occurs during the deoxygenation of cyclic molecules in the presence of hydrogen.

View Article Online
DOI: 10.1039/D5TA00078E



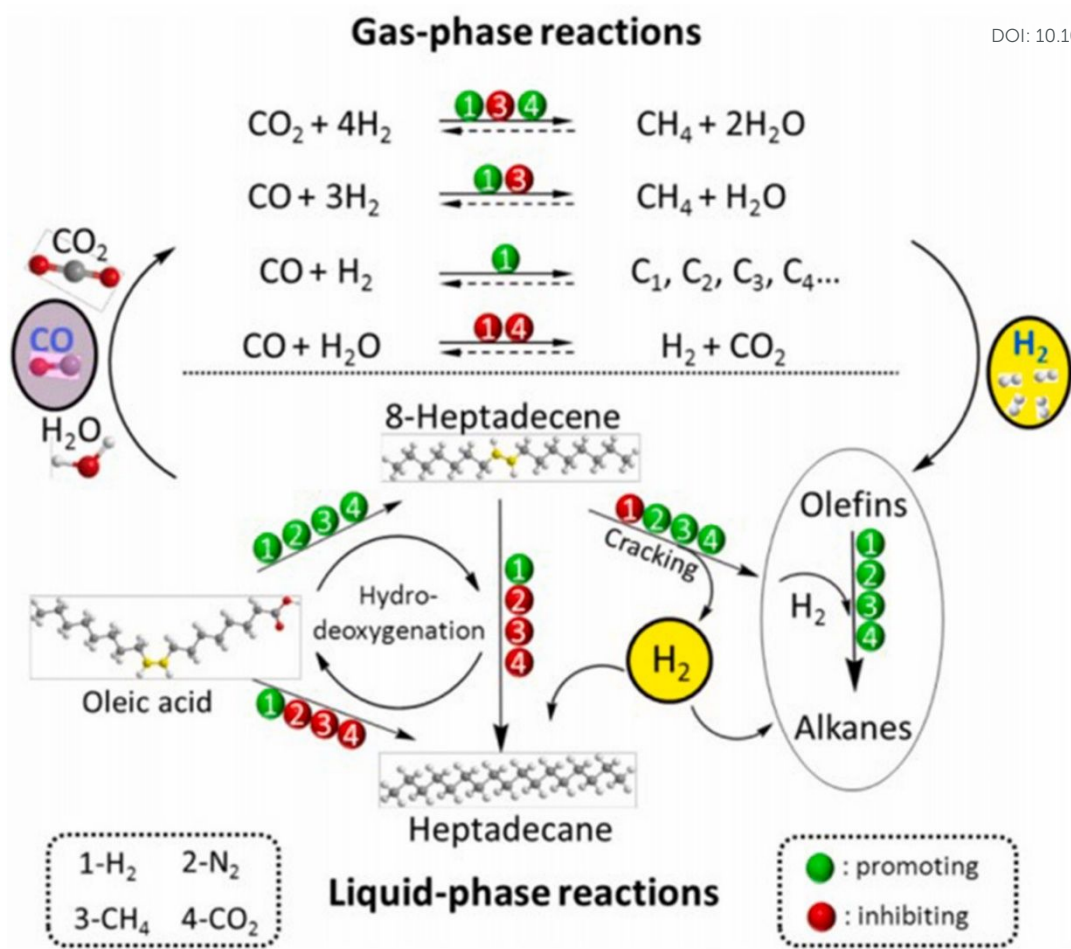


Figure 8: The impact that the four distinct reaction gasses have on the reaction route that leads to the deoxygenation of oleic acid are depicted in Figure 5. This reference is protected by copyright ⁴¹⁹.

Previous experiments, discussed in this paragraph, have shown that deoxygenation is more effective when air contains hydrogen. Increasing the amount of hydrogen present in the process facilitates the improvement of the hydrodeoxygenation route and decreases cracking, which ultimately results in an increase in the yield of saturated linear hydrocarbons. The addition of hydrogen at a high pressure increases the cost of the process. To improve the performance of the catalysts and the effectiveness of deoxygenation, research is being conducted in inert settings.



1.7 Recent developments and future outlook in deoxygenation reaction on production of renewable biofuels

[View Article Online](#)

DOI: 10.1039/D5YA00078E

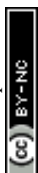
In contemporary times, petroleum fuel plays a significant role in the domains of transportation and industry, both of which are indispensable in the daily lives of people worldwide. Demand was anticipated to rise in tandem with the growing population throughout the period of globalization. The transportation sector, which includes petrol, jet fuel, and diesel fuels, is one of the major sectors that consumes most of the worldwide energy. This has accelerated economic progress in every country. Nevertheless, a negative consequence of this use is the release of greenhouse gases, particularly carbon dioxide (CO₂), by direct combustion. Carbon dioxide (CO₂) contributes directly to climate change and global warming. Moreover, this petroleum-based fuel originates from restricted sources and is expected to be depleted in a few decades owing to its extensive consumption to satisfy the rising demand. Therefore, there is a critical need for renewable, sustainable, and alternative green fuels that can replace petroleum-based diesel in terms of their lack of pollution, economic attractiveness, and ability to reduce waste. Green fuels derived from renewable sources, such as corn oil, palm oil, animal fats, sunflower oil, and microalgae, can effectively mitigate CO₂ emissions by absorbing and using CO₂ for the photosynthetic cycle. During the initial stages of renewable energy production, the product was referred to as a first-generation green fuel, with a primary focus on biodiesel production through transesterification or esterification procedures.

This hypothesis might be substantiated through an examination conducted by Gideon et al., which focused on the production of biodiesel using tall oil fatty acids (TOFA) and experimenting with different types of catalysts⁴²³. The data reported that on a homogenous catalyst, sulfuric acid (H₂SO₄) obtained 96.76% FAME under optimum conditions at 55 °C using 0.5% catalyst concentration for 1h with a methanol: oil ratio of 15:1. On the other hand, while using a heterogeneous catalyst called Amberlyst BD20 ion-exchange resin, a conversion



rate of 90% was achieved under the following conditions: a methanol-to-oil ratio of 20.8, catalyst amount of 23.4% relative to the oil mass, and a reaction period of 4.7 hours at a constant temperature between 75 and 80 °C. Abhishek also investigated the impact of the W/ZrO₂ catalyst on the conversion of microalgal lipids to 94.58% and found that it could be utilized for up to three rounds without any noticeable loss of catalyst.²⁴² Notably, the majority of the fuel characteristics of biodiesel obtained comply with the specifications set by ASTM 6751 and EN 14214 standards. Nonetheless, biodiesel is not ideal as a direct replacement for B-100 because the inclusion of oxygen atoms in biodiesel results in the formation of sediments and polymers, in addition to the viscosity of the fuel. This could result in injector fouling and filter clogging. The primary difficulties associated with FAME biodiesel are its instability during long-term storage, small ignition point, poor oxidation resistance and susceptibility to autoxidation at room temperature. These issues arise from the presence of mono- and poly unsaturated fatty acids, making biodiesel prone to oxidative deterioration⁴²⁴.

Therefore, second-generation green fuels have been created with the aim of fully substituting fossil fuels. This green fuel, referred as SAF or bio-jet fuel for air transportation, possesses a paraffinic molecular framework similar to that of conventional diesel or kerosene/gasoline fuels. Green fuel is favorable because of its higher thermal temperature, energy density, cetane number, high stability, and low oxygen content, making it better quality than biodiesel. Many studies have been conducted, and a few processes have been certified for producing jet fuel owing to certain properties. However, to date, only up to 50% of jet fuel is blended with petroleum fuel, and the use of HEFA and FT fuels may lead to performance concerns^{425,426}. The lack of aromatic compounds in these fuels leads to a reduced emission of particles, but it can also cause fuel pump leakage owing to insufficient expansion of the elastic polymers⁴²⁵. Nevertheless, the manufacture of hydrocarbons containing significant amounts of aromatic compounds and cycloparaffins for aviation applications must comply with the



rigorous standards specified in ASTM D1655, which establishes the requirements for aviation turbine fuel⁴²⁷. Hence, the ASTM D7566 standard includes the addition of FT-SPK plus aromatics (FT-SPK/A) to increase the aromatic content to a maximum of 20 wt.%. Despite this, the fuel composition is still unsuitable for consumption by aircraft turbine engines until it is blended with commercial jet fuel. The economic viability of HEFA procedures was proven by the substantial fuel output (86-91% feedstock) observed in previous studies^{428,429}.

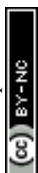
In the early development of second-generation green fuel, hydrodeoxygenation followed by selective cracking/isomerization was chosen as the favorable pathway to produce a high yield of the product. This process uses non-edible resource with high TGs or FFAs contents. In addition to utilizing non-edible oils for the creation of second-generation SAF, there are various other alternative feedstocks and technologies worth considering. These alternatives include lignocellulosic biomass, municipal solid waste (MSW), and oil derived from microalgae. Study reported Yani et al. showed hydrodeoxygenation by NiO/NbOPO₄ catalyst producing green fuel yield ranging from 69% to 82% with highest selectivity with 58% of C₁₅ followed by C₁₂ (15.04%)⁴¹⁶. However, the calorific value (44.03 MJ/kg) was higher than that reported by Orozco but acceptable by the Indonesian National Standard (43 MJ/kg)⁴³⁰. An additional study conducted by Tsitsias et al. revealed that the use of a Ni/CeZr catalyst for 20 h of continuous operation at a temperature of 300 °C resulted in approximately 80% of C₁₅-C₁₈ hydrocarbons, which is considered to be acceptable⁴³¹. The data also showed high selectivity for C₁₇, revealing the dominance of the deCO_x pathway⁴³¹. In another separate study, Makcharoen examined the production of bio-jet fuel by using crude palm kernel oil with a 5% Pt/C catalyst and showed 58% bio-jet fuel yield with selectivity towards n-C₈-C₁₆ around 28%¹⁴¹. Nonetheless, the cold flow properties were found to be poor; thus, the addition of HZSM-5 to the Pt/C catalyst promoted cracking, aromatization, and isomerization, resulting in a reduction in the freezing point to 30 °C and aromatic content to 8%, thus shifting the boiling



range of the liquid product. Research has shown that involving H_2 into the HDO process improves the catalyst's longevity and reduces carbon emissions in the form of CO and CO_2 yet these methods necessitate a substantial amount of H_2 to produce the desirable hydrocarbons.

Instead of employing expensive hydrodeoxygenation techniques, deoxygenation with N_2 could be a viable alternative for producing second generation green fuel. This method offers substantial economic benefits compared with conventional hydroprocessing methods. A study conducted by Aziz et al. examined the transformation of Nyamplung oil into green fuel by employing a NiAg/ZH catalyst at 350 °C for 3 h. Their results showed a petrol selectivity of 4%, kerosene selectivity of 5%, and green fuel selectivity of 62%⁴³². Further research by Why et al. employed a Pd/C catalyst to convert jet fuel from PKO, which demonstrated the highest yield (99%) and favorable jet paraffin selectivity (□73%) but a lower aromatic concentration, resulting in a higher fuel blend²⁵¹. This clearly shows that the noble metal catalyst has high potential as the best catalyst for green fuel production.

However, the use of noble metals as catalysts is disadvantageous owing to their high manufacturing costs. Therefore, future prospects for green fuel production involve enhancing the quality, removing oxygen, increasing the yield, and improving the selectivity toward diesel or jet fuel chains. Additionally, efforts should be made to improve the properties of SAF by adjusting the aromatic content to the desired level without compromising the yield. Furthermore, the aim is to reduce production costs by utilizing non-noble metal catalysts and eliminating the need for external H_2 . Researchers have developed substitute catalysts made of non-noble elements to prevent the consumption of precious metal catalysts. Numerous investigations have indicated that catalysts made of nickel can be as efficient as noble metals in the manufacturing of environmentally friendly diesel fuel for the reasons mentioned above. As a result, Ni metal has been created because of its superior features, such as a large number of active sites and high acidity, which enhances the effectiveness of the catalyst. In addition,



monometallic Ni catalysts have a high impact on excess cracking, producing more undesirable products and leading to catalyst deactivation during coke formation. Hence, to improve the catalyst properties, bimetallic catalysts can be produced by adding a second metal to inhibit coke formation and increase the hydrocarbon yield has been studied. The objective of future green fuel production involves lowering manufacturing expenses in order to achieve a commercially feasible scale of equipment that is both economically viable and yields high catalytic activity. This can be accomplished in two ways. The first option is to employ economical or industrial scrap of transition metals such as Ni and Co, as the predecessor for the catalyst. Palm kernel oil (PKO) is a refined waste output that can also reduce the rivalry between energy, supply, and sustenance. Furthermore, by advancing catalysts or implementing technology that eliminates the need for an external hydrogen supply, it is possible to reduce the operational pressure and the amount of hydrogen consumed.

Conclusion

Deoxygenation represents a potentially viable alternative method for converting biofuels from renewable feedstocks, specifically non-edible oils such as ceiba and palm kernel oil (PKO), into hydrocarbon-fuel-like fuels that are identical in chains and comparable in quality to conventional fuels. However, numerous obstacles must be overcome before attaining this objective. The primary emphasis of research has been on the deoxygenation of inedible feedstock. Nevertheless, the composition of biomass oil is intricate, frequently comprising of various free fatty acids and esters. Therefore, further research should be conducted on novel catalysts by using non-noble metals such as iron-based catalysts and catalytic deoxygenation processes tailored to various biomass feedstocks. Iron is the fourth most abundant transition element in the Earth's crust. It is environmentally safe and plays a crucial role in society as a significant metal. Furthermore, catalysts containing iron (Fe) exhibited a more efficient water



gas shift process, characterized by a lower hydrogen to carbon monoxide (H_2/CO) ratio and a strong affinity for oxygen. This affinity facilitates the breaking of carbon-oxygen (C-O) bonds by binding to the oxygen atom in the C=O group of oleic acid. These iron oxide species possess a robust affinity for oxygen-deprived regions, allowing them to increase the adhesion and activation of oxygenated compounds more efficiently than nickel. However, the selectivity and activity of catalysts during the conversion of biomass feedstock into biofuels may be impeded by the complex composition of these materials. Catalyst deactivation is an additional significant obstacle in the deoxygenation process. Irrespective of the catalyst composition (noble or non-noble metal), the formation of even a negligible amount of coke leads to toxicity and causes deactivation. The major findings of this review are that bimetallic NiCo catalysts on magnetite supports demonstrate high efficiency in converting PKO into SA), achieving significant kerosene range selectivity through deoxygenation. Additionally, optimizing catalyst design and exploring alternative feedstocks are crucial for improving energy efficiency, reducing environmental impact, and ensuring the scalability of SAF production. Future research should focus on developing novel, iron-based catalysts to enhance the deoxygenation of complex biomass oils, ensuring greater efficiency and selectivity while reducing catalyst deactivation. Additionally, efforts should be directed toward creating catalysts resistant to coke formation or those that can be easily regenerated to optimize the sustainability and economic viability of biofuel production. Consequently, in the future, it is necessary to develop novel catalysts that are resistant to coke formation or can be regenerated through straightforward processes. As previously stated, economic factors support the advancement of catalysts composed of iron-based catalysts.



Acknowledgement

View Article Online
DOI: 10.1039/D5YA00078E

This research was financially supported by the Ministry of Higher Education, Malaysia, for niche area research under the Higher Institution Centre of Excellence (HICoE) program (JPT(BKPI)1000/016/018/28 Jld.3(2) & NANOCAT-2024E) and the financial support from the PUTRA grant-UPM (Vot No: 9344200), MOSTI-e Science (Vot No: 5450746), Geran Putra Berimpak (GPB) UPM/800-3/3/1/GPB/2018/9658700

References

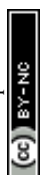
- 1 J. Rosen, *New York Times*.
- 2 S. H. H. Al-Jaberi, U. Rashid, F. A. J. Al-Doghachi, G. Abdulkareem-Alsultan and Y. H. Taufiq-Yap, *Energy Convers. Manag.*, 2017, **139**, 166–174.
- 3 A. G. Alsultan, N. Asikin Mijan, N. Mansir, S. Z. Razali, R. Yunus and Y. H. Taufiq-Yap, *ACS Omega*, 2021, **6**, 408–415.
- 4 Climate Change - NASA Science, <https://science.nasa.gov/climate-change/>, (accessed 28 December 2024).
- 5 N. A. M. Aziz, R. Yunus, H. A. Hamid, A. A. K. Ghassan, R. Omar, U. Rashid and Z. Abbas, *Sci. Rep.*, 2020, **10**, 1–17.
- 6 X. Y. Ooi, W. Gao, H. C. Ong, H. V. Lee, J. C. Juan, W. H. Chen and K. T. Lee, *Renew. Sustain. Energy Rev.*, 2019, **112**, 834–852.
- 7 H. S. Roh, I. H. Eum, D. W. Jeong, B. E. Yi, J. G. Na and C. H. Ko, *Catal. Today*, 2011, **164**, 457–460.
- 8 P. Kumar, S. R. Yenumala, S. K. Maity and D. Shee, *Appl. Catal. A Gen.*, 2014, **471**, 28–38.
- 9 F. Hameed Kamil, A. Salmiaton, R. Mohamad Hafriz Raja Shahrizzaman, R. Omar, A. Ghassan Alsultsan, H. K. Faten, A. Salmiaton, R. M. H. R. Shahrizzaman, R. Omar



- and A. G. Alsultsan, *Bull. Chem. React. Eng. Catal.*, 2017, **12**, 81–88.
- 10 G. Abdulkareem-Alsultan, N. Asikin-Mijan, L. K. Obeas, R. Yunus, S. Z. Razali, A. Islam and Y. Hin Taufiq-Yap, *Chem. Eng. J.*, 2022, **429**, 132206.
 - 11 N. Arun, R. V Sharma and A. K. Dalai, *Renew. Sustain. Energy Rev.*, 2015, **48**, 240–255.
 - 12 S. Kouider Elouahed, N. Asikin-Mijan, A. Alsultan G., O. Kaddour, M. R. Yusop, H. Mimoun, S. Samidin, N. Mansir and Y. H. Taufiq-Yap, *Energy Convers. Manag.*, 2024, **303**, 118185.
 - 13 T.-Y. Y. . Abdulkareem-Alsultan G., Asikin-Mijan N., Lee H.V., G. Abdulkareem-Alsultan, N. Asikin-Mijan, H. V. Lee and Y. H. Taufiq-Yap, in *Innovations in Sustainable Energy and Cleaner Environment. Green Energy and Technology*, ed. R. A. Gupta A., De A., Aggarwal S., Kushari A., Springer Singapore, 2020, pp. 489–504.
 - 14 N. Asikin-Mijan, H. V. Lee, J. C. Juan, A. R. Noorsaadah, H. C. Ong, S. M. Razali and Y. H. Taufiq-Yap, *Appl. Catal. A Gen.*, 2018, **552**, 38–48.
 - 15 N. Asikin-Mijan, H. V. Lee, Y. H. Taufiq-Yap, G. Abdulkrem-Alsultan, M. S. Mastuli and H. C. Ong, *Energy Convers. Manag.*, 2017, **141**, 325–338.
 - 16 N. Mansir, H. M. Sidek, S. H. Teo, N.-A. Mijan, A. G. Alsultan, C. H. Ng, M. R. Shamsuddin and Y. H. Taufiq-Yap, *Bioresour. Technol. Reports*, 2022, **17**, 100988.
 - 17 E. Abd-Alkuder Salman, K. Abaid Samawi, M. Fawzi Nassar, G. Abdulkareem-Alsultan and E. Abdulmalek, *J. Electroanal. Chem.*, 2023, **945**, 117629.
 - 18 L. Hermida, A. Z. Abdullah and A. R. Mohamed, *Renew. Sustain. Energy Rev.*, 2015, **42**, 1223–1233.
 - 19 M. Ameen, M. T. Azizan, S. Yusup, A. Ramli and M. Yasir, *Renew. Sustain. Energy Rev.*, 2017, **80**, 1072–1088.
 - 20 M. M. X. Lum, K. H. Ng, S. Y. Lai, A. R. Mohamed, A. G. Alsultan, Y. H. Taufiq-



- Yap, M. K. Koh, M. A. Mohamed, D. V. N. Vo, M. Subramaniam, K. S. Mulya and N. Imanuella, *Process Saf. Environ. Prot.*, 2023, **176**, 580–604.
- 21 A. Zheng, Z. Huang, G. Wei, K. Zhao, L. Jiang, Z. Zhao, Y. Tian and H. Li, *Iscience*, 2020, **23**, 100814.
- 22 S. Z. Razali, R. Yunus, D. Kania, S. A. Rashid, L. H. Ngee, G. Abdulkareem-Alsultan and B. M. Jan, *J. Mater. Res. Technol.*, 2022, **21**, 2891–2905.
- 23 S. Janampelli and S. Darbha, *Catal. Today*, 2018, **309**, 219–226.
- 24 C. Detoni, F. Bertella, M. M. V. M. Souza, S. B. C. Pergher and D. A. G. Aranda, *Appl. Clay Sci.*, 2014, **95**, 388–395.
- 25 L. N. Silva, I. C. P. Fortes, F. P. De Sousa and V. M. D. Pasa, *Fuel*, 2016, **164**, 329–338.
- 26 N. Asikin-Mijan, J. C. Juan, Y. H. Taufiq-Yap, H. C. Ong, Y. C. Lin, G. Abdulkareem-Alsultan and H. V. Lee, *Catal. Commun.*, 2023, **182**, 106741.
- 27 K. Abaid Samawi, E. Abd-Alkuder Salman, B. Abd-Alsatar Alshekhly, M. Fawzi Nassar, M. Yousefzadeh Borzehandani, G. Abdulkareem-Alsultan, M. Alif Mohammad Latif and E. Abdulmalek, *Comput. Theor. Chem.*, 2022, **1212**, 113725.
- 28 A. Abdulkareem Ghassan, N.-A. Mijan and Y. Hin Taufiq-Yap, in *Nanorods and Nanocomposites*, 2020.
- 29 S. Oh, J. H. Lee, I.-G. Choi and J. W. Choi, *Renew. Energy*, 2020, **149**, 1–10.
- 30 K. A. Rogers and Y. Zheng, *ChemSusChem*, 2016, **9**, 1750–1772.
- 31 K. A. Samawi, S. J. Abdulrazzaq, M. Zorah, M. Al-Bahrani, H. A. M. A. Mahmoud, G. Abdulkareem-Alsultan, A. G. Taki and M. F. Nassar, *J. Solid State Chem.*, 2024, **334**, 124690.
- 32 G. Abdulkareem-Alsultan, N. Asikin-Mijan and Y. H. Taufiq-Yap, in *Key Engineering Materials*, 2016, vol. 707, pp. 175–181.



- 33 S. T. Lim, S. Sethupathi, A. G. Alsultan and Y. Munusamy, *Energy and Fuels*, 2021, **35**, 16212–16221. View Article Online
DOI:10.1039/D5YA00078E
- 34 N. Hongloi, P. Prapainainar, A. Seubsai, K. Sudsakorn and C. Prapainainar, *Energy*, 2019, **182**, 306–320.
- 35 K. B. Baharudin, Y. H. Taufiq-Yap, J. Hunns, M. Isaacs, K. Wilson and D. Derawi, *Microporous Mesoporous Mater.*, 2019, **276**, 13–22.
- 36 N. Asikin-Mijan, H. Mohd Sidek, A. G. AlSultan, N. A. Azman, N. A. Adzahar and H. C. Ong, *Catalysts*, 2021, **11**, 1470.
- 37 R. S. R. M. Hafriz, I. Nor Shafizah, A. Salmiaton, N. A. Arifin, R. Yunus, Y. H. Taufiq Yap and S. Abd Halim, *Comparative study of transition metal-doped calcined Malaysian dolomite catalysts for WCO deoxygenation reaction*, King Saud University, 2020, vol. 13.
- 38 F. Batool, T. A. Kurniawan, A. Mohyuddin, M. H. D. Othman, I. Ali, G. Abdulkareem-Alsultan, A. Anouzla, H. H. Goh, D. Zhang, F. Aziz and K. Wayne Chew, *Chem. Eng. Sci.*, 2024, **293**, 120057.
- 39 M. Safa Gamal, N. Asikin-Mijan, M. Arumugam, U. Rashid and Y. H. Taufiq-Yap, *J. Anal. Appl. Pyrolysis*, 2019, **144**, 104690.
- 40 A. G. Alsultan, N. Asikin-Mijan, L. K. Obeas, A. Islam, N. Mansir, S. H. Teo, S. Z. Razali, M. F. Nassar, S. Mohamad and Y. H. Taufiq-Yap, *Catalysts*, 2022, **12**, 566.
- 41 N. A. Abdul Razak, N.-A. Mijan, Y. H. Taufiq-Yap and D. Derawi, *J. Clean. Prod.*, 2022, **366**, 132971.
- 42 M. H. Wondi, R. Shamsudin, R. Yunus, G. A. Alsultan and A. H. Iswardi, *J. Food Process Eng.*, DOI:10.1111/jfpe.13426.
- 43 I. Shah, R. Adnan, A. G. Alsultan and Y. H. Taufiq-Yap, *J. Dispers. Sci. Technol.*, 2020, **0**, 1–16.



- 44 A. Shamil Albazzaz, *J. Energy, Environ. Chem. Eng.*, 2018, **3**, 40. View Article Online
DOI: 10.1039/D5YA00078E
- 45 A. M. Robinson, J. E. Hensley and J. Will Medlin, *ACS Catal.*, 2016, **6**, 5026–5043.
- 46 T. Nordgreen, T. Liliedahl and K. Sjöström, *Fuel*, 2006, **85**, 689–694.
- 47 A. Afiqah-Idrus, G. Abdulkareem-Alsultan, N. Asikin-Mijan, M. Fawzi Nassar, L. Voon, S. Hwa Teo, T. Agustiono Kurniawan, N. Athirah Adzahar, M. Surahim, S. Zulaika Razali, A. Islam, R. Yunus, N. Alomari and Y. Hin Taufiq-Yap, *Energy Convers. Manag. X*, 2024, **23**, 100589.
- 48 R. E. Nugraha, A. R. Y. Sunarti, H. Tehubijuluw and Z. Mumtazah, *J. Kim. Ris.*, 2022, **7**, 81–93.
- 49 S. Li and J. Gong, *Chem. Soc. Rev.*, 2014, **43**, 7245–56.
- 50 K. A. Samawi, B. A. Mohammed, E. A. A. Salman, H. A. M. A. Mahmoud, A. Z. Sameen, S. M. Mohealdeen, G. Abdulkareem-Alsultan and M. F. Nassar, *Phys. Chem. Chem. Phys.*, 2024, **26**, 9284–9294.
- 51 European Commission, EUR-Lex - 52019DC0640 - EN - EUR-Lex, <https://eur-lex.europa.eu/legal-content/EN/TXT/?uri=COM%3A2019%3A640%3AFIN%0Ahttps://eur-lex.europa.eu/legal-content/EN/TXT/?qid=1596443911913&uri=CELEX:52019DC0640#document2%0Ahttps://eur-lex.europa.eu/legal-content/IT/ALL/?uri=CELEX:52019DC0640%0Ahttps://>, (accessed 20 January 2024).
- 52 K. A. Samawi, E. A. A. Salman, H. A. Hasan, H. A. M. A. Mahmoud, S. M. Mohealdeen, G. Abdulkareem-Alsultan, E. Abdulmalek and M. F. Nassar, *Mol. Syst. Des. Eng.*, 2024, **9**, 464–476.
- 53 S. T. Lim, S. Sethupathi, A. G. Alsultan, L. K. Leong and Y. H. Taufiq-Yap, *Key Eng. Mater.*, 2020, **853 KEM**, 228–234.



- 54 Paris Agreement, The Paris Agreement | UNFCCC, <https://unfccc.int/process-and-meetings/the-paris-agreement>, (accessed 20 January 2024). View Article Online
DOI: 10.1039/D5YA00078E
- 55 N. Asikin, H. V. Lee, G. A. Alsultan and T. Yap, *Mater. Sci. Forum*, 2016, **840**, 353–358.
- 56 M. S. Forum, DOI:10.4028/www.scientific.net/MSF.840.353.
- 57 G. Ceballos, P. R. Ehrlich, A. D. Barnosky, A. García, R. M. Pringle and T. M. Palmer, *Sci. Adv.*, 2015, **1**, e1400253.
- 58 P. M. Cox, R. A. Betts, C. D. Jones, S. A. Spall and I. J. Totterdell, *Nature*, 2000, **408**, 184–187.
- 59 R. E. Gullison, P. C. Frumhoff, J. G. Canadell, C. B. Field, D. C. Nepstad, K. Hayhoe, R. Avissar, L. M. Curran, P. Friedlingstein and C. D. Jones, *Science (80-.)*, 2007, **316**, 985–986.
- 60 H. Chang, G. Abdulkareem-Alsultan, Y. H. Taufiq-Yap, S. Mohd Izham and S. Sivasangar, *Fuel*, 2024, **355**, 129459.
- 61 E. J. Dlugokencky, L. P. Steele, P. M. Lang and K. A. Masarie, *J. Geophys. Res.*, 2022, **99**, 17021–17043.
- 62 A. P. Schurer, M. E. Mann, E. Hawkins, S. F. B. Tett and G. C. Hegerl, *Nat. Clim. Chang.*, 2017, **7**, 563–567.
- 63 H. A. Alrazen, S. M. Aminossadati, H. A. Mahmood, M. M. Hasan, G. Abdulkreem-Alsultan and M. Konarova, *Energy*, 2023, **282**, 128754.
- 64 M. X. Y. Ravindran, N. Asikin-Mijan, H. C. Ong, D. Derawi, M. R. Yusof, M. S. Mastuli, H. V. Lee, W. N. A. S. Wan Mahmood, M. S. Razali, G. Abdulkareem Al-Sultan and Y. H. Taufiq-Yap, *J. Anal. Appl. Pyrolysis*, 2022, **168**, 105772.
- 65 N. A. Adzahar, N. Asikin-Mijan, M. I. Saiman, G. A. Alsultan, M. S. Mastuli, M. R. Shamsuddin and Y. H. Taufiq-Yap, *RSC Adv.*, 2022, **12**, 16903–16917.



- 66 I. E. Agency, *World energy outlook*, OECD/IEA Paris, 2009. View Article Online
DOI: 10.1039/D5YA00078E
- 67 L. K. Obeas, A. khalid ghalib, G. A. kareem-Alsultan, N. A.- Mijan and R. Yunus, *Orient. J. Chem.*, 2021, **37**, 256–268.
- 68 K. Davron, T. A. Kurniawan, B. Akbarbek, E. Rasulbek, N. Shavkat, B. Zebo, F. Batool and G. AbdulKareem-Alsultan, *J. Taiwan Inst. Chem. Eng.*, 2024, **166**, 105481.
- 69 H. Wang, Z. Lei, X. Zhang, B. Zhou and J. Peng, *Energy Convers. Manag.*, 2019, **198**, 111799.
- 70 N. Asikin-Mijan, D. Derawi, N. Salih, J. Salimon, G. A. Alsultan, M. S. Mastuli and M. X. Y. Ravindran, *Innov. Thermochem. Technol. Biofuel Process.*, 2022, 197–219.
- 71 B. Pillot, M. Muselli, P. Poggi and J. B. Dias, *Energy Policy*, 2019, **127**, 113–124.
- 72 S. H. Teo, C. H. Ng, A. Islam, G. Abdulkareem-Alsultan, C. G. Joseph, J. Janaun, Y. H. Taufiq-Yap, S. Khandaker, G. J. Islam, H. Znad and M. R. Awual, *J. Clean. Prod.*, 2022, **332**, 130039.
- 73 K. L. Yu, B. S. Zainal, H. Mohamed, P. J. Ker, H. C. Ong, H. B. Zaman, G. Abdulkareem-Alsultan and Y. H. Taufiq-Yap, *Int. J. Hydrogen Energy*, DOI:10.1016/j.ijhydene.2024.04.023.
- 74 U.S. Energy Information Administration, Biomass explained - U.S. Energy Information Administration, <https://www.eia.gov/energyexplained/biomass/>, (accessed 5 April 2024).
- 75 U. S. Department of Energy, 5 Everyday Products Made from Biomass: A Few May Surprise You | Department of Energy, <https://www.energy.gov/eere/articles/5-everyday-products-made-biomass-few-may-surprise-you>, (accessed 5 April 2024).
- 76 W. Dizayee, M. M. Hamarashid, M. Zorah, H. A. M. A. Mahmoud, M. Al-Bahrani, A. G. Taki, G. Abdulkareem-Alsultan and M. F. Nassar, *J. Alloys Compd.*, 2024, **1004**, 175825.



- 77 E. Emmanouilidou, A. Lazaridou, S. Mitkidou and N. C. Kokkinos, *J. Mol. Struct.*, 2024, **1306**, 137870. View Article Online
DOI: 10.1039/D5YA00078E
- 78 Megawati, Z. A. S. Bahlawan, A. Damayanti, R. D. A. Putri, B. Triwibowo, H. Prasetiawan, S. P. K. Aji and A. Prawisnu, *Mater. Today Proc.*, 2022, **63**, S373–S378.
- 79 M. Sadeghi and M. H. Husseini, *J. Appl. Chem. Res.*, 2013, **7**, 39–49.
- 80 I. Abrantes, A. F. Ferreira, A. Silva and M. Costa, *J. Clean. Prod.*, 2021, **313**, 127937.
- 81 T. A. Kurniawan, M. Riaz, A. Mohyuddin, A. Haider, S. Ali, G. Abdulkareem-
Alsultan, M. H. D. Othman, H. H. Goh, A. Anouzla, H. E. Al-Hazmi, F. Aziz, Y.
Wibisono, T. D. Kusworo, S. A. A. Alkhadher and M. M. H. Khan, *Inorganic
membrane: a game changer for gas separation and purification*, Springer International
Publishing, 2024, vol. 78.
- 82 T. A. Kurniawan, S. Khan, A. Mohyuddin, A. Haider, T. M. T. Lei, M. H. D. Othman,
H. H. Goh, D. Zhang, A. Anouzla, F. Aziz, M. Mahmoud, I. Ali, S. Haddout, G.
AbdulKareem-Alsultan and S. A. A. Alkhadher, *Chem. Pap.*, 2024, **78**, 6843–6871.
- 83 J. Holladay, Z. Abdullah and J. Heyne, *U.S. Dep. Energy - Off. Energy Effic. Renew.
Energy*, 2020, **September**, Report No. DOE/EE-2041.
- 84 International Energy Agency, Aviation - IEA, <https://www.iea.org/energy-system/transport/aviation>, (accessed 17 January 2024).
- 85 IATA, IATA - Air Passenger Numbers to Recover in 2024,
<https://www.iata.org/en/pressroom/2022-releases/2022-03-01-01/>.
- 86 F. N. Maadh, E. Abdulmalek, M. F. Ismail, S. A. A. Ahmad and G. Abdulkreem-
Alsultan, *High Energy Chem.*, 2024, **58**, 16–58.
- 87 A. Islam, S. H. Teo, M. T. Islam, A. H. Mondal, H. Mahmud, S. Ahmed, M. Ibrahim,
Y. H. Taufiq-Yap, A. A. G., M. L. Hossain, M. C. Sheikh, A. I. Rasee, A. I. Rehan, R.
M. Waliullah, M. E. Awual, M. M. Hasan, M. S. Hossain, K. T. Kubra, M. S. Salman,



- M. N. Hasan and M. R. Awual, *Renew. Sustain. Energy Rev.*, DOI:10.1016/j.rser.2024.115033.
- 88 C. Gutiérrez-Antonio, F. I. Gómez-Castro and S. Hernández, *Chem. Eng. Trans.*, 2018, **69**, 319–324.
- 89 A. R. Abu Talib, Y. S. M. Altarazi, J. Yu, E. Gires, M. Fahmi Abdul Ghafir, A. Tahmasebi, T. Yusaf, A. G. Alsultan and R. Yunus, *Fuel*, 2024, **378**, 132860.
- 90 M. Y. Albalushi, G. Abdulkreem-Alsultan, N. Asikin-Mijan, M. I. bin Saiman, Y. P. Tan and Y. H. Taufiq-Yap, *Catalysts*, 2022, **12**, 1537.
- 91 L. Zhang, T. L. Butler and B. Yang*, *Green Energy to Sustain. Strateg. Glob. Ind.*, 2020, 85–110.
- 92 A. Ghassan Alsultan, N. Asikin-Mijan, L. Kareem Obeas, A. Isalam, N. Mansir, M. Fawzi Nassar, S. Zulaika Razali, R. Yunus and Y. Hin Taufiq-Yap, *Biochar - Product. Technol. Prop. Appl.*, DOI:10.5772/intechopen.104984.
- 93 ICAO, Carbon offsetting and reduction scheme for international aviation (CORSIA), https://info.carbon-clear.com/hubfs/Factsheets/CORSIA/CORSIA_Factsheet_EN.pdf?submissionGuid=c319185f-35af-4e9a-b10a-8875f97a53c2, (accessed 2 April 2024).
- 94 H. Chang, H. V. Lee, Y. H. Taufiq-Yap, G. Abdulkareem-Alsultan and S. Seenivasagam, *Renew. Energy*, 2025, **238**, 121882.
- 95 IATA, *Int. Air Transp. Assoc.*, 2021, 1–3.
- 96 IATA, *IATA Fact sheet*, 2023, 1–3.
- 97 and M. F. N. Alshaer, Fadwa, Mohammed Zorah, HassabAlla MA Mahmoud, L. M. Abdalgadir, Anmar Ghanim Taki, Bassam A. Mohammed, G. Abdulkareem-Alsultan, *Mater. Today Commun.*, 2023, 107836.
- 98 A. ASTM, *DoiOrg/101520/D7566-19*.



- 99 B. S. Zainal, K. L. Yu, H. C. Ong, H. Mohamed, P. J. Ker, G. Abdulkareem-^{View Article Online}
^{DOI: 10.1039/D5YA00078E}Alsultan, Y. H. Taufiq-Yap and T. I. Mahlia, *Process Saf. Environ. Prot.*, 2024, **192**, 424–436.
- 100 N. A. Adzahar, G. AbdulKareem-Alsultan, N. A. Mijan, M. S. Mastuli, H. V. Lee and
 Y. H. Taufiq-Yap, *Energy*, 2025, **314**, 133957.
- 101 G. Omer-Alsultan, A. A. Alsahlani, G. Mohamed-Alsultan, G. Abdulkareem-Alsultan,
 M. F. Nassar, T. A. Kurniawan and Y. H. Taufiq-Yap, *Towards zero emission:
 exploring innovations in wind turbine design for sustainable energy a comprehensive
 review*, Springer London, 2024.
- 102 S. Kramer, G. Andac, J. Heyne, J. Ellsworth, P. Herzig and K. C. Lewis, *Front. Energy
 Res.*, 2022, **9**, 782823.
- 103 T. A. Kurniawan, M. Ali, A. Mohyuddin, A. Haider, M. H. D. Othman, A. Anouzla, H.
 H. Goh, D. Zhang, W. Dai, F. Aziz, M. I. Khan, I. Ali, M. Mahmoud, S. A. A.
 Alkhadher and G. A. Alsultan, *Process Saf. Environ. Prot.*, 2025, **193**, 643–664.
- 104 S. Samidin, A. Anuar, G. Abdulkareem-Alsultan, N. Asikin-Mijan, W. N. R. W.
 Isahak, L. H. Voon, S. Y. Lai, S. M, S. Ali, M. R. Shamsuddin and Y. H. Taufiq-Yap,
Chem. Pap., DOI:10.1007/s11696-024-03795-7.
- 105 S. Samidin, W. N. R. W. Isahak, K. N. Ahmad, N. A. Mijan, M. R. Yusop, A. Samsuri,
 G. Abdulkareem-Alsultan and M. A. Yarmo, *Fuel*, 2024, **373**, 132370.
- 106 N. A. Mohamad Aziz, Y. K. Ling, H. Mohamed, B. S. Zainal, H. B. Zaman and A. G.
 Alsultan, *IOP Conf. Ser. Earth Environ. Sci.*, DOI:10.1088/1755-1315/1372/1/012032.
- 107 S. De Jong, K. Antonissen, R. Hoefnagels, L. Lonza, M. Wang, A. Faaij and M.
 Junginger, *Biotechnol. Biofuels*, 2017, **10**, 1–18.
- 108 N. Azri, R. Irmawati, U. I. Nda-Umar, M. I. Saiman, Y. H. Taufiq-Yap and G.
 Abdulkareem-Alsultan, *Pertanika J. Sci. Technol.*, 2024, **32**, 1141–1159.
- 109 G. Abdulkareem-alsultan, H. Voon, N. Asikin-mijan, S. Samidin and N. Athirah,



- Techno-Economic , Environmental , Policy Status and Perspectives on Sustainable Resource Conversion Into Transportation Fuels*, Elsevier, Second Edi., 2024.
- 110 G. Liu, B. Yan and G. Chen, *Renew. Sustain. Energy Rev.*, 2013, **25**, 59–70.
- 111 G. Abdulkareem-alsultan, N. Asikin-mijan, M. Fawzi, S. Samidin, N. Athirah and L. Hwei, *Hydrogen Production From Methanol Reforming Processes*, Elsevier, Second Edi., 2024.
- 112 H. Wei, W. Liu, X. Chen, Q. Yang, J. Li and H. Chen, *Fuel*, 2019, **254**, 115599.
- 113 G. Abdulkareem-Alsultan, N. Asikin-Mijan, M. F. Nassar, S. Samidin, N. A. Adzahar, L. H. Voon, T. A. Kurniawan and Y. H. Taufiq-Yap, *Biodiesel Blend With Different Alcohol Emission Evaluation*, Elsevier, Second Edi., 2024.
- 114 G. A. Alsultan, N. Asikin-Mijan, H. V. Lee, A. S. Albazzaz and Y. H. Taufiq-Yap, *Energy Convers. Manag.*, 2017, **151**, 311–323.
- 115 R. S. R. M. Hafriz, S. H. Habib, N. A. Raof, M. Y. Ong, C. C. Seah, S. Z. Razali, R. Yunus, N. M. Razali and A. Salmiaton, *Energy Convers. Manag. X*, 2024, **24**, 100749.
- 116 C. S. Smoljan, J. M. Crawford and M. A. Carreon, *Catal. Commun.*, 2020, **143**, 106046.
- 117 D. Septriana, 2023, **23**, 128–141.
- 118 R. S. R. M. Hafriz, S. H. Habib, N. A. Raof, S. Z. Razali, R. Yunus, N. M. Razali and A. Salmiaton, *J. Taiwan Inst. Chem. Eng.*, 2024, **165**, 105700.
- 119 B. S. N. Afzanizam, B. M. J. M. Nazri, T. Chongcheng and N. Johan, *Am-Eur J Sustain Agric.*
- 120 T. G. Kreutz, E. D. Larson, G. Liu and R. H. Williams, in *25th annual international Pittsburgh coal conference*, International Pittsburgh Coal Conference Pittsburgh, Pennsylvania, 2008, vol. 29.
- 121 D. Leckel, *Energy & Fuels*, 2009, **23**, 2342–2358.



- 122 R. Luque, A. R. de la Osa, J. M. Campelo, A. A. Romero, J. L. Valverde and P. Sanchez, *Energy Environ. Sci.*, 2012, **5**, 5186–5202.
- 123 S. L. Soled, E. Iglesia, R. A. Fiato, J. E. Baumgartner, H. Vroman and S. Miseo, *Top. Catal.*, 2003, **26**, 101–109.
- 124 M. A. Vannice and R. L. Garten, *J. Catal.*; (United States).
- 125 A. P. Steynberg, M. E. Dry, B. H. Davis and B. B. Breman, in *Fischer-Tropsch Technology*, eds. A. Steynberg and M. B. T.-S. in S. S. and C. Dry, Elsevier, 2004, vol. 152, pp. 64–195.
- 126 C. H. Zhang, Y. Yang, B. T. Teng, T. Z. Li, H. Y. Zheng, H. W. Xiang and Y. W. Li, *J. Catal.*, 2006, **237**, 405–415.
- 127 J. Li, X. Cheng, C. Zhang, W. Dong, Y. Yang and Y. Li, *Catal. Letters*, 2016, **146**, 2574–2584.
- 128 D. Xu, W. Li, H. Duan, Q. Ge and H. Xu, *Catal. Letters*, 2005, **102**, 229–235.
- 129 M. F. Shahriar and A. Khanal, *Fuel*, 2022, **325**, 124905.
- 130 A. Ringsred, S. van Dyk and J. J. Saddler, *Appl. Energy*, 2021, **287**, 116587.
- 131 T. Hanaoka, T. Miyazawa, K. Shimura and S. Hirata, *Fuel Process. Technol.*, 2015, **129**, 139–146.
- 132 B.-Y. Yu and C.-C. Tsai, *Chem. Eng. Res. Des.*, 2020, **159**, 47–65.
- 133 X. Xue, X. Hui, P. Singh and C.-J. Sung, *Fuel*, 2017, **210**, 343–351.
- 134 M. J. A. Romero, A. Pizzi, G. Toscano, G. Busca, B. Bosio and E. Arato, *Waste Manag.*, 2016, **47**, 62–68.
- 135 M. Žula, M. Grilc and B. Likozar, *Chem. Eng. J.*, 2022, **444**, 136564.
- 136 M. S. Sowe, A. R. Lestari, E. Novitasari, M. Masruri and S. M. Ulfa, *Bull. Chem. React. Eng. Catal.*, 2022, **17**, 135–145.
- 137 Y. Wu, X. Liu, J. Zhang, Y. Zhang, X. Li, H. Xia and F. Wang, *Ind. Eng. Chem. Res.*,



- 2022, **61**, 12338–12348.
- 138 S. Shao, X. Hu, W. Dong, X. Li, H. Zhang, R. Xiao and Y. Cai, *J. Clean. Prod.*, 2021, **282**, 124331.
- 139 A. Çakan, B. Kiren and N. Ayas, *Mol. Catal.*, 2023, **546**, 113219.
- 140 A. A. Ayandiran, P. E. Boahene, S. Nanda, A. K. Dalai and Y. Hu, *Mol. Catal.*, 2022, **523**, 111358.
- 141 M. Makcharoen, A. Kaewchada, N. Akkarawatkhoosith and A. Jaree, *Energy Convers. Manag. X*, 2021, **12**, 100125.
- 142 S. Khan, K. M. Qureshi, A. N. Kay Lup, M. F. A. Patah and W. M. A. Wan Daud, *Biomass and Bioenergy*, 2022, **164**, 106563.
- 143 C. Papadopoulos, E. Kordouli, L. Sygellou, K. Bourikas, C. Kordulis and A. Lycourghiotis, *Fuel Process. Technol.*, 2021, **217**, 106820.
- 144 H. Pan, X. Zhou, S. Xie, Z. Du, G. Li, C. Zhang, Y. Luo and X. Zhang, *Biomass and Bioenergy*, 2022, **165**, 106592.
- 145 M. Azkaar, Z. Vajglova, P. Mäki-Arvela, A. Aho, N. Kumar, H. Palonen, K. Eränen, M. Peurla, L. A. Kulikov and A. L. Maximov, *Fuel*, 2020, **278**, 118193.
- 146 T. Li, J. Cheng, R. Huang, J. Zhou and K. Cen, *Bioresour. Technol.*, 2015, **197**, 289–294.
- 147 X. Wu, P. Jiang, F. Jin, J. Liu, Y. Zhang, L. Zhu, T. Xia, K. Shao, T. Wang and Q. Li, *Fuel*, 2017, **188**, 205–211.
- 148 G. J. Bishop and B. Elvers, *Handb. Fuels Energy Sources Transp.*, 2021, 503–527.
- 149 P. Bartocci, R. Tschentscher, Y. Yan, H. Yang, G. Bidini and F. Fantozzi, *Biofuel Prod. Technol. Crit. Anal. Sustain.*, 2020, 1–36.
- 150 A. G. Romero-Izquierdo, F. I. Gómez-Castro, C. Gutiérrez-Antonio, S. Hernández and M. Errico, *Chem. Eng. Process. Intensif.*, 2021, **160**, 108270.

View Article Online
DOI: 10.1039/D5YA00078E



- 151 S. M. Yui, in *Catalytic Hydroprocessing of Petroleum and Distillates*, CRC Press, 2020, pp. 236–252. View Article Online
DOI: 10.1039/D5YA00078E
- 152 E. Zikhonjwa, 2021.
- 153 D. T. Sarve, S. K. Singh and J. D. Ekhe, *Inorg. Chem. Commun.*, 2022, **139**, 109397.
- 154 S. Chuklina, A. Zhukova, Y. Fionov, M. Kadyko, A. Fionov, D. Zhukov, A. Il'icheva, L. Podzorova and I. Mikhaleiko, *ChemistrySelect*, 2022, **7**, e202203031.
- 155 S. Sahebdehfar, P. M. Bijani and F. Yaripour, *Fuel*, 2022, **310**, 122443.
- 156 T. K. Phung, L. P. Hernández, A. Lagazzo and G. Busca, *Appl. Catal. A Gen.*, 2015, **493**, 77–89.
- 157 K. Shimura, S. Yoshida, H. Oikawa and T. Fujitani, *Catalysts*, DOI:10.3390/catal13091303.
- 158 A. de Reviere, D. Gunst, M. Sabbe and A. Verberckmoes, *J. Ind. Eng. Chem.*, 2020, **89**, 257–272.
- 159 Y. Nakagawa, M. Yabushita and K. Tomishige, *RSC Sustain.*, 2023, **1**, 814–837.
- 160 Y. Shi, A. S. Weller, A. J. Blacker and P. W. Dyer, *Catal. Commun.*, 2022, **164**, 106421.
- 161 Y. Kim, H. B. Im, U. H. Jung, J. C. Park, M. H. Youn, H.-D. Jeong, D.-W. Lee, G. B. Rhim, D. H. Chun and K. B. Lee, *Fuel*, 2019, **256**, 115957.
- 162 L. Attanatho, S. Lao-ubol, A. Suemanotham, N. Prasongthum, P. Khowattana, T. Laosombut, N. Duangwongsa, S. Larpiattaworn and Y. Thanmongkhon, *SN Appl. Sci.*, 2020, **2**, 1–12.
- 163 P. Panpian, T. T. V. Tran, S. Kongparakul, L. Attanatho, Y. Thanmongkhon, P. Wang, G. Guan, N. Chanlek, Y. Poo-arporn and C. Samart, *Fuel*, 2021, **287**, 119831.
- 164 J. Gulbinski, L. Ren, V. Vattipalli, H. Chen, J. Delaney, P. Bai, P. Dauenhauer, M. Tsapatsis, O. A. Abdelrahman and W. Fan, *Ind. Eng. Chem. Res.*, 2020, **59**, 22049–



22056.

View Article Online
DOI: 10.1039/D5YA00078E

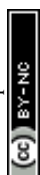
- 165 F. Jin, Y. Yan and G. Wu, *Catal. Today*, 2020, **355**, 148–161.
- 166 Z. Buniazet, A. Cabiach, S. Maury, D. Bianchi and S. Lorient, *Appl. Catal. B Environ.*, 2019, **243**, 594–603.
- 167 A. Milbrandt, C. Kinchin and R. McCormick, *Feasibility of producing and using biomass-based diesel and jet fuel in the United States*, National Renewable Energy Lab.(NREL), Golden, CO (United States), 2013.
- 168 A. Ahmad, F. Banat and H. Taher, *Environ. Technol. Innov.*, 2020, **20**, 101138.
- 169 A. Iram, D. Cekmecelioglu and A. Demirci, *Processes*, 2020, **9**, 38.
- 170 J. Baeyens, H. Zhang, J. Nie, L. Appels, R. Dewil, R. Ansart and Y. Deng, *Renew. Sustain. Energy Rev.*, 2020, **131**, 110023.
- 171 M. Bomgardner, *Chem. Eng. News*, 2012, **90**, 8.
- 172 R. Davis, M. J. Bidy, E. Tan, L. Tao and S. B. Jones, *Biological conversion of sugars to hydrocarbons technology pathway*, Pacific Northwest National Lab.(PNNL), Richland, WA (United States), 2013.
- 173 R. K. Mawhood, E. Gazis, R. Hoefnagels, S. De Jong and R. Slade, .
- 174 J. C. McAuliffe, A. T. Nielsen, C. M. Peres, D. V Vavilina and D. H. Wells, *Google Patents*, 2015.
- 175 B. Kim, S. Lee, D. Jeong, J. Yang, M.-K. Oh and J. Lee, *PLoS One*, 2014, **9**, e105322.
- 176 A. N. Phan and T. M. Phan, *Fuel*, 2008, **87**, 3490–3496.
- 177 H. Chen, M. Ding, Y. Li, H. Xu, Y. Li and Z. Wei, *J. Traffic Transp. Eng. (English Ed.)*, 2020, **7**, 791–807.
- 178 P. Obando-Pacheco, A. J. Justicia-Grande, I. Rivero-Calle, C. Rodríguez-Tenreiro, P. Sly, O. Ramilo, A. Mejías, E. Baraldi, N. G. Papadopoulos and H. Nair, *J. Infect. Dis.*, 2018, **217**, 1356–1364.



- 179 D. Kim, M. Hanifzadeh and A. Kumar, *Environ. Prog. Sustain. Energy*, 2018, **37**, 7.
19.
- 180 R. Sotelo-Boyás, Y. Liu and T. Minowa, *Ind. Eng. Chem. Res.*, 2011, **50**, 2791–2799.
- 181 Y. Sugami, E. Minami and S. Saka, *Fuel*, 2016, **166**, 376–381.
- 182 C. A. Scaldaferri and V. M. D. Pasa, *Fuel*, 2019, **245**, 458–466.
- 183 M. Herskowitz, M. V Landau, Y. Reizner and D. Berger, *Fuel*, 2013, **111**, 157–164.
- 184 T. Kurniawan, A. Setiawan, N. A. Putri, A. Irawan, A. B. D. Nandiyanto and Y. Bindar, *Biomass Convers. Biorefinery*, 2023, **13**, 6847–6858.
- 185 A. Zikri and M. Aznury, in *IOP conference series: materials science and engineering*, IOP Publishing, 2020, vol. 823, p. 12026.
- 186 N. Srihanun, P. Dujjanutat, P. Muanruksa and P. Kaewkannetra, *Catalysts*, 2020, **10**, 241.
- 187 M. Ruangudomsakul, N. Osakoo, J. Wittayakun, C. Keawkumay, T. Butburee, S. Youngjan, K. Faungnawakij, Y. Poo-arporn, P. Kidkhunthod and P. Khemthong, *Mol. Catal.*, 2022, **523**, 111422.
- 188 M. M. Gui, K. T. Ñ. Lee and S. Bhatia, *Energy*, 2008, **33**, 1646–1653.
- 189 R. R. Watson and F. De Meester, *Handbook of cholesterol*, Wageningen Academic Publishers, 2016.
- 190 A. M. N. Renzaho, J. K. Kamara and M. Toole, *Renew. Sustain. Energy Rev.*, 2017, **78**, 503–516.
- 191 M. Khanna, W. Wang, T. W. Hudiburg and E. H. Delucia, *Nat. Commun.*, 2017, **8**, 1–9.
- 192 D. F. Correa, H. L. Beyer, H. P. Possingham, S. R. Thomas-Hall and P. M. Schenk, *Renew. Sustain. Energy Rev.*, 2017, **74**, 1131–1146.
- 193 D. J. Garcia and F. You, *J. Clean. Prod.*, 2018, **182**, 313–330.



- 194 W. Gerbens-Leenes and A. Y. Hoekstra, *Energy Environ. Sci.*, 2011, **4**, 2658–2668. View Article Online
DOI:10.1039/D5YA00078E
- 195 M. Munir, M. Saeed, M. Ahmad, A. Waseem, M. Alsaady, S. Asif, A. Ahmed, M. Shariq Khan, A. Bokhari, M. Mubashir, L. Fatt Chuah and P. Loke Show, *Fuel*, 2023, **332**, 126265.
- 196 M. Munir, M. Ahmad, M. Mubashir, S. Asif, A. Waseem, A. Mukhtar, S. Saqib, H. Siti Halimatul Munawaroh, M. K. Lam, K. Shiong Khoo, A. Bokhari and P. Loke Show, *Bioresour. Technol.*, 2021, **328**, 124859.
- 197 H. Bibi, M. Ahmad, A. I. Osman, A. A. Alsahli, M. Munir, A. H. Al-Muhtaseb, D. W. Rooney and S. Sultana, *GCB Bioenergy*, 2024, **16**, 1–25.
- 198 B. Chaudhry, M. Ahmad, M. Munir, M. Fawzy Ramadan, M. Munir, C. Ussemame Mussagy, S. Faisal, T. M. M. Abdellatief and A. Mustafa, *Sustain. Energy Technol. Assessments*, DOI:10.1016/j.seta.2024.103781.
- 199 J. Heller, *Physic nut, Jatropha curcas L.*, Bioversity International, 1996, vol. 1.
- 200 G. Corro, N. Tellez, E. Ayala and A. Marinez-Ayala, *Fuel*, 2010, **89**, 2815–2821.
- 201 Y. Y. Tye, K. T. Lee, W. N. W. Abdullah and C. P. Leh, *Renew. Sustain. Energy Rev.*, 2016, **60**, 155–172.
- 202 X.-H. Yu, R. Rawat and J. Shanklin, *BMC Plant Biol.*, 2011, **11**, 1–10.
- 203 C. H. Bindhu, J. R. C. Reddy, B. Rao, T. Ravinder, P. P. Chakrabarti, M. S. L. Karuna and R. B. N. Prasad, *J. Am. Oil Chem. Soc.*, 2012, **89**, 891–896.
- 204 MPOC, Malaysian Palm Oil Industry Has A Long-Term Plan To Address EU Regulation, <https://mpoc.org.my/malaysian-palm-oil-industry-has-a-long-term-plan-to-address-eu-regulation/>, (accessed 5 April 2024).
- 205 S. Aznam Shah, Malaysia increases green fuel mix to B20, <https://themalaysianreserve.com/2020/02/21/malaysia-increases-green-fuel-mix-to-b20/>, (accessed 5 April 2024).



- 206 Y. Basiron and Y. Foong-Kheong, *J. Oil Palm, Environ. Heal.*
- 207 F. Y. Ng, F. K. Yew, Y. Basiron and K. Sundram, *J. Oil Palm, Environ. Heal.*
- 208 A. L. S. Murta, M. A. V. De Freitas, C. G. Ferreira and M. M. D. C. L. Peixoto, *Renew. Energy*, 2021, **164**, 521–530.
- 209 Y. Subramaniam and T. A. Masron, *Energy Convers. Manag. X*, 2021, **10**, 100064.
- 210 Supply Chain, How oil palm is grown - Golden Agri-Resources, <https://goldenagri.com.sg/oil-palm-grown/>, (accessed 5 April 2024).
- 211 C. Y. May, M. A. Ngan, C. K. Yoo, R. A. Majid, A. Y. K. Chung, H. L. L. Nang, C. S. Foon, Y. C. Liang, P. C. Wei and N. M. Han, *Palm Oil Dev.*, 2005, **23**, 3–7.
- 212 N. S. Sulaiman, M. D. Sintang, S. Mantihal, H. M. Zaini, E. Munsu, H. Mamat, S. Kanagaratnam, M. H. A. Jahurul and W. Pindi, *Heliyon*, 2022, **8**, e11041.
- 213 S. Mekhilef, S. Siga and R. Saidur, *Renew. Sustain. Energy Rev.*, 2011, **15**, 1937–1949.
- 214 M. H. M. Yasin, R. Mamat, G. Najafi, O. M. Ali, A. F. Yusop and M. H. Ali, *Renew. Sustain. Energy Rev.*, 2017, **79**, 1034–1049.
- 215 K. T. Lee, C. Ofori-Boateng, K. T. Lee and C. Ofori-Boateng, *Sustain. biofuel Prod. from oil palm biomass*, 2013, 107–146.
- 216 G. K. A. Parveez, E. Hishamuddin, S. K. Loh, M. Ong-Abdullah, K. M. Salleh, M. Bidin, S. Sundram, Z. A. A. Hasan and Z. Idris, *J. Oil Palm Res.*, 2020, **32**, 159–190.
- 217 A. R. González, Y. J. O. Asencios, E. M. Assaf and J. M. Assaf, *Appl. Surf. Sci.*, 2013, **280**, 876–887.
- 218 A. N. K. Lup, F. Abnisa, W. M. A. W. Daud and M. K. Aroua, *Appl. Catal. A Gen.*, 2017, **541**, 87–106.
- 219 M. Peroni, I. Lee, X. Huang, E. Baráth, O. Y. Gutiérrez and J. A. Lercher, *Acs Catal.*, 2017, **7**, 6331–6341.



- 220 P. Arora, E. L. Grennfelt, L. Olsson and D. Creaser, *Chem. Eng. J.*, 2019, **364**, 376–389. View Article Online
DOI: 10.1039/D5YA00078E
- 221 S. M. Kim, M. E. Lee, J.-W. Choi, D. J. Suh and Y.-W. Suh, *Catal. Commun.*, 2011, **16**, 108–113.
- 222 M. Elkelawy, H. A.-E. Bastawissi, A. M. Radwan, M. T. Ismail and M. El-Sheekh, in *Handbook of algal biofuels*, Elsevier, 2022, pp. 331–361.
- 223 S. Maroa and F. Inambao, *J. Energy South. Africa*, 2019, **30**, 1–13.
- 224 L. Jeczmioneck and K. Porzycka-Semczuk, *Fuel*, 2014, **128**, 296–301.
- 225 C. González, P. Marín, F. V Díez and S. Ordóñez, *Ind. Eng. Chem. Res.*, 2016, **55**, 2319–2327.
- 226 S. R. Yenumala, S. K. Maity and D. Shee, *Catal. Sci. Technol.*, 2016, **6**, 3156–3165.
- 227 L. Qu, X. Jiang, Z. Zhang, X. Zhang, G. Song, H. Wang, Y. Yuan and Y. Chang, *Green Chem.*, 2021, **23**, 9348–9376.
- 228 S. Khan, A. N. Kay Lup, K. M. Qureshi, F. Abnisa, W. M. A. Wan Daud and M. F. A. Patah, *J. Anal. Appl. Pyrolysis*, 2019, **140**, 1–24.
- 229 R. W. Gosselink, S. A. W. Hollak, S. W. Chang, J. Van Haveren, K. P. De Jong, J. H. Bitter and D. S. Van Es, *ChemSusChem*, 2013, **6**, 1576–1594.
- 230 S. De, B. Saha and R. Luque, *Bioresour. Technol.*, 2015, **178**, 108–118.
- 231 B. P. Pattanaik and R. D. Misra, *Renew. Sustain. Energy Rev.*, 2017, **73**, 545–557.
- 232 US Energy, DOE Explains...Catalysts | Department of Energy, <https://www.energy.gov/science/doe-explainscatalysts>, (accessed 5 April 2024).
- 233 W. Collection, 1882, **44**, 1800–1882.
- 234 V. Fourmond, N. Plumeré and C. Léger, *Nat. Rev. Chem.*, 2021, **5**, 348–360.
- 235 P. Kalita, B. Basumatary, P. Saikia, B. Das and S. Basumatary, *Energy Nexus*, 2022, **6**, 100087.



- 236 P. S. Sreeprasanth, R. Srivastava, D. Srinivas and P. Ratnasamy, *Appl. Catal. A Gen.*, 2006, **314**, 148–159. View Article Online
DOI: 10.1039/B5YA00078E
- 237 R. O. Araujo, V. O. Santos, F. C. P. Ribeiro, J. da S. Chaar, A. M. Pereira, N. P. S. Falcão and L. K. C. de Souza, *Energy Convers. Manag.*, 2021, **228**, 113636.
- 238 N. Degirmenbasi, N. Boz and D. M. Kalyon, *Appl. Catal. B Environ.*, 2014, **150**, 147–156.
- 239 Y. Shitao, X. Cao, S. Wu, Q. Chen, L. Li and H. Li, *Ind. Crops Prod.*, 2020, **150**, 112362.
- 240 O. Ejeromedoghene, *Mater. Today Proc.*, 2021, **47**, 1580–1583.
- 241 J. I. Orege, A. O. Adeyemo, O. F. Adeyinka, O. B. Omitola, A. Usman and E. I. Adeyeye, *Orient. J. Chem.*, 2020, **36**, 106.
- 242 A. Guldhe, P. Singh, F. A. Ansari, B. Singh and F. Bux, *Fuel*, 2017, **187**, 180–188.
- 243 O. Ogunkunle, O. O. Oniya and A. O. Adebayo, *Energy Policy Res.*, 2017, **4**, 21–28.
- 244 S. Chozhavendhan, M. V. P. Singh, B. Fransila, R. P. Kumar and G. K. Devi, *Curr. Res. Green Sustain. Chem.*, 2020, **1**, 1–6.
- 245 A. K. Endalew, Y. Kiros and R. Zanzi, *Energy*, 2011, **36**, 2693–2700.
- 246 U. Habib, F. Ahmad, M. Awais, N. Naz, M. Aslam, M. Urooj, A. Moqem, H. Tahseen, A. Waqar and M. Sajid, *J. Chem. Environ.*, 2023, **2**, 14–53.
- 247 N. S. Lani, N. Ngadi, N. Y. Yahya and R. A. Rahman, *J. Clean. Prod.*, 2017, **146**, 116–124.
- 248 Z. Huang, Z. Zhao, C. Zhang, J. Lu, H. Liu, N. Luo, J. Zhang and F. Wang, *Nat. Catal.*, 2020, **3**, 170–178.
- 249 P. Li, B. Niu, H. Pan, Y. Zhang and D. Long, *J. Clean. Prod.*, 2023, **384**, 135653.
- 250 K. B. Tan, Y. Qiu, Y. Li, B. Chen, L. Xia, D. Cai, S. Ali, J. Huang and G. Zhan, *Mol. Catal.*, 2024, **565**, 114361.



- 251 E. S. K. Why, H. C. Ong, H. V. Lee, W. H. Chen, N. Asikin-Mijan, M. Varman and W. J. Loh, *Energy*, 2022, **239**, 122017. View Article Online
DOI: 10.1039/D5YA00078E
- 252 E. S. K. Why, H. C. Ong, H. V. Lee, W. H. Chen, N. Asikin-Mijan and M. Varman, *Energy Convers. Manag.*, 2021, **243**, 114311.
- 253 Y. Zheng, J. Wang, D. Li, C. Liu, Y. Lu, X. Lin and Z. Zheng, *Int. J. Hydrogen Energy*, 2021, **46**, 27922–27940.
- 254 S. Janampelli and S. Darbha, *Catal. Commun.*, 2019, **125**, 70–76.
- 255 D. Y. Murzin, M. E. Martínez-Klimov, P. Mäki-Arvela, Z. Vajglova, M. Alda-Onggar, I. Angervo, N. Kumar, K. Eränen, M. Peurla, M. H. Calimli, J. Muller, A. Shchukarev and I. L. Simakova, *Energy and Fuels*, 2021, **35**, 17755–17768.
- 256 S. Chen, W. Wang, X. Li, P. Yan, W. Han, T. Sheng, T. Deng, W. Zhu and H. Wang, *J. Energy Chem.*, 2022, **66**, 576–586.
- 257 H. Baek, K. Kashimura, T. Fujii, S. Tsubaki, Y. Wada, S. Fujikawa, T. Sato, Y. Uozumi and Y. M. A. Yamada, *ACS Catal.*, 2020, **10**, 2148–2156.
- 258 T. Bangjang, A. Kaewchada and A. Jaree, *Can. J. Chem. Eng.*, 2021, **99**, 435–446.
- 259 A. Ali and C. Zhao, *Chinese J. Catal.*, 2020, **41**, 1174–1185.
- 260 L. Yang and M. A. Carreon, *ACS Appl. Mater. Interfaces*, 2017, **9**, 31993–32000.
- 261 Y. Liu, X. Yang, H. Liu, Y. Ye and Z. Wei, *Appl. Catal. B Environ.*, 2017, **218**, 679–689.
- 262 S. Lei, S. Qin, B. Li and C. Zhao, *J. Catal.*, 2021, **400**, 244–254.
- 263 S. Xie, C. Jia, A. Prakash, M. I. Palafox, J. Pfaendtner and H. Lin, *ACS Catal.*, 2019, **9**, 3753–3763.
- 264 H. Liu, J. Han, Q. Huang, H. Shen, L. Lei, Z. Huang, Z. Zhang, Z. K. Zhao and F. Wang, *Ind. Eng. Chem. Res.*, 2020, **59**, 17440–17450.
- 265 C. C. Tran, D. Akmach and S. Kaliaguine, *Green Chem.*, 2020, **22**, 6424–6436.



- 266 X. Cao, J. Zhao, F. Long, X. Zhang, J. Xu and J. Jiang, *Appl. Catal. B Environ.*, 2022, **305**, 121068. Article Online
DOI: 10.1039/D2YA00078E
- 267 L. Zhou, W. Lin, K. Liu, Z. Wang, Q. Liu, H. Cheng, C. Zhang, M. Arai and F. Zhao, *Catal. Sci. Technol.*, 2020, **10**, 222–230.
- 268 F. Paquin, J. Rivnay, A. Salleo, N. Stingelin and C. Silva, *J. Mater. Chem. C*, 2015, **3**, 10715–10722.
- 269 T. Burimsitthigul, B. Yoosuk, C. Ngamcharussrivichai and P. Prasassarakich, *Renew. Energy*, 2021, **163**, 1648–1659.
- 270 J. Zhang, C. Zhao, C. Li, S. Li, C.-W. Tsang and C. Liang, *Catal. Sci. Technol.*, 2020, **10**, 2948–2960.
- 271 E. Puello-Polo, Y. Pájaro and E. Márquez, *Catalysts*, 2020, **10**, 894.
- 272 F. Wang, W. Zhang, J. Jiang, J. Xu, Q. Zhai, L. Wei, F. Long, C. Liu, P. Liu, W. Tan and D. He, *Chem. Eng. J.*, 2020, **382**, 122464.
- 273 J. Wang, X. Chen, X. Chen, C. Zhao, Y. Ling and C. Liang, *Sustain. Energy Fuels*, 2022, **6**, 3025–3034.
- 274 L. Skuhrovcová, H. de Paz Carmona, Z. Tišler, E. Svobodová, M. Michálková, K. Strejcová, R. Velvarská and U. Akhmetzyanova, *Mol. Catal.*, 2023, **537**, 112930.
- 275 N. Kaewtrakulchai, A. Smuthkochorn, K. Manatura, G. Panomsuwan, M. Fuji and A. Eiad-Ua, *Materials (Basel)*, DOI:10.3390/ma15196584.
- 276 M. F. Wagenhofer, E. Baráth, O. Y. Gutiérrez and J. A. Lercher, *ACS Catal.*, 2017, **7**, 1068–1076.
- 277 S. Thongkumkoon, W. Kiatkittipong, U. W. Hartley, N. Laosiripojana and P. Daorattanachai, *Renew. Energy*, 2019, **140**, 111–123.
- 278 M. Peronia, G. Mancino, E. Baráth, O. Y. Gutiérrez and J. A. Lercher, *Appl. Catal. B Environ.*, 2016, **180**, 301–311.



- 279 M. Ruangudomsakul, N. Osakoo, C. Keawkumay, C. Kongmanklang, T. Butburee, S. Kiatphuengporn, K. Faungnawakij, N. Chanlek, J. Wittayakun and P. Khemthong, *Catal. Today*, 2021, **367**, 153–164.
- 280 S. Phimsen, W. Kiatkittipong, H. Yamada, T. Tagawa, K. Kiatkittipong, N. Laosiripojana and S. Assabumrungrat, *Energy Convers. Manag.*, 2017, **151**, 324–333.
- 281 X. Chen, X. Chen, C. Li and C. Liang, *Sustain. Energy Fuels*, 2020, **4**, 2370–2379.
- 282 S. Kawi, Y. Kathiraser, J. Ni, U. Oemar, Z. Li and E. T. Saw, *ChemSusChem*, 2015, **8**, 3556–3575.
- 283 N. Gao, J. Salisu, C. Quan and P. Williams, *Renew. Sustain. Energy Rev.*, 2021, **145**, 111023.
- 284 Z. Zhang, J. Cheng, Y. Zhu, H. Guo and W. Yang, *Fuel*, 2020, **269**, 117465.
- 285 S.-U. Lee, E. S. Kim, T.-W. Kim, J.-R. Kim, K.-E. Jeong, S. Lee and C.-U. Kim, *J. Ind. Eng. Chem.*, 2020, **83**, 366–374.
- 286 Q. Tan, Y. Cao and J. Li, *Renew. Energy*, 2020, **150**, 370–381.
- 287 Y. Zhu, Z. Zhang, J. Cheng, H. Guo and W. Yang, *Int. J. Hydrogen Energy*, 2021, **46**, 3898–3908.
- 288 P. Chintakanan, T. Vitidsant, P. Reubroycharoen, P. Kuchonthara, T. Kida and N. Hinchiranan, *Fuel*, 2021, **293**, 120472.
- 289 A. Zitouni, R. Bachir, W. Bendedouche and S. Bedrane, *Fuel*, 2021, **297**, 120783.
- 290 J. Cheng, Y. Shao, H. Guo, Z. Zhang, Y. Mao, L. Qian, K. Xin and W. Yang, *Fuel*, 2022, **318**, 123679.
- 291 A. Ramesh, K. Shanthi and M.-T. Nguyen-Le, *Mol. Catal.*, 2022, **518**, 112113.
- 292 W. Hunsiri, N. Chaihad, C. Ngamcharussrivichai, D. N. Tungasmita, P. Reubroycharoen and N. Hinchiranan, *Fuel Process. Technol.*, 2023, **248**, 107825.
- 293 M. S. Kuttiyathil, K. Sivaramakrishnan, L. Ali, T. Shittu, M. Z. Iqbal, A. Khaleel and



- M. Altarawneh, *Bioresour. Technol. Reports*, 2023, **22**, 101437.
- 294 M. S. Gamal, N. Asikin-Mijan, W. N. A. W. Khalit, M. Arumugam, S. M. Izham and Y. H. Taufiq-Yap, *Fuel Process. Technol.*, 2020, **208**, 106519.
- 295 J. de Barros Dias Moreira, D. Bastos de Rezende and V. Márcia Duarte Pasa, *Fuel*, 2020, **269**, 117253.
- 296 V. K. Soni, S. Dhara, R. Krishnapriya, G. Choudhary, P. R. Sharma and R. K. Sharma, *Fuel*, 2020, **266**, 117065.
- 297 M. Y. Choo, L. E. Oi, T. C. Ling, E. P. Ng, Y. C. Lin, G. Centi and J. C. Juan, *J. Anal. Appl. Pyrolysis*, 2020, **147**, 104797.
- 298 J. A. Melo, M. S. de Sá, A. Moral, F. Bimbela, L. M. Gandía and A. Wisniewski, *Nanomaterials*, DOI:10.3390/nano11071659.
- 299 M. Safa-Gamal, N. Asikin-Mijan, M. Arumugam, W. N. A. W. Khalit, I. Nur Azreena, F. S. Hafez and Y. H. Taufiq-Yap, *J. Anal. Appl. Pyrolysis*, 2021, **160**, 105334.
- 300 C. Muangsuwan, W. Kriprasertkul, S. Ratchahat, C. G. Liu, P. Posoknistakul, N. Laosiripojana and C. Sakdaronnarong, *ACS Omega*, 2021, **6**, 2999–3016.
- 301 N. Asikin-Mijan, G. AbdulKareem-Alsultan, M. S. Mastuli, A. Salmiaton, M. Azuwa Mohamed, H. V. Lee, Y. H. H. Taufiq-yap, A. G. Alsultan, A. G. Alsultan, A. G. Alsultan, N. A. Mijan, G. A. Alsultan, M. S. Mastuli, A. Ali, M. A. Mohamed, H. V Voon, Y. H. H. Taufiq-yap, E. S. Chan, I. P. Jain, A. Rownaghi, M. Anwar, K. Wilson and A. Lee, *Fuel*, 2022, **325**, 124917.
- 302 M. Saidi and A. Zhandnezhad, *J. Environ. Manage.*, 2023, **326**, 116761.
- 303 A. Athirah, N. Othman and M. N. M. Jaafar, *Malaysian J. Catal.*, 2023, **7**, 1–5.
- 304 P. S. Shinde, P. S. Suryawanshi, K. K. Patil, V. M. Belekar, S. A. Sankpal, S. D. Delekar and S. A. Jadhav, *J. Compos. Sci.*, 2021, **5**, 75.
- 305 J. Huang, A. Jones, T. D. Waite, Y. Chen, X. Huang, K. M. Rosso, A. Kappler, M.



- Mansor, P. G. Tratnyek and H. Zhang, *Chem. Rev.*, 2021, **121**, 8161–8233. View Article Online
DOI: 10.1039/D5YA00078E
- 306 H. Wang, K. H. L. Zhang, J. P. Hofmann and F. E. Oropeza, *J. Mater. Chem. A*, 2021, **9**, 19465–19488.
- 307 W. H. Lee, M. H. Han, Y.-J. Ko, B. K. Min, K. H. Chae and H.-S. Oh, *Nat. Commun.*, 2022, **13**, 605.
- 308 H. N. Bhatti, Z. Iram, M. Iqbal, J. Nisar and M. I. Khan, *Mater. Res. Express*, 2020, **7**, 15802.
- 309 S. Xia, K. Hu, C. Lei and J. Jin, *Org. Lett.*, 2020, **22**, 1385–1389.
- 310 Z. Li, X. Wang, S. Xia and J. Jin, *Org. Lett.*, 2019, **21**, 4259–4265.
- 311 D. Wang and Z. Li, *Res. Chem. Intermed.*, 2017, **43**, 5169–5186.
- 312 G. Chen, Y. Zhu, H. M. Chen, Z. Hu, S. Hung, N. Ma, J. Dai, H. Lin, C. Chen and W. Zhou, *Adv. Mater.*, 2019, **31**, 1900883.
- 313 F. N. I. Sari, S. Abdillah and J.-M. Ting, *Chem. Eng. J.*, 2021, **416**, 129165.
- 314 M. Minella, G. Marchetti, E. De Laurentiis, M. Malandrino, V. Maurino, C. Minero, D. Vione and K. Hanna, *Appl. Catal. B Environ.*, 2014, **154**, 102–109.
- 315 A. Safarzadeh-Amiri, J. R. Bolton and S. R. Cater, *J. Adv. Oxid. Technol.*, 1996, **1**, 18–26.
- 316 X. Yu, J. Chen and T. Ren, *RSC Adv.*, 2014, **4**, 46427–46436.
- 317 Y. Zhai, X. Ren, Y. Sun, D. Li, B. Wang and S. F. Liu, *Appl. Catal. B Environ.*, 2023, **323**, 122091.
- 318 F.-P. Wu, L.-L. Qiu, Y.-P. Zhao, Z.-P. Fu, J. Xiao, J. Li, F.-J. Liu, J. Liang and J.-P. Cao, *Fuel Process. Technol.*, 2023, **252**, 107977.
- 319 R. Deplazes, C. A. Teles, C. Ciotonea, A. Sfeir, N. Canilho, F. Richard and S. Royer, *Catal. Today*, 2024, **430**, 114514.
- 320 W. Widayat, D. Andhika Putra and I. Nursafitri, *Mater. Today Proc.*, 2019, **13**, 97–



- 102.
- 321 Z. Zhang, J. Ye, D. Tan, Z. Feng, J. Luo, Y. Tan and Y. Huang, *Fuel*, 2021, **290**, 120039.
- 322 Z. Zhang, J. Li, J. Tian, Y. Zhong, Z. Zou, R. Dong, S. Gao, W. Xu and D. Tan, *Fuel Process. Technol.*, 2022, **230**, 107213.
- 323 Z. Zhang, J. Tian, J. Li, C. Cao, S. Wang, J. Lv, W. Zheng and D. Tan, *Fuel Process. Technol.*, 2022, **233**, 107317.
- 324 E. C. S. Santos, T. C. Dos Santos, R. B. Guimarães, L. Ishida, R. S. Freitas and C. M. Ronconi, *RSC Adv.*, 2015, **5**, 48031–48038.
- 325 J. Dantas, E. Leal, D. R. Cornejo, R. H. G. A. Kiminami and A. C. F. M. Costa, *Arab. J. Chem.*, 2020, **13**, 3026–3042.
- 326 K. Liu, R. Wang and M. Yu, *Renew. energy*, 2018, **127**, 531–538.
- 327 V. Sebastian Cabeza, .
- 328 A. I. Cotar, A. M. Grumezescu, K.-S. Huang, G. Voicu, C. M. Chifiriuc and R. Radulescu, *Biointerface Res. Appl. Chem.*
- 329 W. Xie and J. Li, *Renew. Sustain. Energy Rev.*, 2023, **171**, 113017.
- 330 L. Bai, A. Tajikfar, S. Tamjidi, R. Foroutan and H. Esmacili, *Renew. Energy*, 2021, **170**, 426–437.
- 331 A. Ara, R. Khattak, M. S. Khan, B. Begum, S. Khan and C. Han, *Catalysts*, 2022, **12**, 1–19.
- 332 D. Ho, X. Sun and S. Sun, *Acc. Chem. Res.*, 2011, **44**, 875–882.
- 333 J. Wallyn, N. Anton, D. Mertz, S. Begin-Colin, F. Pertion, C. A. Serra, F. Franconi, L. Lemaire, M. Chipier and H. Libouban, *ACS Appl. Mater. Interfaces*, 2018, **11**, 403–416.
- 334 G. S. Aguilar-Moreno, E. Navarro-Cerón, A. Velázquez-Hernández, G. Hernández-



- Eugenio, M. Á. Aguilar-Méndez and T. Espinosa-Solares, *Renew. Energy*, 2020, **147**, 204–213. View Article Online
DOI: 10.1016/j.renene.2020.109786
- 335 X. Song, C. Ren, Q. Zhao and B. Su, *Chem. Eng. J.*, 2020, **381**, 122586.
- 336 A. Gallo-Cordova, J. Lemus, F. J. Palomares, M. P. Morales and E. Mazario, *Sci. Total Environ.*, 2020, **711**, 134644.
- 337 A. Wang, P. Sudarsanam, Y. Xu, H. Zhang, H. Li and S. Yang, *Green Chem.*, 2020, **22**, 2977–3012.
- 338 Z.-H. Zhang and R. Balasubramanian, *Appl. Energy*, 2015, **146**, 270–278.
- 339 N. M. Ribeiro, A. C. Pinto, C. M. Quintella, G. O. Da Rocha, L. S. G. Teixeira, L. L. N. Guarieiro, M. do Carmo Rangel, M. C. C. Veloso, M. J. C. Rezende and R. Serpa da Cruz, *Energy & fuels*, 2007, **21**, 2433–2445.
- 340 W. Z. Tawfik, M. Esmat and S. I. El-Dek, *Appl. Nanosci.*, 2017, **7**, 863–870.
- 341 A. Fadli, A. Adnan and A. S. Addabsi, in *IOP Conference Series: Materials Science and Engineering*, IOP Publishing, 2019, vol. 622, p. 12013.
- 342 H. Chen, X. Zhang, J. Zhang and Q. Wang, *Catal. Sci. Technol.*, 2018, **8**, 1126–1133.
- 343 N. A. A. Razak, N.-A. Mijan, K. B. Baharuddin, Y. H. Taufiq-Yap and D. Derawi, *Biomass and Bioenergy*, 2024, **186**, 107269.
- 344 R. Kaewmeesri, J. Nonkumwong, W. Kiatkittipong, N. Laosiripojana and K. Faungnawakij, *J. Environ. Chem. Eng.*, 2021, **9**, 105128.
- 345 H. Zhang, H. Lin and Y. Zheng, *Appl. Catal. B Environ.*, 2014, **160–161**, 415–422.
- 346 J. G. Dickinson and P. E. Savage, *J. Mol. Catal. A Chem.*, 2014, **388**, 56–65.
- 347 Y. H. Kim, P. H. Hor, X. L. Dong, F. Zhou and Z. X. Zhao, *Solid State Commun.*, 2013, **156**, 85–89.
- 348 C. H. Bartholomew, *Appl. Catal. A Gen.*, 2001, **212**, 17–60.
- 349 Z. Hao, Q. Zhu, Z. Jiang, B. Hou and H. Li, *Fuel Process. Technol.*, 2009, **90**, 113–



- 121.
- 350 S. Echeandia, B. Pawelec, V. L. Barrio, P. L. Arias, J. F. Cambra, C. V Loricera and J. L. G. Fierro, *Fuel*, 2014, **117**, 1061–1073.
- 351 A. Ausavasukhi, Y. Huang, A. T. To, T. Sooknoi and D. E. Resasco, *J. Catal.*, 2012, **290**, 90–100.
- 352 M. S. Zanuttini, M. A. Peralta and C. A. Querini, *Ind. Eng. Chem. Res.*, 2015, **54**, 4929–4939.
- 353 R. Singh, N. Chakinala, K. Mohanty and A. G. Chakinala, *J. Environ. Chem. Eng.*, 2023, **11**, 111518.
- 354 W. Lonchay, G. Bagnato and A. Sanna, *Bioresour. Technol.*, 2022, **361**, 127727.
- 355 G. F. Froment, *Catal. Rev.*, 2008, **50**, 1–18.
- 356 B. Zhao, J. Zou, C. Chen, Q. He, Q. Tang, L. Liu and J. Dong, *Chem. Eng. J.*, 2023, **478**, 147396.
- 357 N. D. Charisiou, K. Polychronopoulou, N. Dimitratos, M. A. Goula, K. N. Papageridis, V. Sebastian, G. I. Siakavelas and D. Motta, *The effect of noble metal (M: Ir, Pt, Pd) on M/Ce₂O₃- γ -Al₂O₃ catalysts for hydrogen production via the steam reforming of glycerol*, 2020.
- 358 V. Gunasekaran, H. Gurusamy, G. Ravi and Y. Rathinam, *Renew. Energy*, 2024, 120130.
- 359 A. Kunamalla and S. K. Maity, *Fuel*, 2023, **332**, 125977.
- 360 S. Eser, R. Venkataraman and O. Altin, *Ind. Eng. Chem. Res.*, 2006, **45**, 8956–8962.
- 361 S. Eser, R. Venkataraman and O. Altin, *Ind. Eng. Chem. Res.*, 2006, **45**, 8946–8955.
- 362 M. A. A. Aziz, A. A. Jalil, S. Wongsakulphasatch and D.-V. N. Vo, *Catal. Sci. Technol.*, 2020, **10**, 35–45.
- 363 Z. Zhang, X. Zhang, L. Zhang, Y. Wang, X. Li, S. Zhang, Q. Liu, T. Wei, G. Gao and



- X. Hu, *Energy Convers. Manag.*, 2020, **205**, 112301.
- 364 D. Xu, J. Lin, R. Ma, L. Fang, S. Sun and J. Luo, *Renew. Energy*, 2022, **184**, 124–133.
- 365 F. Lin, M. Xu, K. K. Ramasamy, Z. Li, J. L. Klinger, J. A. Schaidle and H. Wang, *ACS Catal.*, 2022, **12**, 13555–13599.
- 366 D. Gao, C. Schweitzer, H. T. Hwang and A. Varma, *Ind. Eng. Chem. Res.*, 2014, **53**, 18658–18667.
- 367 A. N. Kay Lup, F. Abnisa, W. M. A. Wan Daud and M. K. Aroua, *J. Ind. Eng. Chem.*, 2017, **56**, 1–34.
- 368 P. M. Mortensen, H. W. P. de Carvalho, J.-D. Grunwaldt, P. A. Jensen and A. D. Jensen, *J. Catal.*, 2015, **328**, 208–215.
- 369 K. Li, R. Wang and J. Chen, *Energy & Fuels*, 2011, **25**, 854–863.
- 370 N. Asikin-Mijan, H. V. Lee, J. C. Juan, A. R. Noorsaadah, G. Abdulkareem-Alsultan, M. Arumugam and Y. H. Taufiq-Yap, *J. Anal. Appl. Pyrolysis*, 2016, **120**, 110–120.
- 371 H. Tani, T. Hasegawa, M. Shimouchi, K. Asami and K. Fujimoto, *Catal. Today*, 2011, **164**, 410–414.
- 372 D. Purchase, G. Abbasi, L. Bisschop, D. Chatterjee, C. Ekberg, M. Ermolin, P. Fedotov, H. Garelick, K. Isimekhai and N. G. Kandile, *Pure Appl. Chem.*, 2020, **92**, 1733–1767.
- 373 I. Sádaba, M. L. Granados, A. Riisager and E. Taarning, *Green Chem.*, 2015, **17**, 4133–4145.
- 374 L. Santamaría Arana, S. A. Korili and A. Gil Bravo, *Chem. Eng. J.* 455 140551.
- 375 I. Arends and R. A. Sheldon, *Appl. Catal. A Gen.*, 2001, **212**, 175–187.
- 376 S. G. Wettstein, J. Q. Bond, D. M. Alonso, H. N. Pham, A. K. Datye and J. A. Dumesic, *Appl. Catal. B Environ.*, 2012, **117**, 321–329.
- 377 C. Zhao, S. Kasakov, J. He and J. A. Lercher, *J. Catal.*, 2012, **296**, 12–23.



- 378 X. Liu, Z. Li, B. Zhang and M. Hu, *Fuel*, 2017, **204**, 144–151.
- 379 J. Yan, H. Zhang, Z. Yang and Y. Li, *J. Environ. Chem. Eng.*, 2025, **13**, 114968.
- 380 M. Rabaev, M. V Landau, R. Vidruk-Nehemya, A. Goldbourt and M. Herskowitz, *J. Catal.*, 2015, **332**, 164–176.
- 381 S. Bezergianni, A. Dimitriadis, A. Kalogianni and P. A. Pilavachi, *Bioresour. Technol.*, 2010, **101**, 6651–6656.
- 382 M. Anand and A. K. Sinha, *Bioresour. Technol.*, 2012, **126**, 148–155.
- 383 F. Pinto, F. T. Varela, M. Gonçalves, R. N. André, P. Costa and B. Mendes, *Fuel*, 2014, **116**, 84–93.
- 384 P. Šimáček, D. Kubička, G. Šebor and M. Pospíšil, *Fuel*, 2010, **89**, 611–615.
- 385 O. V Kikhtyanin, A. E. Rubanov, A. B. Ayupov and G. V Echevsky, *Fuel*, 2010, **89**, 3085–3092.
- 386 J. Hancsók, M. Krár, S. Magyar, L. Boda, A. Holló and D. Kalló, *Microporous Mesoporous Mater.*, 2007, **101**, 148–152.
- 387 S. Bezergianni and A. Dimitriadis, *Fuel*, 2013, **103**, 579–584.
- 388 A. Srifa, K. Faungnawakij, V. Itthibenchapong, N. Viriya-Empikul, T. Charinpanitkul and S. Assabumrungrat, *Bioresour. Technol.*, 2014, **158**, 81–90.
- 389 A. Sonthalia and N. Kumar, *J. Energy Inst.*, 2019, **92**, 1–17.
- 390 S. D. A. Sharuddin, F. Abnisa, W. M. A. W. Daud and M. K. Aroua, *Energy Convers. Manag.*, 2016, **115**, 308–326.
- 391 A. Srifa, K. Faungnawakij, V. Itthibenchapong and S. Assabumrungrat, *Chem. Eng. J.*, 2014, **278**, 1–10.
- 392 S. T. Mohammed, S. A. Gheni, D. Y. Aqar, K. I. Hamad, S. M. R. Ahmed, M. A. Mahmood, G. H. Abdullah and M. K. Ali, *Process Saf. Environ. Prot.*, 2022, **159**, 489–499.



- 393 Z. Ding, T. Zhao, Q. Zhu, S. Liao, L. Ning, Y. Bi and H. Chen, *Biomass and Bioenergy*, 2020, **143**, 105879. View Article Online
DOI: 10.1039/D5YA00078E
- 394 V. Itthibenchapong, A. Srifa, R. Kaewmeesri, P. Kidkhunthod and K. Faungnawakij, *Energy Convers. Manag.*, 2017, **134**, 188–196.
- 395 T. Ramezani, S. M. Sadrameli, A. Bayat and A. H. S. Dehaghani, *Fuel Process. Technol.*, 2022, **238**, 107514.
- 396 N. A. A. Razak, Y. H. Taufiq-Yap and D. Derawi, *J. Anal. Appl. Pyrolysis*, 2024, 106369.
- 397 F. W. Mezaal, I. Zainol, N. M. Abbass, N. Rahim and A. A. Majhool, *J. Green Eng.*, 2020, **10**, 376–398.
- 398 G. Abdulkareem-Alsultan, N. Asikin-Mijan, N. Mansir, H. V. Lee, Z. Zainal, A. Islam and Y. H. Taufiq-Yap, *J. Anal. Appl. Pyrolysis*, 2019, **137**, 171–184.
- 399 O. N. Syazwani, S. H. Teo, A. Islam and Y. H. Taufiq-Yap, *Process Saf. Environ. Prot.*, 2017, **105**, 303–315.
- 400 T. Morgan, D. Grubb, E. Santillan-Jimenez and M. Crocker, *Top. Catal.*, 2010, **53**, 820–829.
- 401 V. Balasundram, N. Ibrahim, R. M. Kasmani, M. K. A. Hamid, R. Isha, H. Hasbullah and R. R. Ali, *Energy Procedia*, 2017, **142**, 801–808.
- 402 N. Asikin-Mijan, H. V. Lee, T. S. Marliza and Y. H. Taufiq-Yap, *J. Anal. Appl. Pyrolysis*, 2018, **129**, 221–230.
- 403 P. Mäki-Arvela, I. Kubickova, M. Snåre, K. Eränen and D. Y. Murzin, *Energy & Fuels*, 2007, **21**, 30–41.
- 404 M. Snåre, I. Kubičková, P. Mäki-Arvela, K. Eränen and D. Y. Murzin, *Ind. Eng. Chem. Res.*, 2006, **45**, 5708–5715.
- 405 K. C. Kwon, H. Mayfield, T. Marolla, B. Nichols and M. Mashburn, *Renew. Energy*,



- 2011, **36**, 907–915.
- 406 P. Mäki-Arvela, B. Rozmysłowicz, S. Lestari, O. Simakova, K. Eränen, T. Salmi and D. Y. Murzin, *Energy & Fuels*, 2011, **25**, 2815–2825.
- 407 P.-B. Chen, J.-W. Yang, Z.-X. Rao, Q. Wang, H.-T. Tang, Y.-M. Pan and Y. Liang, *J. Colloid Interface Sci.*, 2023, **652**, 866–877.
- 408 L. Boda, G. Onyestyák, H. Solt, F. Lónyi, J. Valyon and A. Thernes, *Appl. Catal. A Gen.*, 2010, **374**, 158–169.
- 409 M. R. De Brimont, C. Dupont, A. Daudin, C. Geantet and P. Raybaud, *J. Catal.*, 2012, **286**, 153–164.
- 410 I. Kubičková, M. Snåre, K. Eränen, P. Mäki-Arvela and D. Y. Murzin, *Catal. Today*, 2005, **106**, 197–200.
- 411 I. H. Choi, K. R. Hwang, J. S. Han, K. H. Lee, J. S. Yun and J. S. Lee, *Fuel*, 2015, **158**, 98–104.
- 412 S. Lestari, P. Mäki-Arvela, K. Eränen, J. Beltramini, G. Q. Max Lu and D. Y. Murzin, *Catal. Letters*, 2010, **134**, 250–257.
- 413 I. Simakova, O. Simakova, P. Mäki-Arvela and D. Y. Murzin, *Catal. Today*, 2010, **150**, 28–31.
- 414 T. Morgan, E. Santillan-Jimenez, A. E. Harman-Ware, Y. Ji, D. Grubb and M. Crocker, *Chem. Eng. J.*, 2012, **189–190**, 346–355.
- 415 H. Heriyanto, S. Murti, S. Is Heriyanti, I. Sholehah and A. Rahmawati, *MATEC Web Conf.*, 2018, **156**, 3032.
- 416 F. T. Yani, H. Husin, Darmadi, S. Muhammad, F. Abnisa, Nurhazanah, F. Nasution and Erdiwansyah, *J. Clean. Prod.*, 2022, **354**, 131704.
- 417 H. Tang, Q. Dai, Y. Cao, J. Li, X. Wei, K. Jibran and S. Wang, *Biomass and Bioenergy*, 2023, **177**, 106927.



- 418 K. Li, F. Zhou, X. Liu, H. Ma, J. Deng, G. Xu and Y. Zhang, *Catal. Sci. Technol.*, 2020, **10**, 1151–1160. View Article Online
DOI: 10.1039/D5YA00078E
- 419 S. Xing, P. Lv, C. Zhao, M. Li, L. Yang, Z. Wang, Y. Chen and S. Liu, *Fuel Process. Technol.*, 2018, **179**, 324–333.
- 420 Z. Cai, Y. Wang, Y. Cao, P. Yu, Y. Ding, Y. Ma, Y. Zheng, K. Huang and L. Jiang, *Fuel*, 2023, **337**, 127175.
- 421 K. Malins, *Fuel*, 2021, **285**, 119129.
- 422 L. Chen, K. Huang, Q. Xie, S. Mun Lam, J. Chung Sin, T. Su, H. Ji ab and Z. Qin, *Cite this Catal. Sci. Technol*, 2021, **11**, 1602.
- 423 G. Lawer-Yolar, B. Dawson-Andoh and E. Atta-Obeng, *Sustain. Chem.*, 2021, **2**, 206–221.
- 424 R. K. Saluja, V. Kumar and R. Sham, *Renew. Sustain. Energy Rev.*, 2016, **62**, 866–881.
- 425 J. Yang, Z. Xin, Q. (Sophia) He, K. Corscadden and H. Niu, *Fuel*, 2019, **237**, 916–936.
- 426 R. Mawhood, E. Gazis, S. de Jong, R. Hoefnagels and R. Slade, *Biofuels, Bioprod. Biorefining*, 2016, **10**, 462–484.
- 427 M. A. Rumizen, *Front. Energy Res.*, 2021, **9**, 1–8.
- 428 E. Halim, C. Lee, W. Wang, J. Lin and Y. Lin, *Int. J. Energy Res.*, 2022, **46**, 1059–1076.
- 429 M. Zanata, S. Tri Wulan Amelia, M. R. Mumtazy, F. Kurniawansyah and A. Roesyadi, in *Materials Science Forum*, Trans Tech Publ, 2019, vol. 964, pp. 193–198.
- 430 L. M. Orozco, D. A. Echeverri, L. Sánchez and L. A. Rios, *Chem. Eng. J.*, 2017, **322**, 149–156.
- 431 A. I. Tsiotsias, S. Hafeez, N. D. Charisiou, S. M. Al-Salem, G. Manos, A. Constantinou, S. AlKhoori, V. Sebastian, S. J. Hinder, M. A. Baker, K.



Polychronopoulou and M. A. Goula, *Renew. Energy*, 2023, **206**, 582–596. [View Article Online](#)
DOI: 10.1039/D5YA00078E

- 432 I. Aziz, L. Adhani, M. I. Maulana, M. Ali Marwono, A. A. Dwiatmoko and S. Nurbayti, *J. Kim. Val.*, 2022, **8**, 240–250.



Data Availability Statement

[View Article Online](#)
DOI: 10.1039/D5YA00078E

No primary research results, software or code have been included and no new data were generated or analysed as part of this review.

